



BIOS

Research Doctorate School in BIOMolecular Sciences

RESEARCH PROJECT
2010-2012

**Investigating the molecular basis of *Xotx1*,
Xotx2 and *Xotx5* differential actions during
Xenopus laevis development**

Doctorate Course: Molecular Biotechnology

Cycle: XXV

SSD BIO06

Laboratory: Unità di Biologia Cellulare e dello Sviluppo, SS12 Abetone e Brennero 4, Pisa

Supervisor/ Tutor: Prof. Robert Vignali

Student: Pamela Mancini

A noi due, e, e

“Noi siamo in piedi e camminiamo con parti del nostro corpo che sarebbero servite per pensare se si fossero sviluppate in un'altra parte dell'embrione.”

“We are standing and walking with parts of our body which could have been used for thinking had they developed in another part of the embryo.”

Hans Spemann, 1943

Index

Abstract	Pag. 1
1- Introduction	Pag. 3
1.1- The <i>orthodenticle</i> gene of <i>Drosophila melanogaster</i>	Pag. 3
1.2- Vertebrate <i>Otx</i> genes	Pag. 6
1.2.1- <i>Paired-like K₅₀</i> homeobox genes	Pag. 6
1.2.2- <i>Otx</i> genes in mammalian anterior development	Pag. 7
1.3- <i>Otx</i> genes and evolution	Pag. 12
1.3.1- <i>Otx</i> genes in the animal kingdom	Pag. 12
1.3.2- <i>Otd/Otx</i> : Insect and Vertebrate nervous system evolution	Pag. 15
1.4- <i>Xenopus laevis</i>	Pag. 17
1.5- <i>Otx</i> genes in <i>Xenopus laevis</i>	Pag. 18
1.5.1- <i>Xotx1</i> (and <i>Xotx4</i>) expression profile	Pag. 18
1.5.2- <i>Xotx2</i> expression profile	Pag. 20
1.5.3- <i>Xotx5/5b</i> expression profile	Pag. 22
1.5.4- <i>Xotx2</i> and <i>Xotx5</i> expression profile in the developing eye	Pag. 24
1.6- <i>Xotx</i> genes and the Organizer	Pag. 25
1.7- <i>Xotx</i> genes in the developing retina: bipolar <i>versus</i> photoreceptor fate	Pag. 30
1.8- <i>Xotx</i> genes and cement gland induction	Pag. 32
2- Aim	Pag. 37
3- Materials and methods	Pag. 39
3.1- DNA constructs section I	Pag. 39
3.2- DNA constructs section II	Pag. 41
3.3- <i>Xenopus laevis</i> embryos	Pag. 45

3.4- <i>In situ</i> hybridization	Pag. 45
3.5- RNAs methods, embryo microinjections and animal cap assays	Pag. 45
3.6- Oligo antisense Morpholino	Pag. 46
3.7- RT-PCR	Pag. 47
3.8- Two-hybrid screening	Pag. 48
3.9- GST-pull down assay	Pag. 48
3.10- Western blotting	Pag. 49
3.11- XOP-GFP reporter assay	Pag. 49
3.12- Immunostaining on sections	Pag. 50
3.13- 5' RACE	Pag. 50
3.14- Bioinformatics tools	Pag. 50
4- Results section I	Pag. 51
4.1- Cement gland induction	Pag. 51
4.1 a- Statistical analysis: χ^2 homogeneity test	Pag. 61
4.2- Convergent extension inhibition	Pag. 64
4.3- Neural tissue induction	Pag. 66
5- Results section II	Pag. 70
5.1- XOTX2 and XOTX5 transactivation domain	Pag. 70
5.2- Two-hybrid screen for XOTX2 and XOTX5 potential interactors	Pag. 71
5.3- Potential interactor database search	Pag. 72
5.4- DNA binding ability of potential interactors	Pag. 75
5.5- Expression profiles of potential interactors	Pag. 75
5.5.1- RT-PCR	Pag. 75
5.5.2- <i>In situ</i> hybridization	Pag. 77
5.5.2.1- Early developmental stages	Pag. 77
5.5.2.2- Later developmental stages	Pag. 79
5.6- XOTX interaction domain(s) identification	Pag. 81

5.7- XOTX2 and XOTX5 potential cofactors interaction with XOTX1	Pag. 82
5.8- <i>c29</i>	Pag. 83
5.8.1- C29 and XOTX2/XOTX5 <i>in vitro</i> interaction	Pag. 83
5.8.2- <i>c29</i> localization in the <i>X. tropicalis</i> genome	Pag. 84
5.8.3- C29 <i>in silico</i> secondary structure prediction	Pag. 86
5.8.4- C29 <i>in silico</i> sub-cellular localization prediction	Pag. 87
5.8.5- C29 sub-cellular localization	Pag. 88
5.8.6- <i>c29</i> functional analysis: preliminary data	Pag. 90
5.9- <i>Xusf2</i>	Pag. 94
5.9.1- XUSF2 and XOTX2/XOTX5 <i>in vitro</i> interaction	Pag. 94
5.9.2- XUSF2 and XOTX2/XOTX5 antagonistic action on Rhodopsin promoter	Pag. 95
5.9.3- XUSF2 and XOTX5 microinjection experiments: preliminary data	Pag. 98
6- Discussion section I: Cement gland, convergent extension and neural tissue	Pag. 101
7- Discussion section II: XOTX potential interactors	Pag. 108
8- Conclusions	Pag. 113
9- Bibliography	Pag. 115
10- Ringraziamenti	Pag. 138

Abstract

Otx genes are a class of Vertebrates homeobox genes homologous to the *orthodenticle* gene of *Drosophila melanogaster*. In this study we focus on three members of the *Otx* class in *Xenopus laevis*: *Xotx1*, *Xotx2* and *Xotx5*.

These three homeoproteins show a high level of homology and exploit both common and differential actions during *Xenopus laevis* development. During retinal histogenesis, *Xotx2* drives progenitor cells to a bipolar fate, while *Xotx5* guides retinal precursors toward a photoreceptor fate; analogously, *Xotx2* and *Xotx5* play a similar role in cement gland induction, while *Xotx1* is unable to induce this structure; all three transcription factors seem to be involved in regulating the head organizer activity and convergent extension gastrulation movements.

It has been demonstrated that *Xotx2* and *Xotx5* specific action in frog retina is due to a small amino acid stretch, highly divergent between the two transcription factors and localized downstream of the homeodomain, named retinal specificity box (RS box). Since the specific actions of different transcription factors can be due to their interaction with different cofactors, we have hypothesized that the RS box specific sequences could make XOTX2 and XOTX5 able to interact with different cofactors, thereby leading to the activation of different specific downstream differentiation pathways. To investigate this, we performed two parallel two-hybrid screens, to search for XOTX2 and XOTX5 specific interactors, in order to clarify their divergent action during *Xenopus* retinogenesis. Several candidate interactors of the two homeoproteins have thus been isolated, but all these potential cofactors were found able to interact *in vitro* with both XOTX, and also with XOTX1. However, since XOTX proteins exploit also common actions during *Xenopus* development, the existence of common XOTX interactors is also feasible; besides, a protein that is able to interact *in vitro* with several partners, may interact *in vivo* with only one or few of them simply because it colocalize with them, but not with the others. Thus, we decided to go further with our investigation about identified XOTX hypothetical partners. We performed an

extensive *in silico*-analysis, to find out any homologies with described sequences and we thus selected some of the clones for further analysis: *Xusf1*, *Xusf2*, *Xgrn1*, *Xgrn2* and a hypothetical peptide named *c29*. Furthermore, we mapped the specific domain(s) involved in the interaction with each selected cofactor to XOTX N-terminus. An almost partial co-localization of hypothetical partners and *Xotx* has been found by comparing their expression profiles. After deeply analyzing the data base search results and the expression profiles, we decided to focus our attention on two XOTX hypothetical interactors: USF2, a described transcription factor of bHLH type and C29, a hypothetical so far uncharacterized peptide. We decided to better characterize their molecular interaction with XOTX transcription factors *in vitro* by GST-pull down assays, as well as their *in vivo* possible function by performing gain- and loss-of-function experiments. We have predicted *in silico* the secondary structure of C29 and its subcellular localization; we have demonstrated C29 capability to localize into the nucleus, and we have obtained preliminary data about C29 potential role *in vivo*. Besides, we here describe a possible antagonistic action of XOTX2/XOTX5 and USF2 both *in vitro* and *in vivo*. Moreover, it is known that *Xotx2* and *Xotx5* induce cement gland in *Xenopus laevis* ectoderm, while *Xotx1* does not. Different transcription factors can exert differential actions also on the basis of sequence divergence. Sequence analysis shows the presence of histidine rich and serine rich regions in XOTX1, that are absent in both XOTX2 and XOTX5. We have investigated the molecular basis of XOTX2/5 and XOTX1 differential action in cement gland formation, and we have demonstrated that it is due to the presence/absence of those XOTX1 specific regions. Besides, we have characterized XOTX molecular domains involved in cement gland promoting action, and we have gained some preliminary data concerning XOTX domain(s) involved in neural tissue induction and in regulation of gastrulation movements.

1- Introduction

1.1- The *orthodenticle* gene of *Drosophila melanogaster*

The *Drosophila melanogaster orthodenticle* gene was originally isolated in a large scale screen for *loci* that affect development of the larval cuticle. In *otd* mutants, differently from wild-type flies, all abdomen cuticles point in the same direction, hence the name: *orthodenticle* (Wieschaus et al., 1984). In this study it was demonstrated that *otd* mutant embryos have defects in denticle belt formation, as well as in head development. Besides, it has been shown that *otd* mutant embryos lack antennal (olfactory fruit fly sensory organ) and pre-antennal structures (Cohen and Jurgens, 1990), and that the ocellar region (*ocelli*: three simple light sensitive lenses on the dorsal midline at the top of adult head) is sensitive to *otd* dosage (Wieschaus et al., 1992). The OTD protein contains multiple repeats consisting of single amino acids residues (glycine, serine and glutamine) and pairs of amino acids (i.e. alternating glycine and valine residues). A number of these repeats are the result of the high content of CAG/A sequence in various regions of the coding sequence; the presence of this nucleotide sequence motif has been noted in a number of other developmentally important *Drosophila* proteins, including *Notch* (Wharton et al., 1985a; 1985b) and *single-minded* (Crews et al., 1988). In addition to these repeats, OTD contains a stretch of 19 amino acids precisely repeated in tandem, whose functional role is unknown. Besides, OTD contains several candidate PEST sequences, hypothesized to act as a tag for rapid protein degradation (Finkelstein et al., 1990). Most importantly, OTD protein contains a homeodomain of the paired class K₅₀ (Fig. 1).

```

maagflksqd lqphphsygg phphhsvphg plppgmpmps lgpfglphgl eavgfsqgmw
gdlcypgvnt rkqrrerttf traqldvlea lfgktrypdi fmreevalki nlpesrvqvw
fknrrakcrq qlqqqqqsns lsssknasgg gsgnscssss ansrsnsnnn gsssnntqs
sggnnsnkss qkqgnsqssq qgggssggnn snnnsaaaaa saaaavaaaq sikthhssfl
saaaaasags ikthhssfls aaaaasggtn qsannnsnnn nqgnstpns ssgggsqagg
hlsaaaaaaaa lnvtaahqns splltpats vspvsivckk ehlsqgygss vggggggggg
gassgglng vgvvgvgvgv vgvsqdllrs pydqldagg digagvhhhh siygsaagsn
prllqpggni tpmd ssssit tpsppitpms pqsapqrmp pnrpsptil ppirpicpi
miritsgtis tsniritmpr rpatthrwst lairirsttt wairatrppi lvrhrhpsr
apcprpspr tawitcrri striwcryis sntaavaatt tvqrqqvrv rrvrvrvlv
lvvdvlvvlv lvdldrgaivl pswsstiiss tstsyssisi triitrintr ittaiiiss
ntimmnsdr i

```

Fig. 1. *Drosophila melanogaster* OTD sequence. GenBank accession number: CAA41732.1. Dark grey: homeodomain; light grey: 19 amino acids repeated sequences; green: candidate PEST sequences (tags for rapid protein degradation).

Otd transcripts appear at cellular blastoderm stage, when expression is confined to a broad circumferential stripe at the anterior end of the embryo; this portion of the blastoderm will give rise to many of the structures of the larval head (Jurgens et al., 1986). In *otd* embryos, a number of structures derived from this region are absent or defective (Finkelstein and Perrimon, 1990). Following gastrulation, expression persists in the procephalic head region. Later, a second domain of expression appears in a longitudinal stripe of cells along the ventral midline of the embryo. These cells will generate mixed population of neurons and glia. As development goes on, expression of *otd* continues in the ventral nerve cord and in the head region (Finkelstein et al., 1990). The embryonic brain of *Drosophila* is composed of two supraesophageal ganglia, each subdivided into three neuromeres. The anterior ganglion is subdivided into protocerebral, deuterocephalic and tritocerebral neuromeres; *otd* is expressed mainly in the anteriormost, protocerebral, neuromere, which is deleted almost entirely in *otd* null embryos (Finkelstein and Perrimon, 1990; Cohen and Jurgens, 1991; Hirth et al., 1995; Younossi-Hartenstein et al., 1997) (Fig. 2). Later on in

development, *otd* expression is evident in the eye and antennal primordia and then it covers the *vertex* primordium (the *vertex* is the region comprised between *Drosophila* compound eyes, containing the *ocelli* and associated cuticles) and it extends along the edge of the antennal disc. Besides, *Otd* plays a crucial role in *Drosophila* photoreceptor development (Vandendries et al., 1996) by regulating the expression of opsin genes (Tahayato et al., 2003)

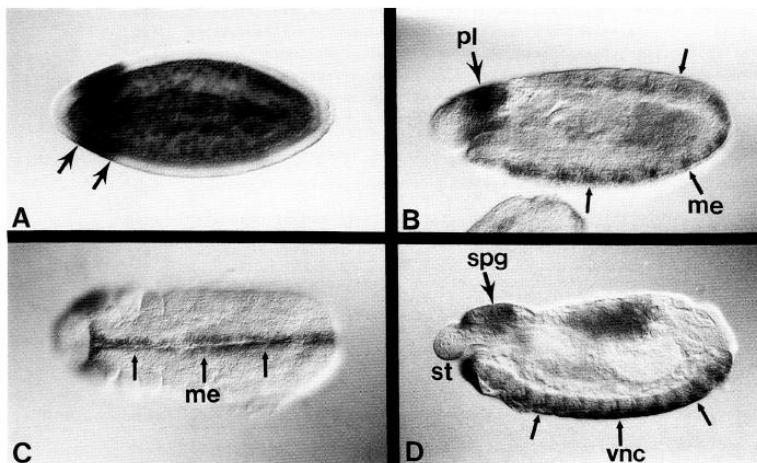


Fig. 2.
Expression of
***otd* transcripts**
during
Drosophila
embryogenesis.

(A-D) Anterior is to the left: (A) dorsal view; (B and D) lateral view; (C) ventral view. (A) A cellular blastoderm-stage embryo in which *otd* expression is

confined to a circumferential stripe extending from 70% to 90% of egg length (arrows). (B, C) Germ-band-extended embryos showing *otd* transcription in the mesectoderm (me, small arrows) and procephalic head region (pl, large arrow). (D) A germ-band-retracted embryo showing *otd* expression in the ventral nerve cord (vnc, small arrows) and in a localized region of the head that includes the supraesophageal ganglion (spg, large arrow). (Figure and caption from Finkelstein et al., 1990).

1.2- Vertebrate *Otx* genes

1.2.1- *Paired-like K₅₀* homeobox genes

Otx genes encode homeodomain transcription factors of the *paired-like* class. The homeodomain is a stretch of 60 amino acid residues and represents a variant of the helix-turn-helix motif found in prokaryotic transcriptional repressors. It is a DNA binding domain formed by three α -helices separated from coiled regions of protein backbone. Helix 3 (recognition helix) binds the DNA major groove, while helix 1 and helix 2 lie outside the DNA double helix. The recognition helix makes contact with both sugar-phosphate backbone and specific bases. An amino-terminus arm makes contact with the DNA minor groove (Lewin, 2003).

Genes belonging to the *paired* class exert primary developmental functions. They are characterized by six invariant amino acid residues in the homeodomain. The residue at position 50 can be a serine (Pax-type), a glutamine (Q₅₀ paired-like) or a lysine (K₅₀ paired-like); the last is the case of *Otx* genes. Only proteins of the first sub-class contain a second DNA binding domain: a *paired* (*prd*) domain (Galliot et al., 1999). This K₅₀ lysine residue has been reported to confer DNA binding specificity (XOTX2: Pannese et al., 1995).

In OTX proteins, the homeodomain is followed by a glutamine rich region, a WSP domain, and, at the C-terminus, by a characteristic region called OTX-tail, generally repeated in tandem, first identified in CRX (Furukawa et al., 1997) (Fig. 3).

The homeodomain of OTX proteins is also involved in their nuclear localization: CRX nuclear localization signal (NLS) is localized in the homeodomain (Fei and Hughes, 2000), as well as, OTX2 NLS (Chatelain et al., 2006). Moreover, it has been demonstrated that the homeodomain is also involved in protein-protein interactions, as in the case of NRL-CRX cooperation (Mitton et al., 2000).

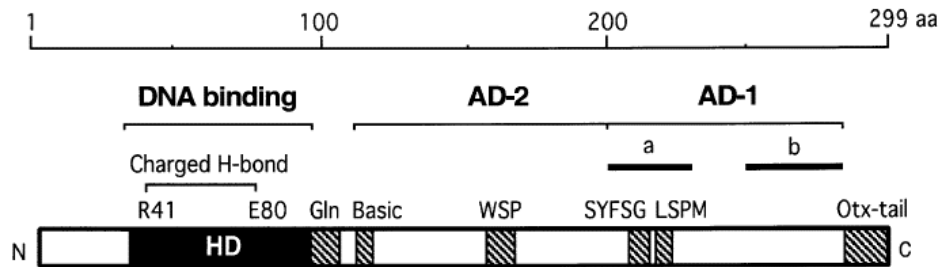


Fig. 3. Scheme of human CRX. HD: homeodomain; Gln: glutamine rich region; Basic: basic region; AD-2/AD-1: transcriptional activation domains; for AD-1, sub-domains “a” and “b” are also shown. Filled boxes represent protein domains shared with OTX1 and OTX2. (Modified from Chen et al., 2002).

1.2.2- *Otx* genes in mammalian anterior development

The study of *Drosophila* gene homologues in Vertebrates has provided a large part of the knowledge of development regulating systems. *Hox* genes are Vertebrates homologues of *Drosophila* homeotic genes; they control Vertebrates axis specification and provide positional cues in the developing neural tube from hindbrain to tail (Hunt et al., 1991). The *Drosophila* homeobox gene *orthodenticle* is involved in fly anterior development (see above), and *Drosophila otd* sequence has been used to identify and clone *otd* Vertebrate homologues *Otx1* and *Otx2* (Simeone et al., 1992; 1993).

The degree of similarity of mouse and fly homologous homeodomains is striking: mouse OTX1 and OTX2 homeodomains differ for 3 and 2 amino acid residues from OTD homeodomain, respectively. OTX1 and OTX2 homeodomains belong to paired-like K_{50} class, as well as OTD (see above), in sharing lysine residue in position 50 (Boncinelli et al., 1993). Murine OTX1 and OTX2 share extensive sequence similarities, even though in OTX1, downstream of the homeodomain, these regions of homology to OTX2 are separated by stretches of additional amino acids containing repetitions of alanine and histidine (Simeone et al., 1993). Nevertheless, OTD and OTX

proteins are highly conserved only in the homeodomain; outside the homeodomain, homology is restricted to few short sequences. OTD lacks also the so-called OTX-tail, which is tandemly duplicated in all Vertebrates OTX (Williams and Holland, 1998).

Together with two other Vertebrates homeobox genes, *Emx1* and *Emx2*, the Vertebrate homologues of *Drosophila empty spiracles*, *Otx* genes are expressed in restricted regions of the developing mouse brain, including the cerebral cortex and olfactory bulbs (Boncinelli et al., 1993) (Fig. 4). These four genes have a role in establishing the limits and the identity of different brain regions of mouse, resembling, at a more anterior level, the functions of *Hox* genes in the embryo posterior part. *Otx* genes are also expressed in sense organ primordia, such as the olfactory epithelium, the developing inner ear and the developing eye, and they exploit a major role in the development of these structures (Boncinelli et al., 1993).

In mouse, *Otx2* null embryos die early in embryogenesis, lack the rostral neuroectoderm fated to become forebrain, midbrain and rostral hindbrain, and show heavy abnormalities in their body plan (Acampora et al., 1995; Ang et al., 1996, Matsuo et al., 1995). Heterozygous *Otx2* +/- embryos, into an appropriate genetic background, show defects in head structures, such as serious brain abnormalities and craniofacial malformations (Matsuo et al., 1995).

Otx1 null mice suffer from spontaneous epileptic seizures and exhibit abnormalities that affect primarily the entire dorsal telencephalic cortex with a more pronounced effect in the temporal and perirhinal areas (Acampora et al., 1996; Weimann et al., 1999). The development of the visual and acoustic sense organs is also impaired, as the ciliary process in the eye and the lateral semicircular duct in the inner ear are lost (Acampora et al., 1996; Morsli et al., 1999).

Rescue experiments replacing lacking one *Otx* gene with the other (Acampora et al., 1998; Acampora and Simeone, 1999; Morsli et al., 1999), have shown an extended functional homology between OTX1 and OTX2,

and lead to argue that the most of the difference between the two *Otx* null mutants phenotypes stems from differences in the expression patterns of the two genes (Acampora et al., 1999a). The clearest exception to the overall *Otx* functional equivalence is provided by the lateral semicircular canal of the inner ear, that is never restored in mice replacing mutant *Otx1* with human *Otx2* (Morsli et al., 1999). The same phenomenon is observed in mice replacing *Otx1* with *otd*; these findings suggest that the ability to specify lateral semicircular canal of the inner ear may be an *Otx1* specific property (Acampora and Simeone, 1999).

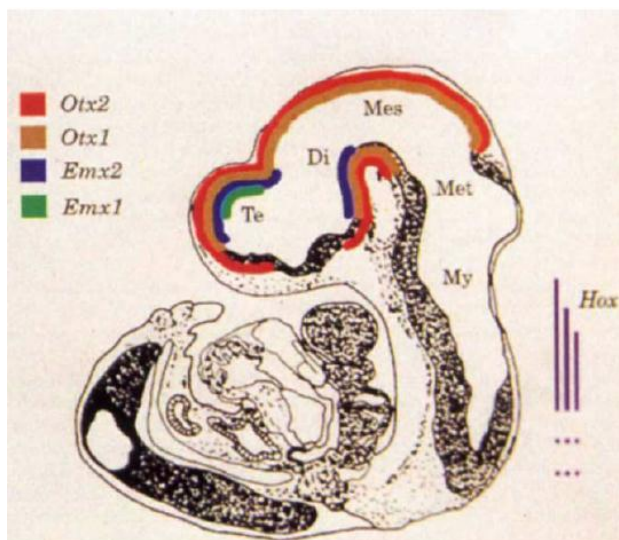


Fig. 4. Schematic representation of *Emx1*, *Emx2*, *Otx1* and *Otx2* expression in developing mouse embryo. Expression of the genes in the developing central nervous system at 10 d.p.c is given in colours. Expression of *Hox* gene family is also indicated. Di: diencephalon; Mes: mesencephalon; Met: metencephalon; My: myelencephalon; Te: telencephalon. (From Boncinelli et al., 1993).

A fundamental step of brain development involving *Otx* genes is the position of the isthmus organizer (IsO), a signaling center located at the mid-hindbrain boundary (Martinez et al., 1991) that expresses signaling molecules that refine and polarize neighbouring neural tissues (Meinhardt, 1983; Rubenstein et al., 1998). *Otx2* plays a crucial role in the IsO positioning together with another homeobox gene, *Gbx2*. *Otx2* defines the anterior fate of the neural plate, while *Gbx2* appears to be the major molecular determinant of metencephalic identity (Bouillet et al., 1995; Chapman and

Rathjen, 1995; von Bubnoff et al., 1995; Wassarman et al., 1997). These two genes are essential for correct positioning of the IsO and they exploit this function through mutual repression (Broccoli et al., 1999; Millet et al., 1999; Simeone et al., 2000).

Otx1 and *Otx2* are also required in a dose dependent manner for the normal development of mouse eye. Both *Otx1* and *Otx2* mutant mice display consistent and profound ocular malformations, including lens, pigmented epithelium, neural retina and optic stalk defects; cell proliferation, differentiation and apoptotic death are severely affected (Martinez-Morales et al., 2001). *Otx2* is essential for the development and maintenance of retinal pigmented epithelium (Martinez-Morales et al., 2001; 2003), and is also expressed in post-mitotic retinal neuroblast cells that have the potential to develop into various cell types, including ganglion cells, bipolar cells and photoreceptors (Bovolenta et al., 1997; Baas et al., 2000).

Another *Otx-like* homeobox gene has been isolated from mouse retina and named *Crx*: cone-rod homeobox containing gene. CRX is a photoreceptor specific transcription factor, playing a crucial role in their differentiation; its expression is restricted to the developing and mature photoreceptor cells. CRX binds and transactivates a specific sequence found upstream of several photoreceptor-specific genes, including the opsin genes of many species, and is essential for differentiation and maintenance of photoreceptor cells (Freund et al., 1997). *Crx* overexpression (obtained by retina retroviral transfection) causes an increase in the frequency of clones containing exclusively rods and a reduction of the frequency of clones containing other retinal cell types (amacrine and Müller glia cells). In addition, photoreceptor cells expressing a dominant negative form of *Crx* failed to form proper photoreceptors outer segments and terminals (Furukawa et al., 1997). Homozygous *Crx* knockout mice are blind at birth without any detectable photoreceptor function; their photoreceptors never develop the outer segment critical for phototransduction, and subsequently degenerate (Furukawa et al., 1999). Heterozygous *Crx*^{+/-} mice have

normally functioning photoreceptors, but their development is delayed (Furukawa et al., 1999). In humans, *Crx* is expressed, together with *Otx2*, in all photoreceptors, from early specification through adulthood and are important for regulating a wide range of photoreceptor-specific genes (Chen et al., 1997; Furukawa et al., 1997; Nishida et al., 2003; Koike et al., 2007; Henning et al., 2008; Corbo et al., 2010; Omori et al., 2011). Mutations in *Crx*, as well as in *Otx2*, are associated with several photoreceptor-specific retinopathies: mutations in *Otx2* or *Crx* can lead to Leber's Congenital Amaurosis (LCA) (Freund et al., 1998; Jacobson et al., 1998; Sohocki et al., 1998; Swaroop et al., 1999; Rivolta et al., 2001; den Hollander et al., 2008; Henderson et al., 2009; Nicols et al., 2010). Mutations in *Crx* are also linked to progressive vision loss in Cone-Rod dystrophy (CORD) and Retinitis Pigmentosa (RP) (Freund et al., 1997; 1998; Swain et al., 1997; Sohocki et al., 1998; Swaroop et al., 1999; Rivolta et al., 2001), whereas LCA-associated alleles of *Otx2* are also associated with more severe diseases (Henderson et al., 2009). It has been demonstrated that *Crx* is a target of *Otx2*, together with other *Crx* direct targets (Nishida et al., 2003; Henning et al., 2007).

In *Drosophila*, the single *otd* gene plays multiple roles in photoreceptor morphogenesis and opsin gene regulation during eye development. OTX1, OTX2 and CRX have been tested for their ability to rescue *otd* function in fly rhabdomeric eye development. Each mammalian gene has been demonstrated to mediate a defined subset of *otd*-dependent functions, with *Otx2* and *Crx* mediating unique cell-specific functions, demonstrating that during evolution OTX proteins have sub-functionalized (Terrell et al., 2012). *Crx* is also expressed in the pineal gland and it is involved in regulating pineal gene expression through the interaction with a specific pineal regulatory element located upstream of pineal-specific genes, and it is important for circadian rhythm regulation (Li et al., 1998).

1.3- *Otx* genes and evolution

1.3.1- *Otx* genes in the animal kingdom

Otd/Otx related genes have been isolated from a wide range of organisms; most of them, up to the Chordates, have only one *Otx* member, with few exceptions of duplications in independent lineages (Li et al., 1996; Umesono et al., 1999) (Fig. 5). An *Otx* related gene is present already in Cnidarians, primitive Metazoans with radial symmetry. In these organisms *Otx* function is associated with cell movements involved in axes formation rather than with head development (Smith et al., 1999). Rising up the evolutionary scale, *Otx* genes have been found in animals with primitive bilateral symmetry such as planarians (Stornaiuolo et al., 1998; Umesono et al., 1999). In these organisms *Otx* expression has been found in regenerating blastemas after transverse sectioning, with an asymmetric distribution: more abundant in regenerating head structures (Stornaiuolo et al., 1998). In planarians, *Otx* expression starts to be related with anterior patterning. Although not directly correlated with a defined anterior structure, the ancient function of *Otx* genes seems to deal with body axis patterning and with making tissues competent to respond to anteriorizing signals (Smith et al., 1999). In the nematode *C.elegans* three members of the *Otx* class have been identified. These three genes are involved in the development of thermo- and chemo-sensory neurons and, as well as *Otx* genes in mouse, their ablation gives rise to different mutant phenotypes affected in these neuronal populations. This variety of phenotypes could be caused by both divergent expression patterns and divergent protein functions (Lanjuin et al., 2003). The first case of head-associated *Otx* expression is found in Annelids, in the leech *Holobdella triserialis* (Bruce and Shankland, 1998). *Otx* related genes have been found in all Chordates, including Urochordates (Wada et al., 1996), Cephalochordates (Williams and Holland, 1996) and Agnathans (Ueki et al., 1998); in all these organisms they are expressed, as in flies, in the anterior

rostralmost part of the body and specifically in the CNS, independently from the complexity of these structures (Fig. 5). In Urochordates and Cephalochordates only one member of the *Otx* family has been isolated, and it is thought to correlate with Vertebrate *Otx2* (Wada et al., 1996; Williams and Holland, 1998); indeed, in addition to amino acid sequence homology and similarity in expression patterns, those genes are expressed in endoderm cells during gastrulation, similar to Vertebrate *Otx2*. This suggests a primitive role of *Otx2* in anterior endoderm to elicit signals specifying anterior neuroectoderm.

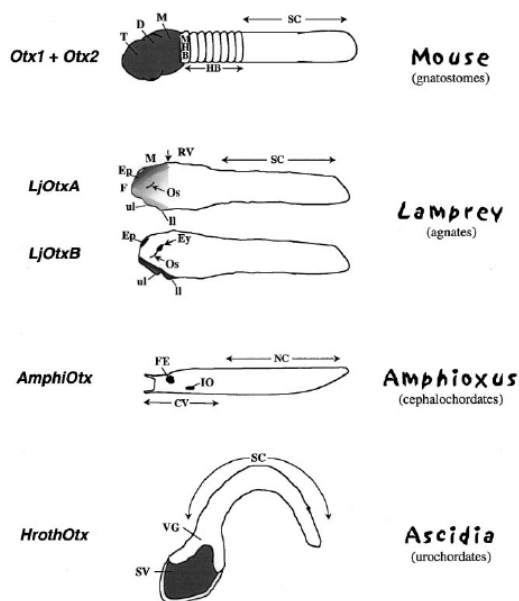


Fig. 5. Schematic representation of *Otx*-related gene expression (grey) in some representative Protochordates (Ascidia and Amphioxus) and Vertebrates (Lamprey and mouse). D: diencephalon; Ep: epiphysis; Ey: eye; F: forebrain; FE: frontal eye; HB: hindbrain; IO: infundibular organ; Il: lower lip; M: mid brain; MHB: mid-hindbrain boundary; NC: nerve cord; Oe: olfactory epithelium; Os: optic stalk; RV: rhombencephalic vesicle; SC: spinal cord; SV: sensory vesicle; T: telencephalon; ul: upper lip; VG: visceral ganglion (Figure and caption from Acampora et al.,

Another ancient *Otx2* function has been proposed: a role in cell movements regulation. This idea is consistent with functional data in frog (Blitz and Cho, 1995; Pannese et al., 1995; Andreazzoli et al., 1997; Vignali et al., 2000) and mouse (Acampora et al., 1995; Matsuo et al., 1995; Ang et al., 1996) that suggest *Otx2* involvement in cell movements occurring during gastrulation.

Otx2 sequences and expression patterns are quite conserved during evolution from low Chordates to Vertebrates (Acampora et al., 2001 and references therein). The duplication event generating *Otx1* branch from the ancestor *Otx2* gene has occurred in gnathostome Vertebrates (Williams and Holland, 1998). This is coherent with *Otx1* new function in specifying Gnathostomes specific structures (i.e. lateral semicircular canal of the inner ear). *Otx1* genes evolve more rapidly than *Otx2*, as also shown by further duplications events occurred in both *Xenopus* (Kablar et al., 1996) and *zebrafish* (Mori et al., 1994) and by the ratio of sequence divergence higher than in *Otx2* genes (Williams and Holland, 1998). These data are reinforced by notable changes in *Otx1* expression patterns in different Vertebrates (Simeone et al., 1993; Mori et al., 1994), that underlie a rapid evolution of the regulatory elements as well. A particular case is that of lamprey: the lamprey genome has two *Otx* cognates *LjOtxA* and *LjOtxB* (Fig. 5). Phylogenetic analyses suggest that *LjOtxA* clusters with Gnathostomes *Otx2* gene, while *LjOtxB* does not belong to either *Otx1* or *Otx2* lineages. Beside, *LjOtxB* is not expressed in lamprey brain, but only in olfactory placode, epiphysis, optic stalks and lower and upper lips, together with *LjOtxA*; moreover, *LjOtxB* is expressed in the eyes where *LjOtxA* is not detected (Fig. 5). Thus, *Otx1* and *Otx2* functions for the development of forebrain and midbrain in Gnathostomes appear to be shouldered by *LjOtxA* alone in lamprey. *LjOtxB* may have diverged from the stem of the *Otx1* and *Otx2* and it may have evolved independently (Ueki et al., 1998), with some weak similarity to *Otx5/Crx* lineage (see below).

Another Gnathostome *Otx* orthology class comprises *Xenopus Otx5/5b*, fish *Xotx5/Crx* and the highly divergent *Crx* gene characterized in Mammals (Plouhinec et al., 2003; Germot et al., 2001). *Otx5* and *Crx* share highly specific expression domains: developing eye and epiphysis (Furukawa et al., 1997; Vignali et al., 2000). Such expression patterns substantially differ from the broad *Otx1* and *Otx2* expression areas, spanning the whole

prosencephalon and diencephalon. Genes of *Crx* orthology class may have been recruited for specific roles in photoreceptors development.

1.3.2- *Otd/Otx*: Insect and Vertebrate nervous system evolution

Until a few years ago it was widely assumed that Insects and Vertebrates nervous system had evolved independently (Garstand, 1928; Lacalli, 1994). This was due to their position at opposite side of the dorso-ventral body axis. Nevertheless, nowadays a common evolutionary origin is supported by several evidences. Two groups of homologues genes, *Hom/Hox* and *Otd/Otx*, play crucial roles in the regional specification of the neuroectoderm fated to form nerve cord/posterior brain and anterior brain, respectively. Many studies carried out in *Drosophila* have shown that Mammalian *Hox* genes could either partially rescue phenotypes due to mutation of their fly orthologues, or elicit responses similar to those of their endogenous counterparts when transiently overexpressed (Bachiller et al., 1994; Malicki et al., 1990; Zhao et al., 1993). On the other side *Drosophila otd* has been used to rescue either mouse *Otx1* or *Otx2* gene. Mice in which a full-coding *otd* was introduced to replace *Otx1* showed the rescue of several abnormalities: brain size, as well as the thickness and cell number of the temporal and perirhinal cortices, that are reduced in *Otx1* *-/-* mice, are very similar to wild-type (Acampora, 1998). Moreover, replacement of *Otx1* *-/-* by *otd* leads to rescue of some sensory and sensory associated structures, such as iris and ciliary process; on the contrary, lateral semicircular canal of the inner ear is never rescued (Fritzch et al., 1986; Torres and Giraldez, 1998), as it is the case when *Otx1* is rescued with *Otx2*. This observation leads to the conclusion that the development of the lateral semicircular canal requires newly established properties specific of *Otx1*. Also mice in which *Otx2* has been substituted with *otd* show an almost partial rescue, providing a proof of *Otd/Otx* functional equivalence. All these data suggest that OTD

and OTX proteins are able to drive cephalic development possibly through the activation of genetic pathways conserved between Insects and Vertebrates, reinforcing the idea that the nervous systems of these two *taxa* are homologous structures sharing a common ancestor (Acampora and Simeone, 1999; Reichert and Simeone, 1999; Sharman and Brand, 1998). *Otd* and *Otx* functions have been established in a common ancestor of fly and mouse and retained during evolution; at the same time, copy number of *Otx* genes and transcriptional/translational regulation have been modified by evolution, leading to the specification of the more complex Vertebrates brain (Acampora and Simeone, 1999; Reichert and Simeone, 1999; Sharman and Brand, 1998). *Otx* gene duplication and modification of sequences and regulatory control may have contributed, from this point of view, to mammalian brain evolution (Boyl et al., 2001). Additional properties may have been acquired also by sequence divergences that endow the proteins with new specific abilities, as may be the case of *Otx1* in the inner ear. As previously mentioned, sequence similarities between *Otx* and *Otd* genes are restricted to the homeodomain; it is possible that while the ability to recognize the same DNA targets by the homeodomain might be evolutionary conserved, beside this, murine *Otx* genes have acquired, outside the homeodomain, additional functional features that are different from those of *otd* (Acampora et al., 2001). As mentioned above, rescue experiments on *otd* mutant flies using Vertebrate *Otx* genes, have shown that *Otx1*, *Otx2* and *Crx* each mediate a defined subset of *otd*-dependent function in the fly eye, showing how OTX proteins have sub-functionalized during evolution (Terrell et al., 2012).

1.4- *Xenopus laevis*

Xenopus laevis (Fig. 6) is a species of the genus *Xenopus*, that belongs to the *Pipidae* family. It is widespread in sub-Saharan Africa. It is commonly known as South Africa clawed frog (or toad). It is an aquatic animal living in stagnant waters where it eats almost every kind of food, directing it into its tongueless mouth using its front limbs. Its body is flat, with lidless eyes on the top of a small head. The hind legs have webbed feet with small claws on three toes, since the greek name *Xenopus* that means “strange foot”.

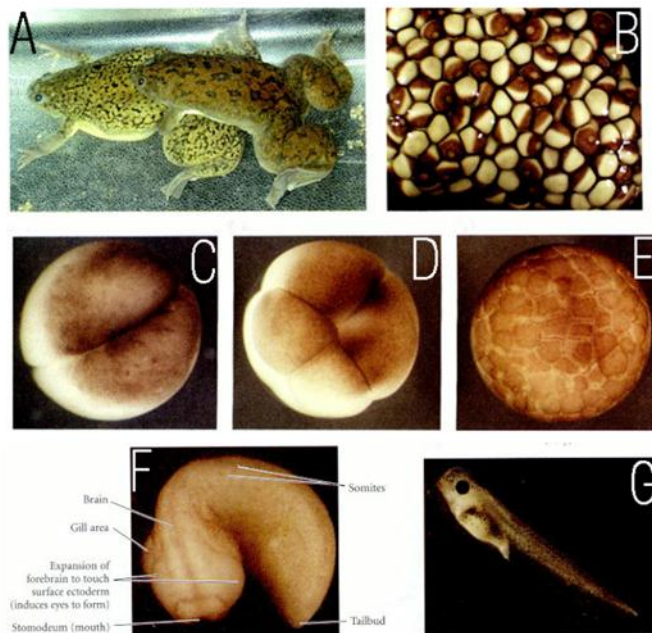


Fig. 6. *Xenopus laevis*. A: Mating frogs, the male grasping the female around the belly and fertilizing the eggs as they are released. B: newly laid clutch of eggs. The brown area of each egg is the pigmented animal cap. The white spot in the middle of the pigment is where the egg nucleus resides. C: 2-cell embryo near the end of its first cleavage. D: An 8-cell embryo. E: Early blastula; the cells get smaller, but the volume of the egg remains the same. F: pre-hatching tadpole, as the protrusions of the forebrain begin to induce eyes to form. G: mature tadpole, having swum away from the egg mass and feeding independently. (modified from Gilbert, 2000)

Many years ago it was discovered that it could be used for human pregnancy tests; this led to the worldwide distribution of *Xenopus laevis* which turned out to be an ideal laboratory animal and from the '60 it is commonly used as a model system in many laboratories all over the world. As a model system it presents several advantages. For instance, eggs are large and embryos are suitable for microsurgical dissections; its development is rapid and *in vitro* fertilization is quite simple. However, there are some drawbacks: it is pseudotetraploid and it requires about 3 years to reach sexual maturity.

1.5- Otx genes in *Xenopus laevis*

In *Xenopus laevis* four members of the *Otx* class have been isolated and characterized: *Xotx1* (Kablar et al., 1996), *Xotx2* (Pannese et al., 1995; Blitz and Cho, 1995), *Xotx4* (Kablar et al., 1996), and *Xotx5/5b* (Kuroda et al., 2000; Vignali et al., 2000). *Xotx1* is a homologue of mouse *Otx1*, *Xotx2* is a homologue of mouse *Otx2*, *Xotx5/5b* are homologues of mouse *Crx*; *Xotx4* may be a derived copy of *Xotx1*.

1.5.1- *Xotx1* (and *Xotx4*) expression profile

Xotx1 and *Xotx4* have both been isolated during a *Xenopus* cDNA library screening using murine *Otx1* as probe (Kablar et al., 1996). The peptide sequence of the homeodomain is fully conserved between *Xotx1*, *Xotx4* and mouse *Otx1*, but for a single amino acid change at position 18. Similarity between *Xotx1* and *Otx1* extends outside the homeodomain, where they share serine and histidine rich regions, *Otx1* diagnostic characters, while *Xotx4* differs a little more.

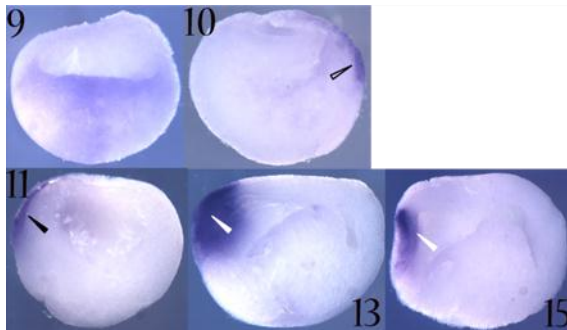


Fig. 7. *Xotx1* expression as detected by *in situ* hybridization on bisected embryos. Embryos stages are indicated. Up is animal/dorsal; down is vegetative/ventral; right is posterior; left is anterior. Empty black arrowhead: dorsal ectoderm; black arrowhead: presumptive anterior neuroectoderm; white arrowhead: anterior neural plate.

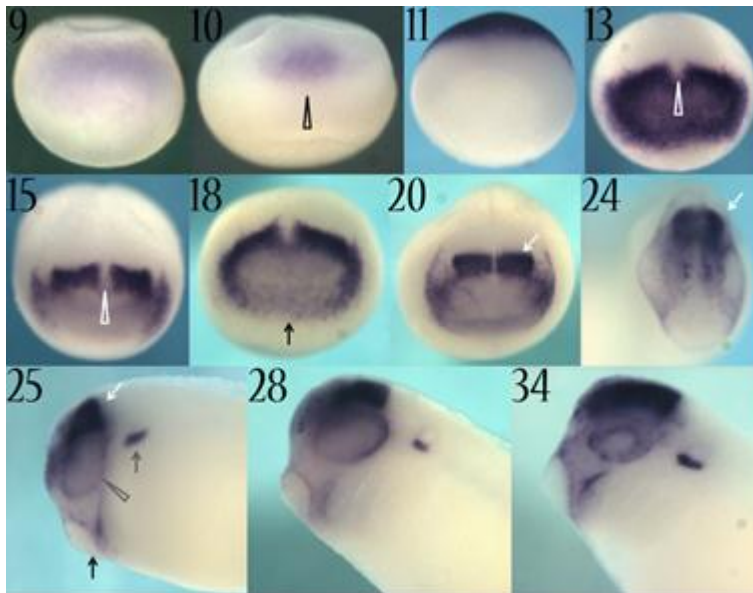


Fig. 8. *Xotx1* expression as detected by *in situ* hybridization on whole embryos. Embryos stages are indicated. Up is animal/dorsal; down is vegetative/ventral; right is posterior; left is anterior. Empty black arrowhead: dorsal ectoderm; white empty arrowhead: notoplate (anterior part); black arrow: cement gland; white arrow: anterior brain; grey arrow: otic vesicle; grey empty arrowhead: otic vesicle.

Xotx1 transcripts become visible by *in situ* hybridization (Fig. 7 and Fig. 8) at stage 10 in the outer layer of the dorsal mesoderm; then, at stage 11, *Xotx1* is detectable in the anterior neural plate; at early neurula stage (13/14) a strong expression is observed in the anterior neuroectoderm, within this area no labeling is detectable in the midline region, putatively corresponding to the anterior part of the notoplate. In the neuroectoderm, transcripts are

present in both the epithelial and sensorial layer. Moreover, transcripts are also detectable in the sensorial layer of the ectoderm at the level of the mesoderm-free zone where the cement gland and the stomodeal-hypophyseal anlagen will appear. At stage 18, *Xotx1* is expressed in the prospective brain regions, but it never reaches the very anterior tip of the brain. This anterior expression persists till tailbud stage (st. 23). Weak labeling is also detectable in the prospective pigmented layer of the eye vesicle. At stage 33 brain expression persists, as well as the exclusion from the most anterior part; *Xotx1* is also expressed in pigmented retinal layer, otic vesicles, olfactory placodes and, at a lower level, in a thin stripe of cells in the cement gland region. At a later stage (st. 37) cephalic expression persists (Kablar et al., 1996).

Xotx4 display a similar, although not perfectly superimposable expression profile (Kablar et al., 1996).

1.5.2- *Xotx2* expression profile

Xotx2 transcripts are primarily detected at stage 9 in the internal region of the dorsal marginal zone, the future Spemann's organizer region. At stage 10, the major expression site is in the migratory deep zone cells that are fated to give rise to prechordal mesendoderm (Keller et al., 1992). In addition it is also expressed in dorsal bottle cells. At stage 10.5, *Xotx2* expression persists in these cell types and posteriorly, above the dorsal blastopore lip, this expression clearly respects the boundary between internal deep zone cells and external cell layer (boundary known as Brachet's cleft) (Keller et al., 1992). Conversely, in the anterior region, *Xotx2* expression extends to cells of the presumptive anterior neuroectoderm (Fig. 9 and Fig. 10).

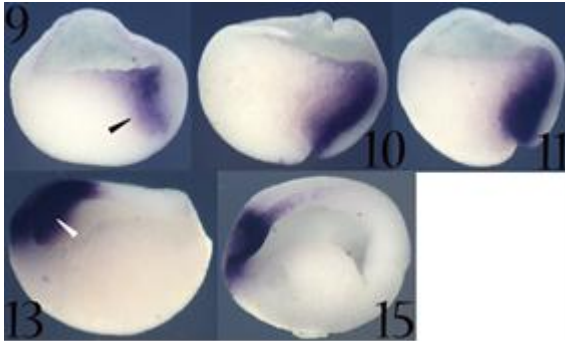


Fig. 9. *Xotx2* expression as detected by *in situ* hybridization on bisected embryos. Embryos stages are indicated. Up is animal/dorsal; down is vegetative/ventral; right is posterior; left is anterior. Black arrowhead: migratory deep zone; white arrowhead: anterior neural plate.

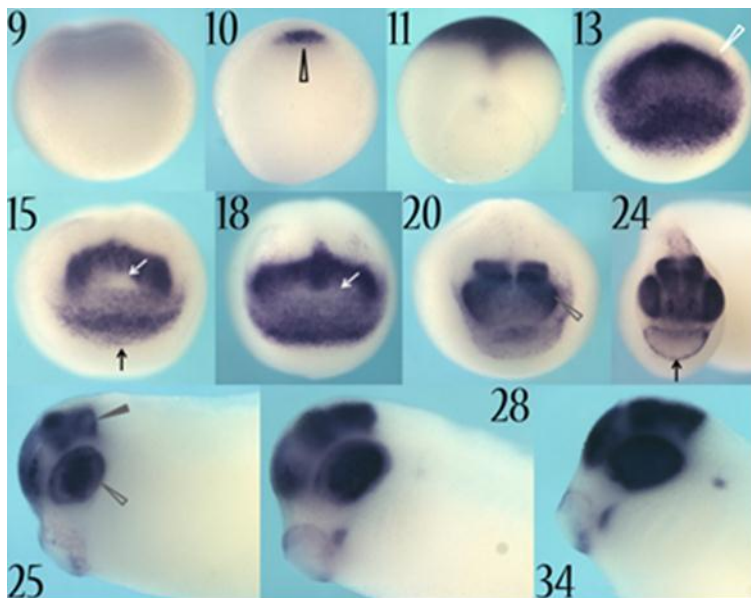


Fig. 10. *Xotx2* expression as detected by *in situ* hybridization on whole embryos. Embryos stages are indicated. Up is animal/dorsal; down is vegetative/ventral; right is posterior; left is anterior. Empty black arrowhead: dorsal migrating zone; white empty arrowhead: presumptive anterior neuroectoderm;

black arrow: cement gland anlage/cement gland; white arrow: optic chiasma; grey empty arrowhead: optic vesicle; grey arrowhead: anterior neural tube/brain.

At neurula stage (st.14), expression is confined to mesoderm and ectoderm cells of anterior/dorsal regions, and to stomodeal-hypophyseal and cement gland anlagen. *Xotx2* is not expressed in the region corresponding to the optic chiasma (Eagleson and Harris, 1990; Pannese et al., 1995). This expression profile persists till stage 18. At tailbud stage (st. 23) *Xotx2* transcripts are present in the anterior part of the brain, excluding optic chiasma area, in whole eye vesicles, in cement gland and in forming

olfactory placodes, where they persist during later phases of olfactory organ development. At stage 33 brain expression is still present, with the exception of chiasmatic region, and *Xotx2* becomes detectable also in otic vesicle. This expression profile persists with no substantial variations till stage 37 (Kablar et al., 1996). (Fig. 9 and Fig. 10)

1.5.3- *Xotx5/5b* expression profile

Xotx5 is initially transcribed at early gastrula stage (st. 10) in the dorsal blastopore lip (Spemann's organizer region). During subsequent gastrula stages this expression persists and intensifies; the major expression site corresponds to the migratory deep zone cells fated to give rise to prechordal mesoderm. At stage 10.5 *Xotx5* expression clearly respects the boundary represented by the Brachet's cleft; at this stage *Xotx5* is also strongly transcribed in the dorsal ectoderm. During later gastrula stages expression disappears from the dorsal blastopore lip, while *Xotx5* transcripts are still detectable in the anterior neuroectoderm, including the whole presumptive anterior neural plate. At early neurula stages (st. 13-14) *Xotx5* expression intensifies in the anterior neural plate, but disappears from a central area corresponding to the presumptive retina and optic chiasma territories. At these stages *Xotx5* transcripts are also detectable in a ventral anterior area corresponding to the cement gland anlage, where it persists until tailbud stage. At stage 17 a new expression site appears, corresponding to the epiphyseal anlage; this expression persists during epiphysis development. From stage 22 the expression in the cement gland anlage becomes weaker and disappears during subsequent developmental stages. Starting from stage 24, a new expression site appears in the eye region, where *Xotx5* is transcribed in a small cluster of cells corresponding to the presumptive neural retina. At stage 27, *Xotx5* is expressed in a broad dorsal region of the neural retina, where it persists till stage 30. At tadpole stage (st. 35) *Xotx5*

expression covers the entire eye region, except for the lens territories (Vignali e al., 2000) (Fig. 11 and Fig. 12).

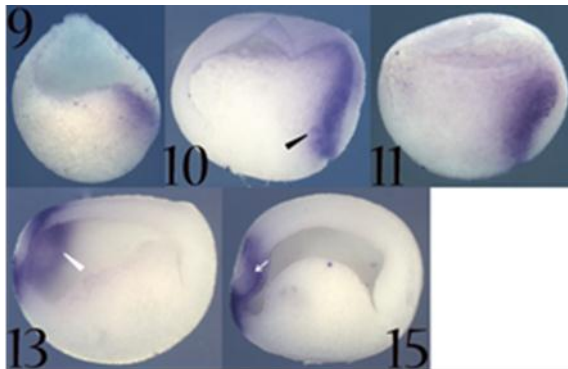


Fig. 11. *Xotx5* expression as detected by *in situ* hybridization on bisected embryos. Embryos stages are indicated. Up is animal/dorsal; down is vegetative/ventral; right is posterior; left is anterior. Black arrowhead: migratory deep zone; white arrowhead: anterior neural plate; white arrow: presumptive optic chiasma region.

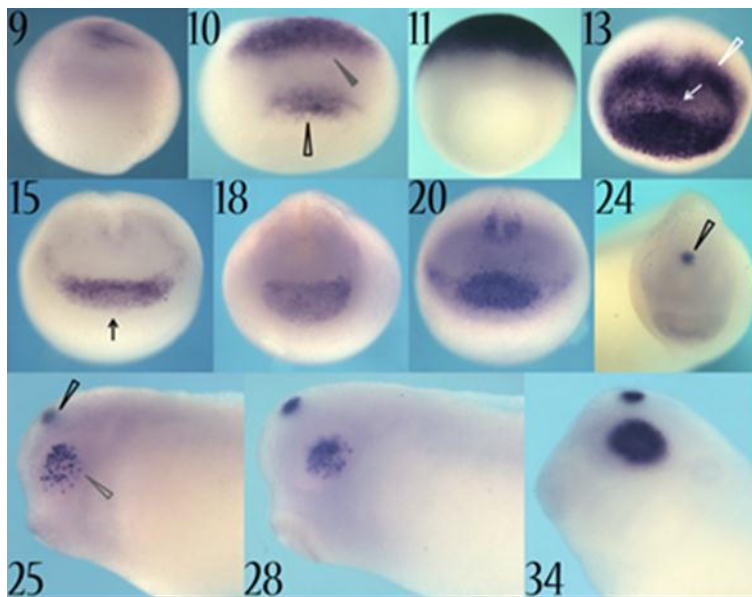


Fig. 12. *Xotx5* expression as detected by *in situ* hybridization on whole embryos. Embryos stages are indicated. Up is animal/dorsal; down is vegetative/ventral; right is posterior; left is anterior. Empty black arrowhead: dorsal migrating zone; grey arrowhead: dorsal ectoderm; white arrow: optic chiasma; white empty arrowhead: presumptive anterior neuroectoderm; black arrow: cement gland anlage/cement gland; grey empty arrowhead: optic vesicle; black empty arrowhead: pineal gland.

neuroectoderm; black arrow: cement gland anlage/cement gland; grey empty arrowhead: optic vesicle; black empty arrowhead: pineal gland.

1.5.4- *Xotx2* and *Xotx5* expression profile in the developing eye

In *Xenopus*, *Xotx2* and *Xotx5* are expressed in different patterns during retinal histogenesis (Fig. 13). At stage 20, *Xotx2* is expressed in the optic vesicles, while *Xotx5* expression in the eye starts only at stage 25, when it is expressed in a small cluster of cells of the presumptive neural retina; at this stage *Xotx2* is expressed throughout the presumptive retinal pigmented epithelium (RPE) and neural retina. A few hours later, at stage 28, *Xotx2* expression has narrowed to the central retina and RPE, while *Xotx5* has expanded. Starting from stage 31, during retinal cells differentiation, the two genes expression patterns seem almost superimposable and they are transcribed in a diffuse fashion throughout all retinal thickness.

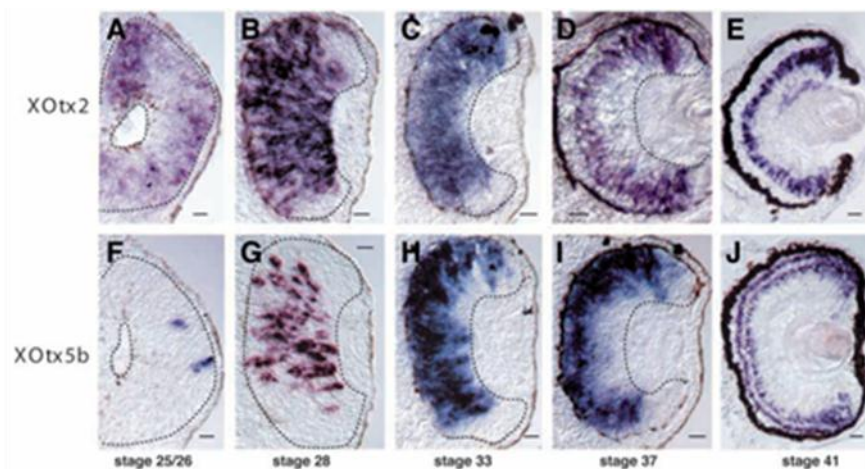


Fig. 13. *In situ* hybridisation on sections of *XOt2* (A-E) and *XOt5b* (*Xotx5*) (F-J). Stages are indicated. Bars: 20 μ m; dashed lines indicate the extent of developing neural retina in A-D,F-I. (Figure and caption modified from Viczian et al., 2003)

At stage 33, the two retinal expression profiles are indistinguishable, in that they are distributed throughout the developing retina except in the most peripheral region, corresponding to the ciliary marginal zone (CMZ). Starting from stage 37 the two gene expression patterns become progressively restricted; at the level of the mature retina (stage 41) *Xotx2* mRNA is

localized only in bipolar cells, while *Xotx5* is transcribed only in photoreceptors and in a subset of bipolar cells (Vicgian et al., 2003). Even more dramatic is the difference in the protein expression patterns: XOTX2 protein is detected only in bipolar cells, while XOTX5 is produced only in photoreceptors, due to precise translational control through the 3'UTR untranslated regions of their mRNA (Fig. 14) (Decembrini et al., 2006).

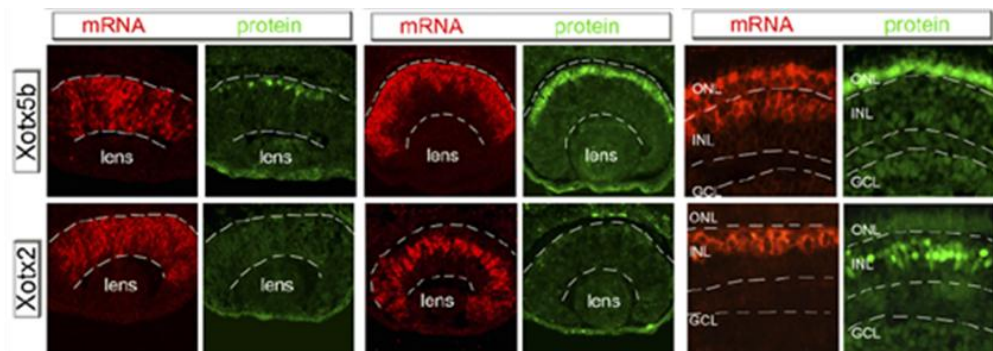


Fig. 14. Translation of the *Xenopus* Homeobox *Xotx5b* (*Xotx5*), and *Xotx2* mRNAs. *In situ* hybridization of *Xotx2* and *Xotx5b* (*Xotx5*) compared to immunostaining of the corresponding proteins on embryonic retinas sections at st. 34 (mid-neurogenesis), st. 37 (late-neurogenesis), and st. 42 (mature embryonic retina). Magnification of central retinal aspect); GCL: ganglion cell layer, INL: inner nuclear layer, ONL: outer nuclear layer. (Figure and caption adapted from Decembrini et al., 2006)

1.6- *Xotx* genes and the Organizer

Neural axial patterning in Vertebrates is the result of inductive events, in which dorsal mesoderm plays a crucial role (Spemann, 1938). Dorsal mesoderm, forming blastopore lip, is called the Organizer because of its ability to recruit cells to form axial structures. The observation that early dorsal lips are able to induce secondary heads, while late dorsal lip transplantations give rise to ectopic posterior structures, led to a distinction between a head and a trunk organizer (Spemann, 1938; Hamburger, 1988). The Organizer itself is induced from signals coming from embryo dorso-

vegetal cells forming the Nieuwkoop center (Nieuwkoop, 1973), and becomes able to induce animal pole ectoderm toward a neural fate, contemporarily establishing its antero-posterior pattern. The neuroectoderm is initially specified as anterior (activation step) and only later posterior neural structures are specified from anterior neuroectoderm (transformation step) (Nieuwkoop, 1952). Regions that will give rise to the head do not undergo convergent extension movements typical of the trunk- and tail-forming regions that are responsible for their elongation.

A number of evidences suggest that *Xotx* genes are involved in head-organizing activity (Pannese et al., 1995; Blitz and Cho, 1995; Kablar et al., 1996; Andreazzoli et al., 1997; Morgan et al., 1999; Vignali et al., 2000).

First of all a common feature of *Xotx* genes is that their early expression patterns correspond to presumptive head regions (Kablar et al., 1996; Pannese et al., 1995; Vignali et al., 2000) that do not undergo convergent extension movements (see above: *Xotx* expression patterns); a number of evidences demonstrated that XOTX proteins play a role in specifying anterior structures, rather than being mere positional markers.

Gain of function experiments have shown that *Xotx2* microinjection results in a delay in gastrulation movements and in a failure of blastopore lip closure. In embryos showing these gastrulation alterations trunk and tail fail to develop properly, the size of these structures is considerably reduced and the embryonic axis is bent dorsally (Pannese et al., 1995). In addition, several embryos show ectopic cement gland formation, as well as the presence of neural tissue in ectopic positions (Fig. 15) (Pannese et al., 1995).

In embryos treated with UV light or retinoic acid (RA) *Xotx2* expression is strongly inhibited, as well as the development of anterior structures, suggesting a direct correlation between this two phenomena and implicating a fundamental role for *Xotx2* in anterior structures development. This also suggests a role of *Xotx2* as an important intermediary between the first positional specification mediated by the cortical rotation originated by sperm

entry (Gerhart et al., 1989) and the establishment of anteroposterior axis (Pannese et al., 1995).

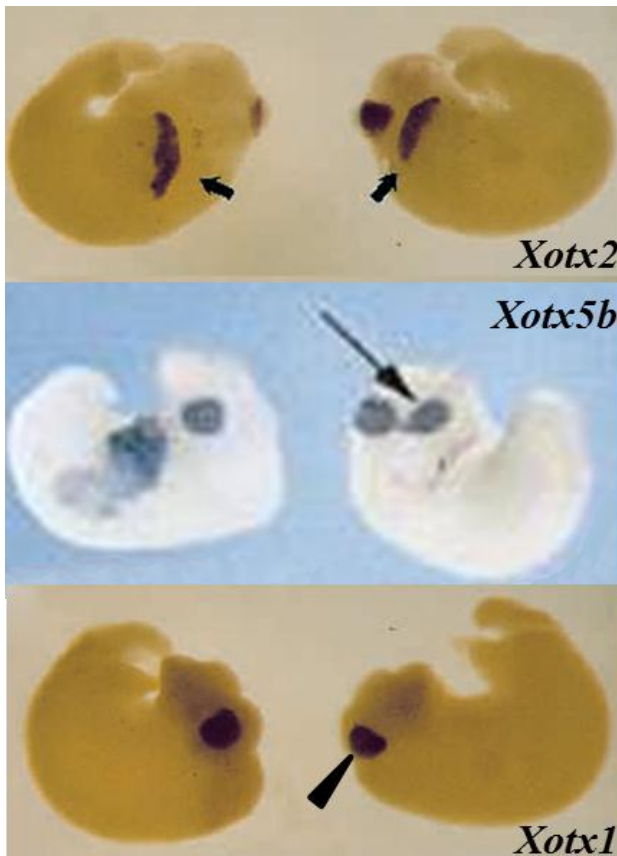


Fig. 15. *Xenopus laevis* embryos injected with *Xotx2*, *Xotx1* and *Xotx5b* (*Xotx5*) mRNA. *Xotx1*, *Xotx2* and *Xotx5b* (*Xotx5*) mRNA microinjection all lead to embryos with typical posterior defects, but only *Xotx2* and *Xotx5b* (*Xotx5*) can induce ectopic cement gland formation. Black bold and thin arrow: ectopic cement gland; black arrowhead: cement gland. (Figures adapted from Andreazzoli et al., 1997; Vignali et al., 2000).

Xotx2 microinjection significantly increases *gooseoid* expression, suggesting that the regulation of *gooseoid* expression is among the functions of *Xotx2* regulatory action during early development, and *gooseoid* has been suggested to play a role in executing Spemann's organizer phenomenon (Cho et al., 1991), thus suggesting a crucial role for *Xotx2* in mediating dorsal blastopore lip activities (Pannese et al., 1995).

It has been shown that *Xotx2* prevents cells that express it from participating in the convergent extension movements that shape the posterior part of the body. *Xotx2* exerts this function by directly activating *XclpH3*, *Xenopus*

homologue of Mammalian calponin; the product of this gene binds both actin and myosin filaments preventing the generation of contractile force and thereby the generation of movements (Morgan et al., 1999).

Phenotypes shown by *Xotx1* injected embryos strongly resemble those obtained after *Xotx2* microinjection (Fig. 15) and analyses performed on exogastrulae have clearly shown that *Xotx1*, as well as *Xotx2*, inhibits convergent extension movements essential for trunk and tail formation (Andreazzoli et al., 1997). It has been hypothesized that *Xotx1* might inhibit convergent extension movements acting on cell adhesion molecules, and that this activity could be either direct or mediated by *Otx1* repression of other genes like *Xbra*, *Pintavillas* and *Xnot*, that are expressed in trunk and tail cells that undergo mediolateral intercalation movements (Andreazzoli et al., 1997). A major difference between *Xotx1* and *Xotx2* overexpression phenotypes is the presence of ectopic cement glands that is never detected in *Xotx1* injected embryos (Andreazzoli et al., 1997). Moreover, *einsteck* experiments performed on injected embryos have shown that *Xotx2* is able to convert a tail organizer into a head organizer, while *Xotx1* seems able only to inhibit the tail-organizing activity of the late blastopore lip, leading to the development of non-posterior bulging structures (swollen vesicles not showing typical tail features), without turning a tail into a head organizer (Andreazzoli et al., 1997). A possible interpretation of these data is that *Xotx1* could be able only to inhibit convergent extension movements, and this should be sufficient only to repress tail-inducing activity. On the other hand, *Xotx2* may also be able to act as specific anteriorizing factor reconstituting a head organizing activity. This hypothesis is consistent with *Xotx2* capability to induce ectopic cement gland, differently from *Xotx1* (Andreazzoli et al., 1997).

Both *Xotx1* and *Xotx2* are activated by the injection of *siamois*, *noggin* and *Xwnt-8*, factors able to trigger head organizer induction, and are repressed by posteriorizing agent such as RA, suggesting, again, an involvement of both in anteriorizing activity (Andreazzoli et al., 1997 and reference therein).

Xotx5 microinjected embryos fully resemble *Xotx2* over-expression phenotype (Fig. 15): failure of blastopore proper closure, posterior defects and ectopic cement glands formation (Vignali et al., 2000). Moreover, *Xotx5*, as well as *Xotx2*, is able to turn a tail organizer into a head organizer (Vignali et al., 2000). Ectopic neural tissue is also detected in injected embryos (Vignali et al., 2000). Further analyses have shown that the induction of ectopic neural tissue may not reflect a direct effect of *Xotx5* within the ectoderm, since in animal cap experiments *Xotx5* is weakly able, if at all, to trigger neural genes (*sox-2*, *nrp-1*) expression (Vignali et al., 2000); however, *Xotx5* may play a role in neural induction somehow sensitizing the anterior dorsal ectoderm towards a neural fate, possibly suppressing the ectodermal fate. On the other hand, *Xotx2* activates general neural and anterior neural markers in isolated ventral ectoderm (Gammill and Sive, 1997; 2001). These differences may be due to objective differences in proteins functions, or may be due to different experimental approaches or to different dosages used for the two transcripts (see Gammill and Sive, 2001). The induction of ectopic cement gland is instead the result of a direct action of *Xotx2*, and maybe of *Xotx5*, within the ectoderm (Vignali et al., 2000). In addition, *Xotx2* efficiently prevents the expression of posterior neural and ventral markers, suggesting that part of the mechanism through which it promotes anterior fate is to repress formation of non-anterior positions (Gammill and Sive, 2001). These data suggest that *Xotx2* and *Xotx5* may perform cooperative roles during early embryogenesis, while they show divergent expression patterns (see above) and different functions (see below) during later developmental stages (Vignali et al., 2000).

Relative size of body regions allocated in early embryogenesis for the development of head and trunk structures are altered in *Xotx* microinjected embryos. Regions specified for presumptive head structures are slightly expanded at the expense of those giving rise to trunk and tail structures. At the same time, reduced trunk and tail structures result from the interference

with convergent extension movements taking place during gastrulation and neurulation and giving rise to more posterior regions (Pannese et al., 1995).

1.7- *Xotx* genes in the developing retina: bipolar versus photoreceptor fate

Vertebrate retina is a highly specialized sensorial tissue whose correct functions depend on the development of its complex cytoarchitecture. This tissue is made up of six different neuronal cell types: bipolar, horizontal, amacrine and ganglion cells and two types of photoreceptors (cones and rods). Besides, a single type of glia cells (Müller glia cells) is present. All these cell types arise from the same retinal multipotent neuroblast cell population and the specification of different neuronal cell types follows a precise temporary and spatially order. The competence model proposes that progenitor cells pass through a series of competence states, during each of which the progenitors are competent to produce a subset of retinal cell types (Livesey and Cepko, 2001). Competence states seem to be intrinsically defined and thus cell fate choices are intrinsically regulated through the definition of progenitor competence. Within a given competence state, the generation of a particular type of cell is regulated by positive and negative extrinsic signals (Livesey and Cepko, 2001). It has been demonstrated that bHLH factors are essential in promoting retinal neurogenesis, but additional factors, like homeodomain containing transcription factors are also crucial in specifying the different cell types (Hatakeyma and Kageyama, 2004 and references therein).

In *Xenopus laevis*, it has been demonstrated that *Xotx2* and *Xotx5* are responsible for bipolar and photoreceptor differentiation respectively (Vicizian et al., 2003). Coherently with their expression pattern in the eye (see above), lipofections of multipotent retinal progenitors cells with constitutively expressed *Xotx2* and *Xotx5* cDNA, lacking 3' UTR regulating elements,

showed dramatically different effects: *Xotx2* drives them to a bipolar fate, while *Xotx5* promotes a photoreceptor fate (Fig. 16) (Viczian et al., 2003; Wang et al., 2005; Decembrini et al., 2006).

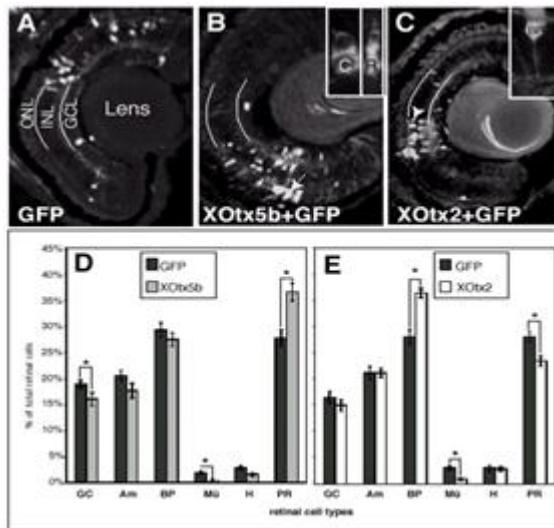


Fig.16. Overexpression of *Xotx5b* (*Xotx5*) or *Xotx2* in developing *Xenopus laevis* retinoblast. (A) Colipofection of GFP and pCS2 vector in the *Xenopus* retinae. A diversity of retinal cell types express the fluorescent marker. (B) Retinae co-lipofected with *Xotx5b* (*Xotx5*) and GFP show an increase in lipofected photoreceptor cells. (C) Retinae co-lipofected with *Xotx2* and GFP vector show an increase in the number of lipofected bipolar cells. (D,E) The graphs show an average of the percentages obtained (Figure and caption adapted from Viczian et al., 2003).

Xotx2 suppresses *Xotx5* photoreceptor inducing action, and the co-lipofection of *Xotx2* with *Xotx5* overrides the latter's ability to promote photoreceptor fate and the combination drives cells towards bipolar fates (Viczian et al., 2003). A small divergent region confers to the two homeoprotein their differential activities in *Xenopus* developing retina. This region has been called retinal specificity box (RS box) and spans amino acid residues 100-109 of XOTX2 and 100-107 of XOTX5 (Fig. 17). The RS box lies directly carboxyterminal to the homeodomain, and the two proteins differ for 6 amino acid residues at this level (Onorati et al., 2007). Swap domain experiments have shown that the RS box is necessary and sufficient to confer to the two transcription factors their specific retinal actions (Onorati et al., 2007). Significantly, deletion of the RS box completely abrogates any cell fate activity of both *Xotx*, while the insertion of the RS box into *Drosophila otd*, which has no cell fate activity in the frog retina, endows it with the retinal activity of either *Xotx2* or *Xotx5*, suggesting that in the absence of the RS

box OTD fails to properly target the gene sets normally activated by either XOTX2 or XOTX5. Moreover the greater ability of XOTX5, compared to XOTX2, to synergize with *Xenopus* NRL to activate the rhodopsin promoter is also switched depending on this box. OTD protein is also able to interact with NRL, demonstrating that the RSbox is not essential for this interaction, but it may modulate this contact in a way that is consistent with the roles of XOTX2 and XOTX5 in frog retinogenesis (Onorati et al., 2007). These data provide strong evidence on how closely related homeodomain factors differentiate their functions to regulate distinct cell fates. To explain RS box capability to modulate XOTX2 and XOTX5 retinal actions two not mutually exclusive possibilities have been proposed: the box refines the DNA binding ability of XOTX proteins towards different sets of promoters, or it modulates interactions with different specific molecular partners of either XOTX protein.

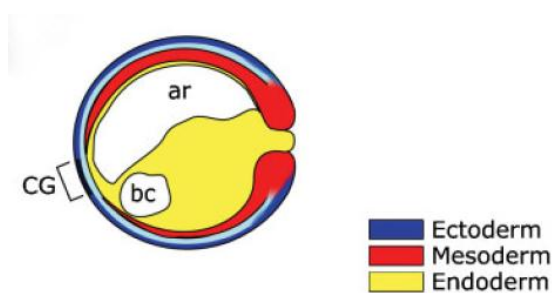


Fig. 17. XOTX2/5b and XOTX5 RS box. On the left are schematics of the two XOTX; on the right are their sequences in the region directly downstream of the homeodomain (HD), with different colors shading the XOTX2 (red) and XOTX5b (XOTX5) (yellow) sequences. Lines are introduced for sequence alignment. The divergent region responsible for the different retinal activities of XOTX2 and XOTX5b (XOTX5) (RS box) is shown in the blue frame. (Figure adapted from Onorati et al., 2007)

1.8- *Xotx* genes and cement gland induction

Cement gland (CG) (or adhesive organ) is a mucus-secreting organ, localized at the extreme anterior of the *Xenopus* embryo where embryonic ectoderm and endoderm contact each other, without mesoderm interposition (Fig. 18); this region corresponds to the chin primordium of Mammals. In all Deuterostomes this region will give rise to the stomodeum (primitive mouth). The adhesive organ secretes a waterproof glue that attaches the newly hatched embryo to a solid support, in a phase when it can swim only poorly

and cannot feed autonomously. It is innervated by the mandibular branch of the trigeminal nerve, whose neurites make the cement gland work as a sensory device that mediates the “stopping response”, to keep the embryo from moving after it is safely attached by glue (Boothby and Roberts, 1992 a, b; Davies et al., 1982; Roberts and Blight, 1975). This mechanism saves energy and makes embryos less obvious to predators.



(light blue), mesoderm (red) and endoderm (yellow) are indicated. (Figure and caption adapted from Wardle and Sive, 2003).

Fig. 18. The *Xenopus* cement gland forming region. The *Xenopus* cement gland (CG; shaded area) forms from the outer layer of ectoderm that overlies the endoderm, in the mesoderm-free area at the anterior of the embryo. This region lies between the dorsal neural plate and ventral epidermis. Outer ectodermal layer (dark blue), inner ectodermal layer

CG arises from the outer or epithelial layer of the ectoderm (Drysdale and Elinson, 1992; Nieuwkoop and Faber, 1967); this layer also gives rise to epidermis, hatching gland, certain neurons and to the ependymal lining of the neural tube.

CG primordium becomes morphologically visible at the onset of neurulation, when a patch of cells, lying anterior to the neural folds, becomes more darkly pigmented than the surrounding tissue. As the neural tube closes, this organ is differentiated and begins secreting mucus before the embryo hatches. Completely differentiated adhesive organ consists in a pseudostratified columnar epithelium, made up by very polarized cells containing mucus and maternal pigment granules (Sive and Bradley, 1996 and reference therein); these cells form a cone shape structure with an oval apex. During successive phases of *Xenopus* development, CG cells decrease in height and become vacuolated to disappear about at stage 45 (Van Evercooren and Picard, 1978). CG degeneration is coordinated with the opening of the mouth and initiation of feeding.

Several genes specifically or preferentially expressed in the *Xenopus* adhesive organ have been isolated: *Xcg* is expressed exclusively in the CG, it is the only known gene to be so restricted and it encodes a mucine like protein (Rones and Sive, unpublished data); *Xag* is expressed at very high levels in the CG and, at lower levels, in the hatching gland, it encodes a novel secreted protein later expressed in the pharynx (Jamrich and Sato, 1989) and in the lung primordium (Bradley and Sive, unpublished data); *Xa* also encodes a novel secreted protein, its expression shows that the CG itself has an antero-posterior pattern, with *Xa* RNA restricted to the posterior cells (Hemmati-Brivanlou et al., 1990), and the *distalless* homeobox genes *Xddl3* and *Xddl4* expressed only in anterior cells (Papalopulu and Kintner, 1993). Trigeminal neurites selectively innervate only the anterior portion of the cement gland (Roberts and Blight, 1975), so that genes expressed asymmetrically may be involved in axonal positioning.

CG is positioned by the overlap of three domains: antero-dorsal domain (AD), ventro-lateral domain (VL) and outer layer ectodermal domain (EO); so that the adhesive organ is defined by the overlap of these three domains: $AD+VL+EO=CG$ (Fig. 19).

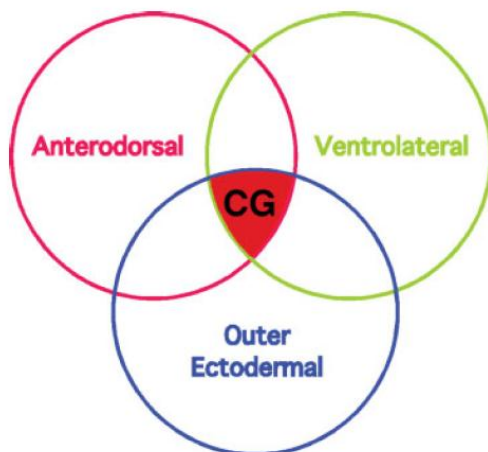


Fig. 19. Overlapping domains position the *Xenopus* cement gland (CG). A Venn diagram shows that three different domains overlap to position the cement gland. Cement gland forms where anterodorsal (AD), ventrolateral (VL) and outer ectodermal (EO) domains overlap; epidermis forms from ectoderm in the VL domain that does not overlap with the AD domain, and anterior neural plate develops from the AD domain that does not overlap with the VL domain. (Figure and caption adapted from Wardle and Sive, 2003)

The AD domain is made up of ectoderm that will form forebrain and CG, of the underlying mesoderm (precordial plate) and of head endoderm (Wardle

and Sive, 2003). Anterodorsal mesoderm and endoderm induce overlying and adjacent ectoderm to assume anterior fate through secreted factors (BMP and *Wnt* antagonists) (Sive and Bradley, 1996; Gamse and Sive, 2000). By mid-gastrula the AD domain is mirrored by *Xotx2* expression domain, which includes anterior neural and CG ectoderm, as well as the mesoderm and endoderm that induce them (Pannese et al., 1995; Blitz and Cho, 1995). *Xotx2* is necessary and sufficient for CG development, since a dominant negative *Otx2* construct prevents CG formation (Gammil and Sive, 2000; Isaacs et al., 1999), conversely *Otx2* misexpression leads to ectopic CG formation (Pannese et al., 1995; Blitz and Cho, 1995; Gammil and Sive, 1997). *Xotx5* is also expressed in the CG anlage and can activate CG fate when misexpressed, suggesting it is also involved in CG determination (Vignali et al., 2000). The ability of *Xotx2* to activate CG fate is limited both temporally and spatially. Firstly, *Xotx2* can activate downstream CG differentiation genes only after mid-gastrula. Secondly, the broad expression of *Xotx2* and its ability to activate both CG and neural cell fates indicates that its CG inducing activity is limited by other factors.

Ventro-lateral domain expresses several characteristic genes such as *bmp4* and *vent2* (Fainsod et al., 1994; Schmidt et al., 1996; Lahder et al., 1996; Onichtchouk et al., 1996). Gradient of BMP signaling in the ectoderm specifies different cell fates (Weinstein and Hemmati-Brivanlou 1999, and reference therein): high levels of BMP signaling lead to epidermal cell fate; intermediate levels activate CG development, as well as other “border” fates, such as neural crest; where there is little or no BMP signaling present neural tissue is formed (Hawley et al., 1995; Sasai et al., 1995; Suzuki et al., 1994; Xu et al., 1995; Wilson et al., 1997; Marchant et al., 1998). Adequate BMP4 levels cooperate with XOTX2 to activate CG formation (Gammil and Sive, 2000).

The embryonic ectoderm is composed of two layers: outer (epithelial layer) and inner (sensorial layer); the CG derives from the outer layer. *Xotx2* and *bmp4* expression is present in both ectodermal layers and other factors

restrict their CG inducing activity to the EO (Wardle and Sive, 2003). The bHLH factor *ESR6e* is expressed in the outer layer (Deblandre et al., 1999; Chalmers et al., 2002) and can alter the fate of ectodermal layers; besides, it normally inhibits primary neuronal differentiation (Chalmers et al., 2002), so that it can select CG fate over neural fate (Wardle and Sive, 2003).

Cement gland induction is a direct effect of *Xotx2* and not a secondary consequence of other tissues induced by *Xotx2* (Gammill and Sive, 1997); moreover, the CG marker *Xcg* is a direct target of *Xotx2* (Gammill and Sive, 1997), while *Xag* is indirectly activated maybe *via* a CRE binding factor acting downstream of *Xotx2*; another factor acting through an Ets-binding site, but not activated by *Xotx2*, cooperates to *Xag* activation (Wardle et al., 2002; Wardle and Sive, 2003); it is not clear if *Xotx2* is also able to self-activate.

2- Aim

In this study we have focused on three members of the *Otx* class in the frog *Xenopus laevis*: *Xotx1*, *Xotx2* and *Xotx5*. As described by Boncinelli et al. (1993), *Otx* genes are Vertebrates homologues of *Drosophila melanogaster orthodenticle* gene (*otd*). As *otd* in the fly, *Otx* genes in Vertebrates are essential for anterior development, and they are involved in central nervous system and sensory organs formation. The three homeoproteins described in the frog exploit both common and specific actions during development: during retinal histogenesis, *Xotx2* drives progenitor cells to a bipolar fate, while *Xotx5*, guides retinal precursors towards a photoreceptor fate (Vicizian et al., 2003); *Xotx2* and *Xotx5* play a similar role in cement gland formation, while *Xotx1* is unable to promote the formation of this structure (Blitz et al., 1995; Pannese et al., 1995; Andreazzoli et al., 1997; Vignali et al., 2000); all three transcription factors seem to be involved in head organizer activity and regulation of gastrulation movements (Andreazzoli et al., 1997; Vignali et al., 2000). These three transcription factors show a high level of homology, but they also contain divergent amino acid stretches. It has been demonstrated that *Xotx2* and *Xotx5* differential action during retinogenesis is due to their highly divergent retinal specificity boxes (RS box) (Onorati et al., 2007). We have hypothesized that the RS boxes could confer to the two transcription factors the capability to differentially interact with diverse cofactors, and, in the aim of identifying XOTX2 and XOTX5 specific interactors we decided to perform two parallel two-hybrid screens using XOTX2 and XOTX5 as baits. This part of the project was performed in collaboration with Dr. Alvaro Galli (CNR, IFC, Pisa). From the screens only common interactors have emerged; however, since a role *in vivo* for these factors is anyway possible, we structurally and functionally characterize the most interesting of these XOTX potential partners. Moreover, we have performed a molecular dissection of the different capability of XOTX2 and XOTX5 in respect to XOTX1 to promote cement gland development, to check the possibility that it could be due to primary amino acid sequence differences. Our aim has been to

functionally characterize the XOTX domains that could be responsible for XOTX differential action in adhesive organ formation. Thus, our general aim has been to try to shed light onto the molecular bases of XOTX actions during *Xenopus laevis* development.

3- Materials and methods

3.1- DNA constructs section I

The main constructs used in section I of this thesis are shown in Fig. 20, and described below.

The *Xotx5* sequence used in the present work was previously described as *Xotx5b*. (Vignali et al., 2000).

pCS2*Xotx5* wild-type construct was previously described in Viczian et al. (2003).

pCS2*Xotx1* wild-type construct was generated as follow: the *Xotx1* 5'UTR (88 nt) +coding region was amplified from *Xenopus laevis* embryos cDNA by using specific primers, both including an EcoRI restriction site at the 5'end; the PCR product was digested with EcoRI and inserted into EcoRI site of pCS2 plasmid vector.

pCS2*Xotx1N5C* and pCS2*Xotx5N1C* swap domain constructs were generated as follows: a KpnI site was inserted in pCS2*Xotx5* wild-type construct by site directed mutagenesis, and similarly a KpnI site was inserted in pCS2*Xotx1* wild-type construct. By using an existing KpnI site in pCS2 plasmid sequence, two fragments were obtained from both pCS2*Xotx1* and pCS2*Xotx5* KpnI mutagenized plasmids by KpnI digestion: pCS2*Xotx1N*-fragment/pCS2*Xotx1C*-fragment and pCS2*Xotx5N*-fragment/pCS2*Xotx5C*-fragment, respectively. Fragments were recombined by *in vitro* DNA ligation, using T4 ligase enzyme (Fermentas), to obtain the swap domain constructs.

pCS2*Xotx1ΔSer* deletion construct corresponds to pCS2*Xotx1* wild-type construct, except for the deletion of the Serine rich region spanning amino acids 139-173. Serine rich region deletion was obtained by PstI digestion, performed after insertion of two PstI restriction sites at Serine rich region borders by site directed mutagenesis. Subsequent DNA re-circularization, using T4 ligase enzyme, allowed to obtain pCS2*Xotx1ΔSer* deletion construct.

pCS2*Xotx1* Δ *His* deletion construct corresponds to pCS2*Xotx1* wild-type construct, except for the deletion of the Histidine rich region spanning amino acids 248-288. The deletion of the Histidine rich region was obtained by NcoI digestion, performed after insertion of two NcoI restriction sites at Histidine rich region borders by site directed mutagenesis. Subsequent DNA re-circularization, using T4 ligase enzyme, allowed to obtain pCS2*Xotx1* Δ *His* deletion construct.

pCS2*Xotx1* Δ *His* Δ *Ser* carries both the Histidine and Serine rich region deletions described above; it was obtained by removal of Serine rich region from pCS2*Xotx1* Δ *His*, as for the generation of pCS2*Xotx1* Δ *Ser* from pCS2*Xotx1* wild-type construct.

pCS2*Xotx5* Δ *RSbox* correspond to pCS2*Xotx5* wild-type construct, except that the region corresponding to *Xotx5* retinal specificity box (spanning amino acid 100-107) was removed by site directed mutagenesis; it was described in Onorati et al. (2007).

pCS2*Xotx5*-177 Δ C, pCS2*Xotx5*-210 Δ C and pCS2*Xotx5*-255 Δ C are deleted constructs lacking different XOTX5 carboxy-terminus portions; they were obtained by the insertion of a stop codon in position 177, 210 and 255, respectively, using site directed mutagenesis.

pCS2*Xotx5*-255 Δ C-*His-rich* correspond to pCS2*Xotx5*-255 Δ C followed by *Xotx1* Histidine rich region coding sequence (cs). *Xotx1* Histidine rich region cs was amplified from pCS2*Xotx1* wild-type construct using specific primers carrying BcuI restriction site. PCR product was digested with BcuI restriction enzyme and inserted into a BcuI site generated in pCS2*Xotx5* wild-type construct by site directed mutagenesis, downstream of aa position 254. This allowed in frame fusion of the Histidine rich region. A stop codon was provided at the end of the Histidine rich box.

All constructs were verified by sequencing.

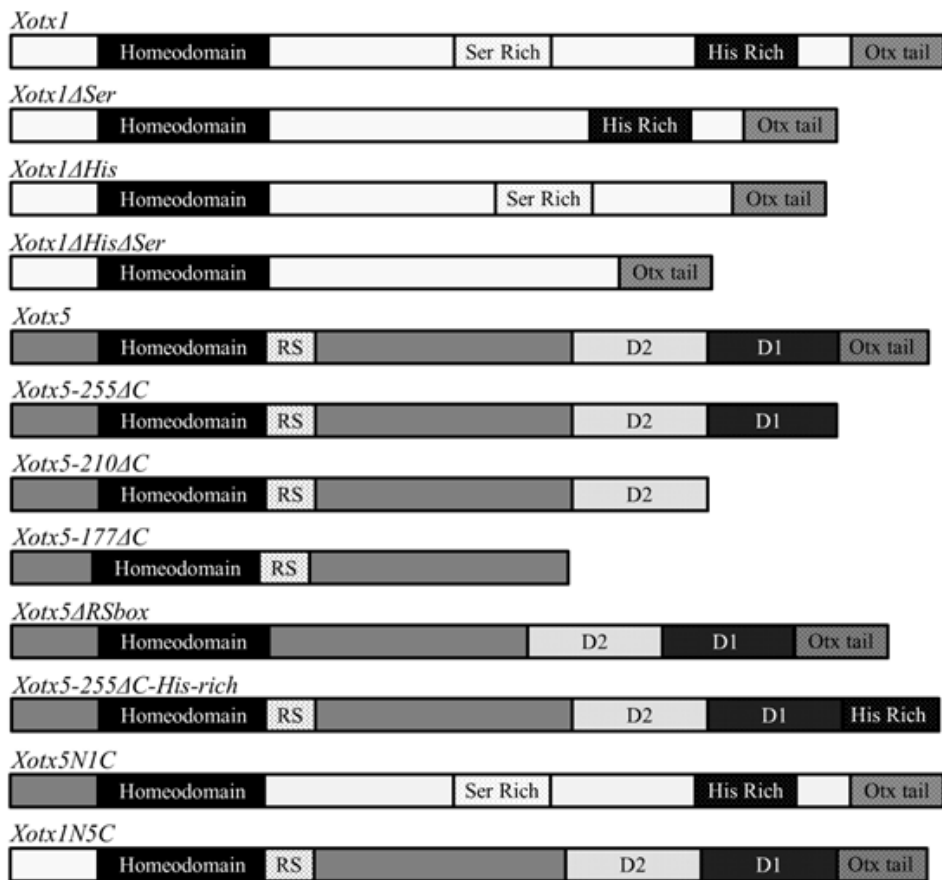


Fig. 20. Schematics of constructs used in section I. Each bar represents a schematic of the construct reported above. Light grey: *Xotx1* constructs, dark grey: *Xotx5* constructs. RS: retinal specificity box; Ser Rich: Serine rich region; His Rich: Histidine rich region. D1: cement gland inducing box domain 1; D2: cement gland inducing box domain 2.

3.2- DNA constructs section II

The main constructs used in section II of this thesis are described below.

For two-hybrid screen specific plasmids pGBDU/pBDGal4Cam/pVp16 were used.

Different portions of *Xotx2/Xotx5* coding regions have been previously cloned in pGBDU and pBDGal4Cam plasmids (Fig. 21):

- pBDGal4Cam*Xotx2*TH1: full length coding region (288 aa)

- pBDGal4Cam*Xotx2*TH2: short N-terminus+homeodomain+RSbox (from aa 25 to aa 98)
 - pBDGal4Cam*Xotx2*TH3: N-terminus+homeodomain+RSbox (from aa 1 to aa 98)
 - pBDGal4Cam*Xotx2*TH4: N-terminus+homeodomain+RSbox+C-terminus portion (from aa 1 to aa 174)
 - pBDGal4Cam*Xotx2*TH5: N-terminus+homeodomain+RSbox+C-terminus portion (from aa 1 to aa 238)
 - pBDGal4Cam*Xotx2*TH6: RSbox+C-terminus portion (from aa 102 to aa 174)
 - pBDGal4Cam*Xotx2*TH7: RSbox+C-terminus (from aa 102 to aa 288)
- pBDGal4Cam*Xotx2*TH8 was generated by the insertion of a stop codon, by site direct mutagenesis, in pBDGal4Cam*Xotx2*TH4 plasmid in correspondence of residue 25.

- pGBDU*Xotx5*TH1: full length coding region (290 aa)
- pGBDU*Xotx5*TH2: short N-terminus+homeodomain+RSbox (from aa 25 to aa 107)
- pGBDU*Xotx5*TH3: N-terminus+homeodomain+RSbox (from aa 1 to aa 107)
- pGBDU*Xotx5*TH4: N-terminus+homeodomain+RSbox+C-terminus portion (from aa 1 to aa 174)
- pGBDU*Xotx5*TH5: N-terminus+homeodomain+RSbox+C-terminus portion (from aa 1 to aa 240)
- pGBDU*Xotx5*TH6: RSbox+C-terminus portion (from aa 99 to aa 174)
- pGBDU*Xotx5*TH7: RSbox+C-terminus (from aa 99 to aa 288)

pGBDU*Xotx5*TH8 was generated by the insertion of a stop codon, by site direct mutagenesis, in pGBDU*Xotx5*TH4 plasmid in correspondence of residue 25.

pBDGal4Cam*Xotx1*TH4 was generated by subcloning *Xotx1* region spanning from 1 to 206 residues, in pBDGalCam EcoRI site. *Xotx1*TH4 fragment was amplified from pCS2*Xotx*FL plasmid using specific primers

both including an EcoRI restriction site at the 5' end, PCR product was digested with EcoRI and inserted into EcoRI site of pBDGal4Cam plasmid vector:

- pBDGal4Cam*Xotx1*TH4: N-terminus+homeodomain+C-terminus portion (from aa 1 to aa 204).

pVp16*Xusf1*TH, pVp16*Xusf2*TH, pVp16*Xgrn1*TH, pVp16*Xgrn2*TH and pVp16*c29*TH plasmids have been isolated from pVp16 *Xenopus laevis* oocyte cDNA library by yeast to hybrid screen. All library fragments were cloned in pVp16 NotI site.

pBSc29TH plasmid has been obtained subcloning *c29* two hybrid isolated fragment (*c29*TH), from pVp16*c29*TH plasmid into NotI site of pBS plasmid.

pBS*Xusf1*/pBS*Xusf2* plasmids were obtained amplifying *Xusf1* and *Xusf2* 5'UTR+partial coding region (CR) from *Xenopus* tailbud cDNA using specific primers all including an EcoRI restriction site at the 5' end, PCR products were digested with EcoRI and inserted into EcoRI site of pBS plasmid vector.

pBS*Xgrn1*/pBS*Xgrn2* plasmids were obtained amplifying *Xgrn1* and *Xgrn2* CR from *Xenopus* tailbud cDNA using specific primers all including an EcoRI restriction site at the 5' end, PCR products were digested with EcoRI and inserted into EcoRI site of pBS plasmid vector.

pCS2*Xusf2* and pCS2*c29* plasmids were obtained amplifying *Xusf2* and *c29* CR from *Xenopus* tailbud cDNA using specific primers all including an EcoRI restriction site at the 5' end, and cloning PCR products into EcoRI site of pCS2 plasmid vector. The *c29* hypothetical coding region was deduced by *c29* cDNA sequence, basing on the first "ATG" codon found.

pYexGST-*Xusf2* and pYexGST-*c29* plasmids were obtained subcloning *Xusf2* and *c29* CR from pCS2*Xusf2* and pCS2*c29* plasmids, inserts have been excised by EcoRI digestion and inserted into EcoRI site of pYex plasmid vector. pYexGST-*nrl* plasmid has been described in Onorati et al. (2007).

pCS2*Xotx2*-myc, pCS2*Xotx5*-myc, pCS2*nrl*-myc and pCS2*XopGFP* plasmids have been described in Onorati et al. (2007).

pCS2*c29CR*-myc plasmid was obtained subcloning *c29* CR from pYex plasmid into EcoRI site of pCS2-myc plasmid.

pCS2*c29NLSstop*-myc plasmid was obtained by the insertion of a stop codon upstream to *c29* hypothetical nuclear localization signal (NLS), corresponding to residue 77, using site directed mutagenesis.

pCS2*RFP* plasmid was obtained subcloning *RFP* coding region from CAG plasmid (kind gift of Dr A. Cellerino), using specific primers both including an EcoRI restriction site at the 5' end, PCR products were digested with EcoRI and inserted into EcoRI site of pCS2 plasmid vector.

pCS2*RFP-c29NLS* plasmid was obtained cloning *C29* hypothetical NLS downstream to *RFP* CR in pCS2*RFP* plasmid.

pCS2*Moc29GFP* sensor plasmid was obtained cloning *c29* oligo antisense morpholino target sequence upstream to *GFP* CR in pCS2*GFP* plasmid.

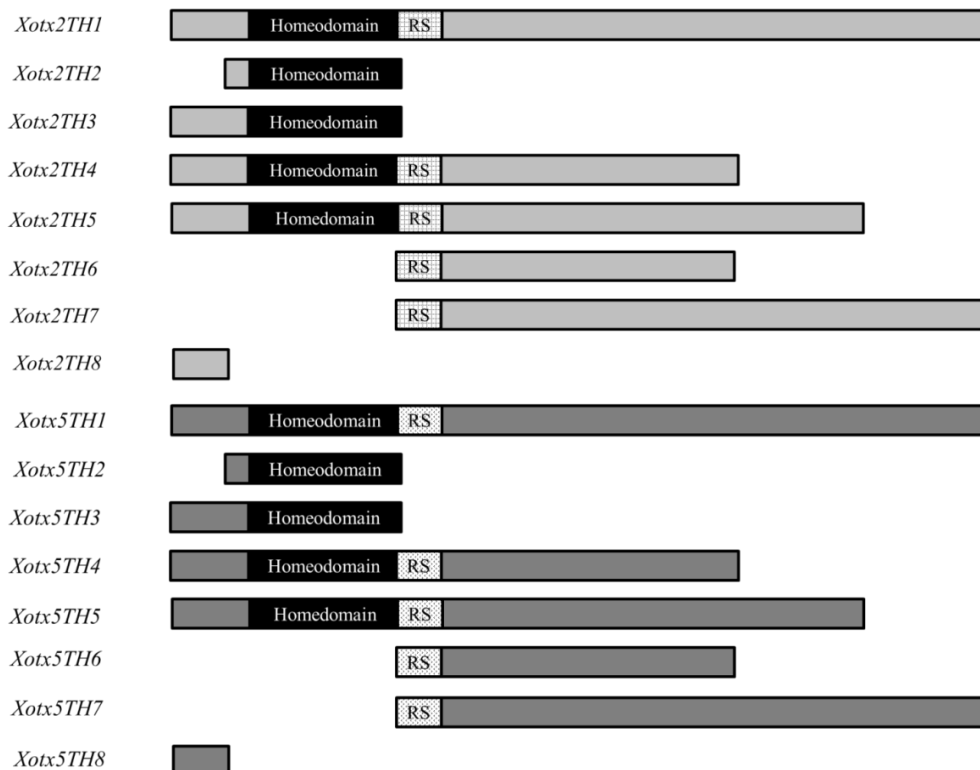


Fig. 21. Schematics of constructs used in section II. Each bar represents a schematic of the constructs reported above. Light grey: *Xotx2* constructs, dark grey: *Xotx5* constructs. RS: retinal specificity box.

3.3- *Xenopus laevis* embryos

Eggs were obtained from *Xenopus laevis* females injected with 800 IU of human gonadotropin; embryos were generated and grown as previously described by Newport and Kirschner (1982) and staged according to Nieuwkoop and Faber (1967).

3.4- *In situ* hybridization

Embryos were processed for whole-mount *in situ* hybridization as described by Harland (1991); for animal cap *in situ* hybridization, Proteinase K was not used. Embryos and caps were bleached after chromogenic reaction as described by Mayor et al. (1995). Probes were generated by *in vitro* transcription of template plasmids, to generate antisense RNAs labeled with digoxigenin; in these reactions, plasmids were linearized with suited restriction enzymes and SP6, T7 or T3 polymerase was used for the synthesis of RNA, depending on the template. We used *Xag* probe (Bradley et al., 1996) for cement gland detection by *in situ* hybridization, and *nrp-1* probe (Knecht et al., 1995) for neural tissue detection. Besides, we use specific probes for expression profiling of the different XOTX candidate interactors, generated from pBS constructs.

3.5- RNAs methods, embryo microinjections and animal cap assays

Capped RNAs were *in vitro* transcribed by SP6 RNA polymerase from linearized pCS2 constructs described above using the mMessage mMachine Kit (Ambion). Embryos were bilaterally (section I experiments) or unilaterally

(section II experiments) injected in the animal region of dorsal or ventral blastomeres of 4-cell stage embryos in 0.1xMMR, 4% Ficoll. Embryos were grown overnight at 14°C and then transferred in 0.1xMMR and cultured at 14°C until tailbud (section I and section II experiments) or later stages (section II experiments). For animal cap assays RNAs were injected in the animal pole region of 1-cell stage embryos. Animal caps were dissected out of stage 9 embryos in 1xMBS, let heal and then cultured in 1xMBS until sibling embryos reached tailbud stage.

3.6- Oligo antisense Morpholino

Loss-of-function experiments were performed using the following oligo antisense Morpholinos (Gene Tool):

Moc29: CACCAGCGTAGTCAGGTACACCCAC, targeting *c29* predicted 5' UTR; 20-40 ng of Moc29 have been injected unilaterally/bilaterally in animal-dorsal blastomeres of 4-cell stage embryos in 0,1X MMR 4% Ficoll.

MoUSF2: CGTCTCAGGCGTTACAGGCCAG, targeting *Xusf2* 5' UTR; 5-10 ng of MoUSF2 have been injected unilaterally in animal dorsal/ventral blastomere of 4-cell stage embryos in 0,1X MMR 4% Ficoll.

MisMoUSF2: CcTCTgAGGCGaTACAGcCCgAG; lowercase letters indicate mis-matched bases; 5-10 ng of MisMoUSF2 have been injected unilaterally in animal dorsal/ventral blastomere of 4-cell stage embryos in 0,1X MMR 4% Ficoll.

Embryos were grown overnight at 14°C and the transferred in 0.1X MMR and cultured at 14°C until tadpole/tailbud stage. LacZ has been used as injection tracer.

3.7- RT-PCR

Total RNA was extracted from animal caps grown until tailbud stage after dissection from injected embryos or from whole wild type embryos at different developmental stages, using NucleoSpin RNAII kit (Macherey-Nagel) and *in vitro* reverse-transcribed using the GoScript Reverse Transcription System (Promega) and oligodT primers.

cDNAs reverse-transcribed from RNAs extracted from animal caps were amplified by PCR using: *Xag* and *Xcg* specific primers described by Gammil and Sive, 1997. All primers were used at 24 cycles with a 55°C annealing temperature.

cDNAs reverse-transcribed from RNAs extracted from whole embryos were amplified by PCR using: *c29* specific primers: Fw: 5'-ATGGAACTGAGCGCTGAACTGAG-3', Rev: 5'-TTTCTTTTAGTGGGAGGTCCACTACT-3' (30 cycles, annealing temperature 55°C); *Xusf1* specific primers: Fw: 5'-GGGAATTCGGGGAAGTACTGGACTGGATAGGTTGG-3', Rev 5'-GGGAATTCGCGGGGCCGTGGATCC-3' (35 cycles, annealing temperature 60°C); *Xusf2* specific primers: Fw: 5'-GGGAATTCTTCCGGGTCGCCCCGGGC-3', Rev 5'-GGGAATTCTCCTGCTTGTCCCAGTGTGGGGTCGG-3' (22 cycles, annealing temperature 66°C); *Xgrn1* specific primers: Fw: 5'-GCACCCAGGGCCAGTGCTTG-3', Rev 5'-GGGGGGCAGCAGTGTTTCATGGTC-3' (25 cycles, annealing temperature 62°C); *Xgrn2* specific primers: Fw: 5'-CATCCCTTGCTCCTCAAAGTCCAGCTC-3', Rev 5'-GGGAATTCTCATAGGAGAGGAGAGAGATTTTCCGTC-3' (22 cycles, annealing temperature 63°C).

In both cases *odc* primers were used as internal control (Bouwmeester et al., 1996).

3.8- Two-hybrid screening

Two-hybrid assay has been used both to find XOTX potential interactors, among polypeptides encoded by a *Xenopus laevis* oocyte library, and to confirm hypothetical protein-protein interactions found. We have used the yeast strain AH 109 of *Saccaromyces cerevisiae*. Yeast cells were transformed with: pGBDU/pBDGal4Cam plasmids (baits), encoding XOTX TH fragments fused in frame with the DNA binding domain of the transcription factor GAL4, and pVp16 plasmids (preys), containing library fragments fused in frame with the activation domain of transcription factor VP16.

3.9- GST-pull down assay

GST-fusion proteins were expressed in *E.coli* BL21 cells. Culture were grown till mid-log phase ($A_{600}=0.7$) in LB medium at 37°C, induced with 1.0mM isopropyl thio- β -D-galactopiranoside, and grown for additional 4 hours at 30°C. Bacterial cells were collected by centrifugation, pellet was resuspended in ice cold PBS and lysed on ice by lysing mix: lysozyme 200 μ g/ml, DTT 10 mM (in AcONa 10 mM pH 5.2), protease inhibitor mix (2mM AEBSF, 1mM EDTA, 130 μ M bestain, 10 μ M E-64, 1 μ M leupeptin, 0.3 μ M aprotinin; final concentration (Sigma-Aldrich)), 1% (v/v) Triton X-100, 10mM MgCl₂ and 100 μ g/ml DNase. Proteins containing solution was recovered by centrifugation.

HEK 293T cells were cultured in Dulbecco's modified Eagle's medium (Gibco/Invitrogen) supplemented with 10% (v/v) fetal bovine serum (Gibco) and with Pen-Strep antibiotics mix (Sigma). Transfections were performed in Opti-MEM medium (Invitrogen). pCS2-myc-tagged constructs transfection were performed using PEI (Sigma-Aldrich), 39.75 μ g pCS2-myc-tagged plasmid+250ng PEGFP tracing plasmid were used for each transfection (92

mm diameter Petri dish). HEK cells were lysed in lysis buffer: in Hepes pH 7.5 50mM, NaCl 50mM, glycerol 1%, Triton-X100, MgCl₂ 1.5 mM, EGTA 5mM, PMSF 1mM, mammalian protease inhibitor cocktail (Sigma), NaVO₄ 1mM. Proteins containing solution was recovered by centrifugation.

Glutathione Sepharose 4B resin (100 ml) (Amersham, GE Healthcare) has been used for each experiment and control. Resin was first incubated with GST-fusion protein, then with myc-tagged proteins. Proteins elution from resin was obtained boiling resin with DYE loading buffer (detailed procedure is described in Onorati et al., 2007).

3.10- Western blotting

Proteins samples were loaded onto a 12% polyacrylamide gel for size separation. Subsequently, proteins were transferred to Immobilon-P Transfer membrane (Millipore) by electroblotting. Monoclonal primary anti-myc antibody (Sigma) and secondary anti mouse IgG peroxidase conjugate (Sigma), were used to detect myc-tagged proteins. To visualize immunoreactive bands was used Immobilon Western Chemiluminiscent HRP Substrate (Millipore), membranes were exposed to Amersham Hyperfilm.

3.11- XOP-GFP reporter assay

HEK 293T cells culture and transfections were performed as described above. Plasmids quantitative for each transfection have been the following: 4µg pCS2*XopGFP*+ 700ng pCS2*RFP* + 1µg pCS2*Xotx2*/pCS2*Xotx5* + 1µg pCS2*c29*/pCS2*Xusf2*. RFP and GFP fluorescence signals were analyzed using flow cytometry. RFP was used as transfection tracer.

3.12- Immunostaining on sections

Immunostaining on section have been performed as described in Viczian et al. (2003). To identify myc-tagged proteins we have used monoclonal primary anti-myc antibody (Sigma) and secondary anti mouse IgG rhodamine conjugate (Sigma), pCS2*memGFP* has been used as cell membrane marker. Nuclei were stained by Hoechst.

3.13- 5' RACE

5' RACE has been performed using the SMART RACE cDNA Amplification Kit (Clontech). RNA extracted from wild-type embryos at developmental stage 23 has been used as template. The specific primer 29Rev 5'-TTTCTTTTAGTGGGAGGTCCACTACTG-3' has been used. PCR fragments have been cloned in the *Stu*I site of pCS2 plasmid vector after "fill-in" reaction using Klenow Polymerase (Promega). Plasmids were analyzed by sequencing.

3.14- Bioinformatics tools

The following bioinformatics tools have been used.

- ClustalW: nucleotide/aminoacid multi-alignment analysis
(<http://www.ebi.ac.uk>)
- Nucleotide/protein BLAST: (<http://www.ncbi.nlm.nih.gov>)
(<http://www.ensembl.org>)
- PsiPred: protein secondary structure *in silico* prediction
(<http://www.bioinf.cs.ucl.ac.uk/psipred>)
- PSORT II: protein subcellular localization sites *in silico* prediction
from amino acid sequence (www.psort.org)

4- Results section I

4.1- Cement gland induction

Previous functional analyses have shown that *Xotx5* and *Xotx2* are both able to promote adhesive organ formation, while *Xotx1* is not (Pannese et al., 1995; Blitz and Cho, 1995; Bradley et al., 1996; Andreazzoli et al., 1997; Gammill and Sive 1997; Kuroda et al., 2000; Vignali et al., 2000). XOTX1, XOTX2 and XOTX5 alignment, performed using ClustalW software (<http://www.ebi.ac.uk/Tools/msa/clustalw2>), shows that the main differences in the primary sequence between these three homeoproteins are a serine (Ser)-rich region (aa 139-173) and a histidine (His)-rich region (aa 248-288), present in XOTX1 but absent in XOTX2 and XOTX5 (Fig. 22 and Fig. 23).

This suggested that the different action of *Xotx2* and *Xotx5* compared to *Xotx1* in CG promoting activity could be due to these differences. Because XOTX2 and XOTX5 are very similar (76% identity overall) and have, in this respect, identical effects in misexpression experiments, we focused our research on *Xotx1* and *Xotx5*. Since the main differences between them reside in the C-terminal part, we first swapped this region between XOTX1 and XOTX5, and used the two chimeric plasmids *Xotx1N5C* (encoding chimeric XOTX1/XOTX5) and *Xotx5N1C* (encoding chimeric XOTX5/XOTX1) in microinjection experiments (see Fig. 20 for schemes). We microinjected the corresponding mRNAs, as well as *Xotx1* and *Xotx5* mRNAs as controls, and checked for ectopic CG formation by whole mount *in situ* hybridization (WISH) using *Xag* as a cement gland marker. Injection of 800 pg *Xotx5* mRNA is able to produce ectopic CG formation in about the 80% of embryos; *Xotx5* retains this activity when injected at progressively lower doses (with correspondingly lower frequencies of ectopic CG) (Fig. 24 A and Tab. 1). On the contrary, injection of 800 pg *Xotx1* mRNA is not able to lead to ectopic adhesive organ development; we did not observe ectopic CG formation even if *Xotx1* mRNA was injected at a higher dose (1,2 ng)

(Fig. 24 A and Tab. 1). Interestingly, injection of 800 pg of *Xotx1N5C* mRNA is able to elicit ectopic CG formation in about 80% of ventral microinjections, thus reproducing *Xotx5* activity, and maintains this capability even at lower doses (Fig. 24 A and Tab. 1). On the contrary, the reciprocal construct, *Xotx5N1C*, is not able to promote ectopic adhesive organs formation, even when we raised the injected mRNA quantity (Fig. 24 A and Tab. 1). We concluded that the XOTX1 and XOTX5 differential ability to promote CG formation is due to their C-terminal part. By performing WISH experiments on injected caps, using *Xag* as a probe, and RT-PCR experiments on mRNA extracted from sibling caps, we fully confirm the observations obtained on whole embryos: the ability to turn on cement gland markers *Xag* and *Xcg* depends on the protein C-terminus (Fig. 24 C, Fig. 25 A and Tab. 2).

To define if the differential action was due to the Ser-rich region, to the His-rich region or both, we compared the activity of three different *Xotx1* constructs lacking either of these specific portions or both, in similar microinjection experiments. *Xotx1ΔSer* is not able to promote ectopic adhesive organ formation either if ventrally injected at 800 pg or at a higher dose (Fig. 24 A and Tab. 1); on the contrary, *Xotx1ΔHis* is able to promote cement glands in about 45% of embryos injected with 800 pg mRNA, and this effect persists even at lower injection doses (with a decrease in frequency of ectopic CGs) (Fig. 24 A and Tab. 1). *Xotx1ΔHisΔSer* injected embryos show ectopic *Xag* expression in more than 50% of injected embryos (Fig. 24 A and Tab. 1). We conclude that XOTX1 is not able to promote CG fate due to the His-rich amino acid stretch.

The data obtained on whole embryos were confirmed in animal cap assays. By WISH analysis, *Xotx1ΔHis* and *Xotx1ΔHisΔSer* injected caps showed high *Xag* expression levels (77,2% positive caps, $n=57$; 85,5%, $n=55$; respectively). *Xotx1ΔSer* injected caps also showed *Xag* expression, though to a lower extent: about 40% of caps ($n=59$) displayed labeling, and in most explants we found a dotted weak *Xag* signal (Fig. 24 C and Tab. 2). RT-PCR analysis performed on sibling injected caps fully confirmed these results:

Xotx1ΔHis and *Xotx1ΔHisΔSer* promote *Xag* expression (though at a lower level respect to full length *Xotx5* or *Xotx1N5C* constructs), while a weaker *Xag* expression is detectable in *Xotx1ΔSer* injected explants; similar results were obtained with another cement gland marker, *Xcg* (Fig. 25 A).

```

XOTX2  MMSYLKQPPYAVNGLSLTASGMDLLHQSVGYPATPRKORRERTTFTRAQLDILEALFAKT 60
XOTX5  MMSYIKQPHYAVNGLTLAGTGMDLLHSAVGYPTNPRKORRERTTFTRAQLDILESFAKT 60
XOTX1  MMSYLKQPPYGMNGLGLTGPMADLLHPSVGYPATPRKORRERTTFTRSQLDVLESFAKT 60
      ***:*** *: :*** *: :...***** :****:*****:***:***:***

                                HOMEODOMAIN                                RSbox
XOTX2  RYPDFMREEVALKINLPE SRVQVWFKNRRAKCRQQQQQQQ----NGGQNKVRFPSKKKTS 116
XOTX5  RYPDFMREEVALKINLPE SRVQVWFKNRRAKCRQQQQQQQ----STGQAKPRFPAKKKTS 114
XOTX1  RYPDFMREEVALKINLPE SRVQVWFKNRRAKCRQQQQQQQQSSSGAGVKS RPAKKKCS 120
      *****:*****:*****:*****:*****:*****:*****:*****:*****

XOTX2  PVREVSSSESGTSGQFSPSS--TSVPVISSTAP-----VSIWSP 154
XOTX5  PARETNSEASTNGQYSPPPP GTAVTPSSASAT-----VSIWSP 153
XOTX1  PARES--SGSESSGQFTPPA[VSSASASSSSSSSSSNSTGNPGLTSAPLNGSSSTA]SSIWSP 179
      *.* * : :*:***:*. :... **:::

XOTX2  ASVSP-----LSDPLSTSSS--CMQRS-----YPMTYTQASGYSQGYAG--STSYFGGM 199
XOTX5  ASISP-----IPDPLSAVTNFCMQRSTG-----YPMTYSQAPAYTQSYGG--SSSYFTGL 201
XOTX1  ASISPGTAPGSGPDPDLGTGSASC MQRSGSSSAASYPMSYSQAAGYTQAYPAPSSSYFSGV 239
      **:***      .***: : *****      ***:***:*. :*. * . * :*** *

XOTX2  DCGSYLSPMHQLSGFGATLSPMGTNAV-----SHLNQSP----VALSSQAYGASSLG 249
XOTX5  DCGSYLSPMHPQLSAPGATLSP IATPTMG-----SHLSQSP----ASLSAQGYGAASLG 251
XOTX1  DCSSYLGPML[SHHHP--HQLSPMAPSSMSGHHHHHHHLSQTSSHHHHHHHQ]GYTSSALP 297
      **.***.*** :      ***:.. : :      **:*..      *.* :***

                                Otx-tail
XOTX2  FNST[DCLDYKDQT--ASWKLNFNA--DCLDYKDQTSSWKFQVL] 288
XOTX5  FTSV[DCLDYKDQT--ASWKLNFNATDCLDYKDQ--SSWKFQVL] 290
XOTX1  FNSS[DCLDYKEQATASSWKLNFNSTDCLDYKDQ--ASWRFQVL] 338
      *. * *****:*. : *****: *****: *****: *****: *****

```

Fig. 22. Multi-alignment of XOTX1, XOTX2 and XOTX5. Sequences multi-alignment has been obtained using ClustaW. “*”: identical residues; “.”: conserved substitution; “.”: semi-conserved substitution. The homoedomain is marked by a shaded dark grey box. The OTX-tail is labelled by a shaded light grey box. XOTX2 and XOTX5 retinal specificity boxes (RS box) and XOTX1 Serine and Histidine rich regions are labelled by open boxes.

```

                                Homeodomain
XOTX5      MMSYIKQPHYAVNGLTLAGTGMDDLHSAVGYPTNPRKQRRERTTFFTRAQLDILESLFAKT 60
XOTX1      MMSYLKQPPYGMNGLGLTGPAMDLLHPSVGYPATPRKQRRERTTFFRSQLDVLESLFAKT 60
          ****:* ** *:* ** *:* ..*****.:*****.:*****:*****:*****

XOTX5      RYPDIFMREEVALKINLPESRVQVWFKNRRACKRQQQQQ-----STGQAKPRPAKKKTS 114
XOTX1      RYPDIFMREEVALKINLPESRVQVWFKNRRACKRQQQQQSSSSGAGVKSPPAKKKCS 120
          *****:*****:*****:*****:*****:*****:*****:*****:*****

XOTX5      PARETNSEASTNGQYSPPPPGLTAVTPSSSASAT-----VSIWSP 153
XOTX1      PARES-SGSESSGQFTPPAVSSSSSSSSSSSSNSTGNPGLTSAPLNGSSSTAS$SIWSP 179
          ****:* * ..:***:**. .:..:***:*:..:*****:..:*****:*****
                                Ser-rich

XOTX5      ASISP-----IPDPLSAVINPCMQRS-----TGYPMYTSQAPAYTQSYGG-SSSYFTGL 201
XOTX1      ASISPGTAPGSGPDPLGTGSASCMQRSGSSSAASYPMSYSQAAGYTQAYPAPSSSYFSGV 239
          *****:*****: : .*****: :*****:*****:*****: . *****:

XOTX5      DCGSYLSFMHPQLSAPGATLSPIAAPTMG-----SHLSQSPASLS----AQGYGAASLG 251
XOTX1      DCSSYLGFVHSHHHP--HQLSPMAPSSMSGHHHHHHHLSQTS$HHHHHHHHH$QGYTSSALP 297
          **.* **.* **.*: . *****:..:*. *****:..: *****:..: ** * : : *
                                His-rich

XOTX5      FTSVDCLDYKQQT--ASWKLNFNATDCLDYKQSSWKFQVLI 290
XOTX1      FNSSDCLDYKEQATASWKLNFNSTDCLDYKQASWRQVLI 338
          *.* *****:..: *****:*****:*****:*****:*****:*****
                                Otx-tail

```

Fig. 23. Multi-alignment of XOTX1 and XOTX5. Sequences multi-alignment has been obtained using ClustaW. "*" : identical residues; "." : conserved substitution; ":" : semi-conserved substitution. Homeodomain: empty box; *Otx*-tail: dashed box; XOTX1 serine rich region: dotted box; XOTX1 histidine rich region: shaded light green box; XOTX5 CGboxD2: shaded light blue box; XOTX5 CGboxD1: shaded dark blue box. Note that XOTX1 His-rich region is inserted in XOTX1 region corresponding to XOTX5 CGboxD1.

These results suggest that the His-rich region mainly, and the Ser-rich region to a lower extent, impair the potential ability of XOTX1 to promote CG formation. However, they do not identify within the C-terminal of XOTX5 the precise region(s) actively involved in this ability.

To localize this, we microinjected *Xenopus* embryos with three different XOTX5 deletion constructs and analyzed *Xag* expression by WISH. We found that *Xotx5-255ΔC* has the same efficiency of full length *Xotx5* in inducing CG formation: 80% of ventrally injected embryos showed *Xag* ectopic expression (Fig. 24 A and Tab. 1). On the other hand, *Xotx5-210ΔC*, though able to lead to *Xag* ectopic expression, is much less efficient compared to full length *Xotx5*: only 25% of embryos showed ectopic CGs. Finally *Xotx5-177ΔC* is not at all able to promote CG formation in whole embryos (Fig 24 A and Tab. 1).

WISH performed on animal caps injected with the same *Xotx5* deletion constructs fully confirm our data: *Xotx5-255ΔC* injected animal caps show a strong *Xag* expression in more than 90% explants ($n=23$), with an efficiency comparable with that of full length *Xotx5* (96% positive caps, $n=88$); *Xotx5-210ΔC* induces marker expression less efficiently (70% of *Xag* positive animal caps; $n=29$); finally, *Xotx5-177ΔC* does not promote any *Xag* transcription in any of injected animal caps ($n=35$) (Fig. 24 C and Tab. 2). RT-PCR analyses performed on sibling injected caps confirm our findings: the level of *Xag* expression in *Xotx5-255ΔC* injected caps is comparable to that of *Xotx5* injected explants; *Xotx5-210ΔC* induces a lower *Xag* expression; in *Xotx5-177ΔC* injected caps, *Xag* gene is very weakly turned on. As a further confirmation, the expression levels of *Xcg* almost completely resemble those of *Xag* (Fig. 25 B).

These data suggest that the C-terminal region corresponding to aa 177-255 of XOTX5 contains the crucial part actively responsible to promote CG and could therefore function as a CG specific region, that we named CGbox; this region is bipartite: aa 177-209 correspond to CGboxD2, the less effective CG promoting domain; aa 210-255 correspond to CGboxD1, the more effective CG promoting domain. In XOTX1 the sequence of this region is disrupted by the His stretch (Fig. 23); it is possible that this stretch simply impairs the ability of the CG specific region; besides, it is possible that the insertion of these His residues turns this region into a repressor of CG

promoting ability. To verify if XOTX1 His-rich region is able to inhibit XOTX5 CG inducing activity, we inserted it downstream of the shortest *Xotx5* construct (*Xotx5-255ΔC*) that is able to promote CG development with the same efficiency of full length *Xotx5*, and tested the activity of the resulting *Xotx5-255ΔC-His-rich* construct (see Fig. 20). The ventral microinjection of this mRNA at the 800 pg dose does not lead to the formation of any ectopic adhesive structure on embryos (Fig. 24 A and Tab. 1). In injected animal caps we found only a very weak *Xag* expression by WISH (Fig 24 C and Tab. 2); by RT-PCR analysis we observed a weaker level of *Xag* and *Xcg* transcripts compared to *Xotx5* and *Xotx5-255ΔC* injected caps (Fig. 25 B).

Because we previously showed that a RS box mediates the specific and diverse abilities of XOTX2 and XOTX5 in the retina (Onorati et al., 2007), we asked whether the RS box is required for their CG promoting ability. We therefore tested *Xotx5ΔRSbox* mRNA in *Xenopus* embryos and analyzed whole embryos and animal cap explants for expression of CG markers. We found that XOTX5 RS box is not at all involved in CG specification: *Xotx5ΔRSbox* was always able to elicit ectopic CG marker expression at the same level of full length *Xotx5*, both in whole embryos and in animal caps (Fig. 24 B, Fig. 24 C, Fig. 25 C, Tab. 2 and Tab. 3).

All the described constructs have also been injected dorsally, showing a similar CG promoting activity; however, in dorsal injections we generally observed a slightly lower frequency in ectopic *Xag* induction (Fig. 24 B and data not shown)

Results section I

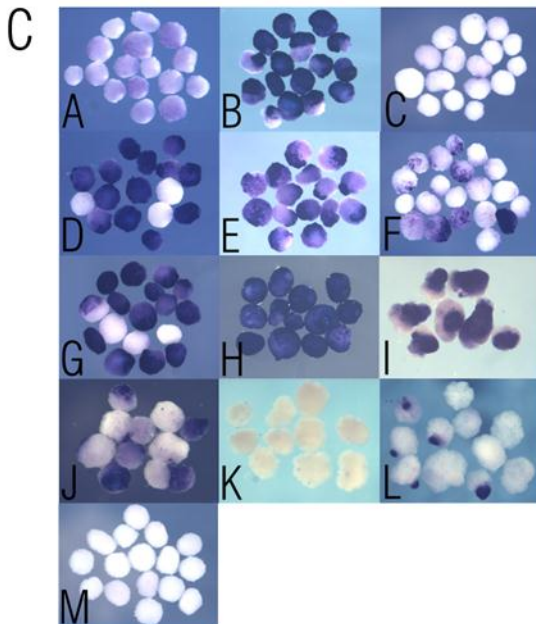
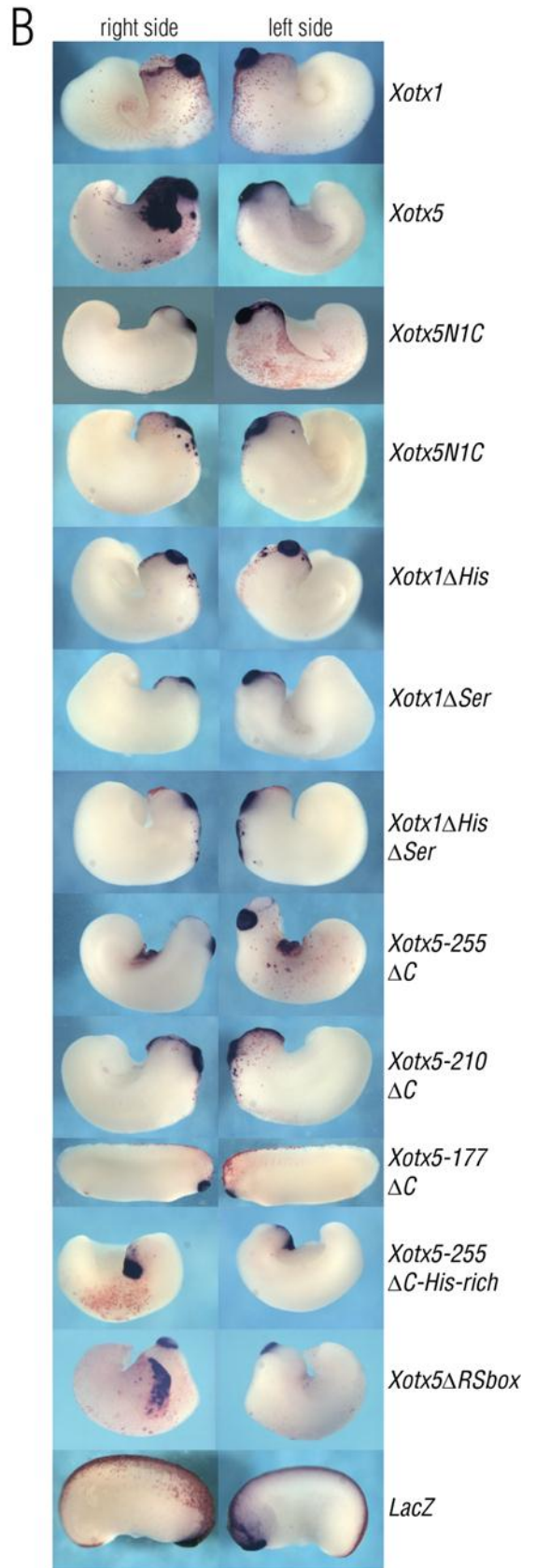
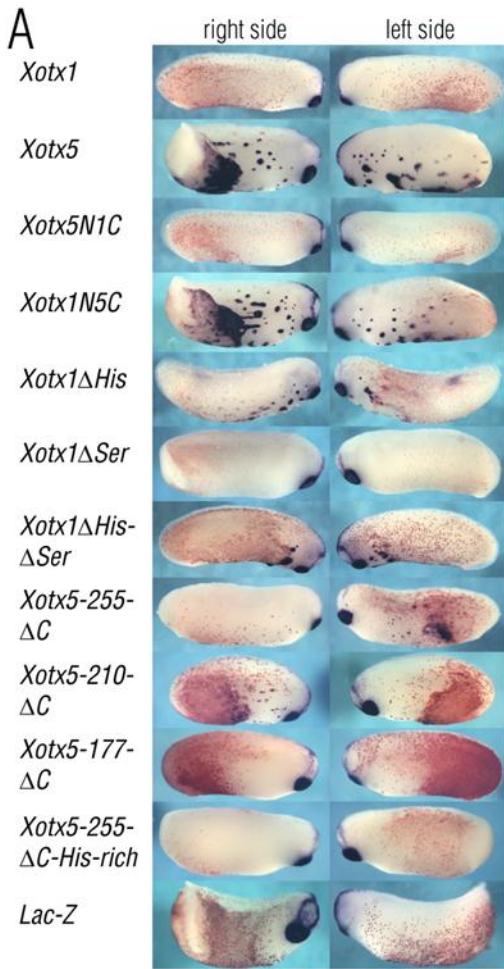


Fig. 24. Results of embryos microinjections and *Xag* *in situ* hybridization: (A, B) A total amount of 800 pg of capped mRNAs corresponding to the different constructs as shown was ventrally (A) or dorsally (B) bilaterally microinjected in *Xenopus* embryos at 4-cell stage, embryos were grown to tailbud stage and processed by *in situ* whole mount hybridization for *Xag* probe (cement gland marker). *Xotx1*, *Xotx2* and *Xotx5* induce posterior defects when overexpressed in *Xenopus* embryos; this activity is maintained by all constructs when microinjected dorsally (B). Lac Z is coinjected as a tracer. Microinjection of LacZ alone is used as negative control. (C) Animal caps were dissected from embryos injected with 800 pg capped-mRNAs as shown and *Xag* expression is detected by *in situ* hybridization. GFP is used as microinjection tracer and GFP alone microinjection is used as negative control. A: *Xotx1*; B: *Xotx5*; C: *Xotx5N1C*; D: *Xotx1N5C*; E: *Xotx1 Δ His*; F: *Xotx1 Δ Ser*; G: *Xotx1 Δ His Δ Ser*; H: *Xotx1 Δ RSbox*; I: *Xotx5-255 Δ C*; J: *Xotx5-210 Δ C*; K: *Xotx5-177 Δ C*; L: *Xotx5-255 Δ C-His-rich*; M: GFP.

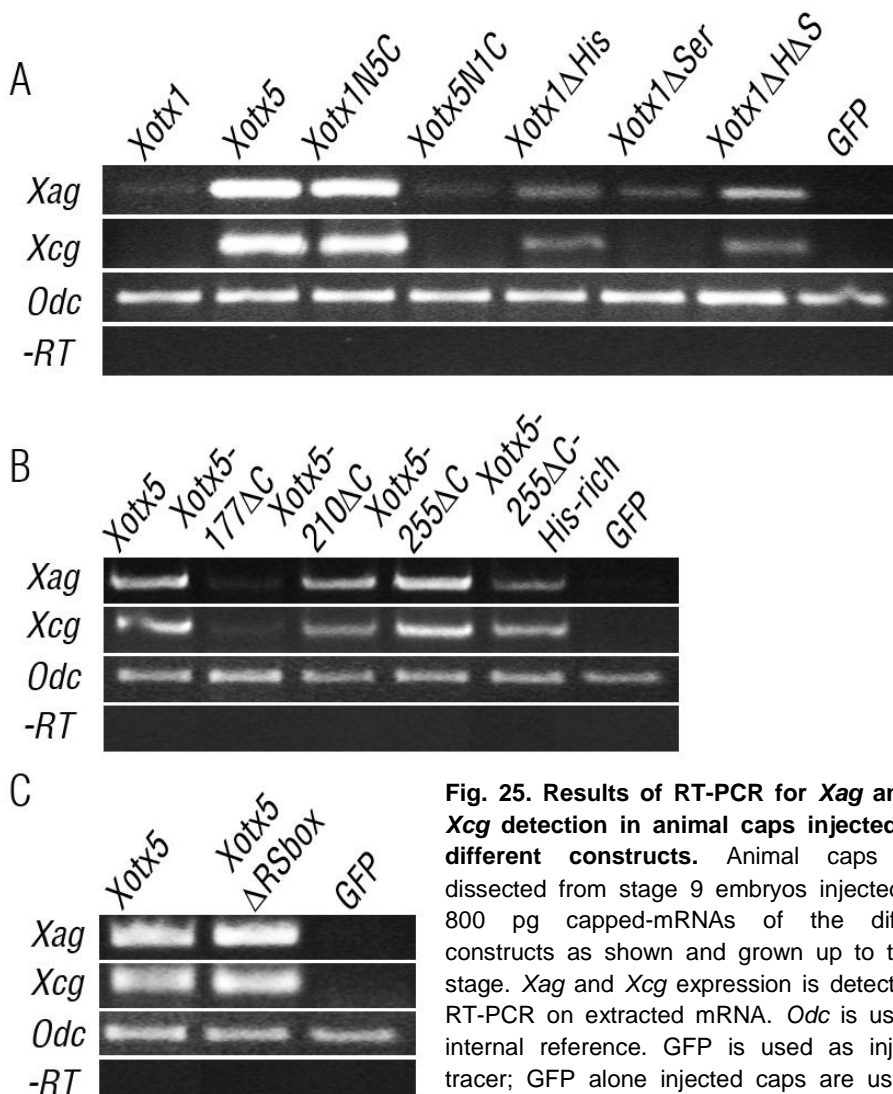


Fig. 25. Results of RT-PCR for *Xag* and for *Xcg* detection in animal caps injected with different constructs. Animal caps were dissected from stage 9 embryos injected with 800 pg capped-mRNAs of the different constructs as shown and grown up to tailbud stage. *Xag* and *Xcg* expression is detected by RT-PCR on extracted mRNA. *Odc* is used as internal reference. GFP is used as injection tracer; GFP alone injected caps are used as negative control.

Tab. 1. Results of microinjection experiments and Xag WISH.

Injected construct	Injection site	Injected dose	Ectopic Xag expression	NO ectopic Xag expression	<i>n</i>
<i>Xotx1</i>	Ventral	1,2ng	3 (1,3%)	222 (98,7%)	225 ^a
		800pg	2 (0,8%)	245 (99,2%)	247 ^b
<i>Xotx5</i>	Ventral	800pg	289 (81,2%)	67 (18,8%)	356 ^c
		500pg	54 (69,2%)	24 (30,8%)	78
		250pg	53 (37,9%)	87 (62,1%)	140
<i>Swap 1N5C</i>	Ventral	800pg	184 (87,2%)	27 (12,8%)	211 ^d
		250pg	27 (27,3%)	72 (72,7%)	99
<i>Swap 5N1C</i>	Ventral	1,2ng	3 (1,8%)	163 (98,2%)	166
		800pg	0 (0%)	208 (100%)	208 ^e
<i>Xotx1ΔHis</i>	Ventral	800pg	72 (46,8%)	82 (53,2%)	154 ^f
		500pg	43 (19%)	183 (81%)	226 ^g
<i>Xotx1ΔSer</i>	Ventral	1,2ng	2 (1,5%)	128 (98,5%)	130
		800pg	0 (0%)	89 (100%)	89 ^h
<i>Xotx1ΔHis ΔSer</i>	Ventral	800pg	62 (57,4%)	46 (42,6%)	108 ⁱ
<i>Xotx5-255ΔC</i>	Ventral	800pg	114 (83,8%)	22 (16,2%)	136 ^l
<i>Xotx5-210ΔC</i>	Ventral	800pg	39 (25,2%)	116 (74,8%)	155
<i>Xotx5-177ΔC</i>	Ventral	800pg	8 (3,7%)	207 (96,3%)	215 ^m
<i>Xotx5-255ΔC- His-Rich</i>	Ventral	800pg	0 (0%)	61 (100%)	61

Data were scored by χ^2 test for homogeneity; in the table are reported data resulting from: ^a: 5 experiments; ^{b, c}: 4 experiments; ^{d, e}: 3 experiments; ^{f, g, h, i, l, m}: 2 experiments. Amount of injected mRNA is indicated in picograms. Injection site is indicated. In brackets embryos relative percentage is indicated. *n*: number of embryos.

Tab. 2. Results of WISH on animal caps injected with the different constructs.

Construct	dose	Xag positive	Xag negative	<i>n</i>
<i>Xotx1</i>	800pg	0 (0%)	78 (100%)	78
<i>Xotx5</i>	800pg	85 (96,6%)	3 (3,4%)	88
<i>Swap1N5C</i>	800pg	62 (84,9%)	11 (15,1%)	73
<i>Swap5N1C</i>	800pg	1 (1,4%)	72 (98,6%)	73
<i>Xotx1ΔHis</i>	800pg	44 (77,2%)	13 (22,8%)	57
<i>Xotx1ΔSer</i>	800pg	25 [23 weak signal] (42,4)	34 (57,6%)	59
<i>Xotx1ΔHisΔSer</i>	800pg	47 [7 weak signal] (85,5%)	8 (14,5%)	55
<i>Xotx5-255ΔC</i>	800pg	21 (91,3%)	2 (8,7%)	23
<i>Xotx5-210ΔC</i>	800pg	20 (69%)	9 (31%)	29
<i>Xotx5-177ΔC</i>	800pg	0 (0%)	35 (100%)	35
<i>Xotx5ΔRSbox</i>	800pg	34 (100%)	0 (0%)	34
<i>Xotx5-255ΔC-HisRich</i>	800pg	12 (48%)	13 (52%)	25
<i>GFP</i>	800pg	0 (0%)	42 (100%)	42

Amount of injected mRNA is indicated in pictograms. In brackets animal cap relative percentage is indicated. Square brackets contain comments. GFP has been used as a tracer; GFP alone has been used as negative control. *n*: number of embryos.

Tab. 3. Results of microinjection experiments and *Xag* WISH.

Injected construct	Injection site	Injected dose	Ectopic <i>Xag</i> expression	NO ectopic <i>Xag</i> expression	<i>n</i>
<i>Xotx5</i>	Dorsal	800pg	52 (38,5%)	83 (61,5%)	135
<i>Xotx5-ΔRSbox</i>	Dorsal	800pg	63 (43,7%)	81 (56,3%)	144

Amount of injected mRNA is indicated in picograms. Injection site is indicated. Brackets indicate embryos relative percentage. *n*: number of embryos.

4.1 a- Statistical analysis: χ^2 homogeneity test

Datasets resulting from the microinjection of different constructs have been tested for homogeneity using chi-square (χ^2) statistical test. We compared results coming from the microinjection of 800pg of different constructs. Statistical analysis results are summarized below.

First of all we verified the dis-homogeneity of the two control datasets: data are not homogeneous, *Xotx1* and *Xotx5* have different effects.

Then we analyzed swap domain constructs effect; data are homogeneous: *Xotx5N1C* and *Xotx1* have the same effect, as well as *Xotx1N5C* and *Xotx5*, confirming that cement gland inducing activity resides in the C-terminus.

When we analyzed deleted construct effects, we found that:

- *Xotx1* and *Xotx1 Δ His* have different effects, confirming that the deletion of the Histidine rich region makes *Xotx1* able to induce cement gland formation;
- *Xotx5* and *Xotx1 Δ His* also have different effects: the deletion of the Histidine rich region makes *Xotx1* able to induce cement gland formation, but the deleted constructs is less efficient in respect to *Xotx5*;

1 st construct	2 nd construct	χ^2 value	p value	homogeneous/ <u>not</u> -homogeneous data
<i>Xotx1</i>	<i>Xotx5</i>	> 3,84	<0,05	<u>not</u> homogeneous
<i>Xotx1</i>	<i>Xotx5N1C</i>	< 3,84	>0,05	homogeneous
<i>Xotx5</i>	<i>Xotx1N5C</i>	< 3,84	>0,05	homogeneous
<i>Xotx1</i>	<i>Xotx1ΔHis</i>	> 3,84	<0,05	<u>not</u> homogeneous
<i>Xotx5</i>	<i>Xotx1ΔHis</i>	> 3,84	<0,05	<u>not</u> homogeneous
<i>Xotx1</i>	<i>Xotx1ΔSer</i>	< 3,84	>0,05	homogeneous
<i>Xotx1</i>	<i>Xotx1ΔHisΔSer</i>	> 3,84	<0,05	<u>not</u> homogeneous
<i>Xotx5</i>	<i>Xotx1ΔHisΔSer</i>	> 3,84	<0,05	<u>not</u> homogeneous
<i>Xotx1ΔHis</i>	<i>Xotx1ΔHisΔSer</i>	< 3,84	>0,05	homogeneous
<i>Xotx5</i>	<i>Xotx5-255ΔC</i>	< 3,84	>0,05	homogeneous
<i>Xotx1</i>	<i>Xotx5-210ΔC</i>	> 3,84	<0,05	<u>not</u> homogeneous
<i>Xotx5</i>	<i>Xotx5-210ΔC</i>	> 3,84	<0,05	<u>not</u> homogeneous
<i>Xotx1</i>	<i>Xotx5-177ΔC</i>	> 3,84	<0,05	<u>not</u> homogeneous
<i>Xotx5</i>	<i>Xotx5-177ΔC</i>	> 3,84	<0,05	<u>not</u> homogeneous
<i>Xotx1</i>	<i>Xotx5-255ΔC-HisRich</i>	< 3,84	>0,05	homogeneous
<i>Xotx5</i>	<i>Xotx5ΔRSbox</i>	< 3,84	>0,05	homogeneous

- *Xotx1* and *Xotx1ΔSer* have the same effect, confirming that removing Serine rich region is not sufficient to confer cement gland inducing activity to the deletion construct;
- *Xotx1* and *Xotx1ΔHisΔSer* have different effects, confirming that the deletion of the Histidine rich and of the Serine rich region makes *Xotx1* able to induce cement gland formation;
- *Xotx5* and *Xotx1ΔHisΔSer* have also different effects, the deletion of the Histidine rich and of the Serine rich region makes *Xotx1* able to induce cement gland formation, but the deleted constructs is still less efficient in respect to *Xotx5*;

- *Xotx1ΔHis* and *Xotx1ΔHisΔSer* have the same effect. From animal cap assays we can appreciate the more efficiency of *Xotx1ΔHisΔSer* in cement gland promoting activity in respect to *Xotx1ΔHis*, this difference is not evident from assays on whole embryos, and there is not any statistical difference between the effects of these two constructs.

When we analyze the effects of *Xotx5* deleted constructs we found that:

- *Xotx5* and *Xotx5-255ΔC* have the same effect, confirming that *Otx*-tail is not at all involved in cement gland inducing activity;
- *Xotx5-210ΔC* is not homogeneous neither with *Xotx1* or with *Xotx5*: upon the removal of this C-terminus portion *Xotx5* is still able to induce cement gland formation, differently from *Xotx1*, but with a lower efficiency in respect to *Xotx5*;
- *Xotx5-177ΔC* is not homogeneous neither with *Xotx5* or with *Xotx1*: almost all residual cement gland inducing activity is lost upon the removal of both CGbox-D1 and CGbox-D2; anyway data obtained are still statistically different from data obtained with the microinjection of *Xotx1*.

Then we analyzed the capability of Histidine rich region to inhibit *Xotx5* cement gland inducing activity; *Xotx5-255ΔC-His-rich* and *Xotx1* microinjections produce homogeneous data sets: therefore, the insertion of *Xotx1* Histidine rich region downstream of *Xotx5* cement gland box inhibits *Xotx5* cement gland inducing function.

Finally, we verified that *Xotx5* RS box is not at all involved in cement gland inducing activity: *Xotx5* and *Xotx5ΔRSbox* produce homogeneous data sets.

4.2- Convergent extension inhibition

Both *Xotx1* and *Xotx5*, mostly if dorsally mis-expressed, produce embryos with posterior defects. All the constructs microinjected in the present work, maintain the capability to produce blastopore closure failure, typical of inhibition of convergent extension movements (Fig 24 B and Tab. 4). By injecting the same dose of mRNA from different constructs, we observed that *Xotx5* is more effective than *Xotx1* in inhibiting convergent extension movements (Tab. 4). If we remove XOTX1 His-rich region the frequency of truncated embryos increases, but does not reach the frequency obtained injecting *Xotx5* (Tab. 4). Embryos injected with Ser-rich deleted *Xotx1*, instead, show the same gastrulation defects frequency of embryos injected with *Xotx1*; *Xotx1* double deleted construct almost mirrored *Xotx1ΔHis* microinjections (Tab. 4). *Xotx5-255ΔC* and *Xotx5-210ΔC* induce trunked embryos with efficiency similar to *Xotx5*; we observed a consistent reduction in gastrulation defects only by injecting *Xotx5-177ΔC* (Tab. 4). The capability to inhibit convergent extension is completely lost when XOTX proteins are interrupted inside the homeodomain region in position corresponding to aa 88 (data not shown). The removal of the RS box does not affect convergent extension inhibition, as well as the insertion of a supplementary His-rich region downstream to *Xotx5-255ΔC* (Tab. 4). We can speculate that the lower effect of *Xotx1* in respect to *Xotx5* is due, almost partially, to the presence of the His-rich region, even if this domain is not able to inhibit *Xotx5* activity in the chimeric construct *Xotx5-255ΔC-His-rich*. On the contrary Ser-rich region does not seem to have any inhibitory effect on XOTX1 convergent extension inhibition capability. Besides, CGboxD1 is not relevant for XOTX5 gastrulation movements regulation, differently from CGboxD2.

Tab. 4. Results of microinjection experiments.

Injected construct	Injection site	Injected dose	Posterior defect	NO posterior defect	<i>n</i>
<i>Xotx1</i>	Dorsal	800pg	72 (32%)	153 (68%)	225 ^a
<i>Xotx5</i>	Dorsal	800pg	181 (84,2%)	34 (15,8%)	215 ^b
<i>Swap 1N5C</i>	Dorsal	800pg	148 (70,1%)	63 (29,9%)	211 ^c
<i>Swap 5N1C</i>	Dorsal	800pg	33 (22,8%)	112 (77,2%)	145 ^d
<i>Xotx1ΔHis</i>	Dorsal	800pg	46 (56,1%)	36 (43,9%)	82 ^e
<i>Xotx1ΔSer</i>	Dorsal	800pg	16 (28,6%)	40 (71,4%)	56
<i>Xotx1ΔHis ΔSer</i>	Dorsal	800pg	38 (48,7%)	40 (51,3%)	78
<i>Xotx5-255ΔC</i>	Dorsal	800pg	95 (72%)	37 (28%)	132 ^f
<i>Xotx5-210ΔC</i>	Dorsal	800pg	79 (81,4%)	18 (18,6%)	97
<i>Xotx5-177ΔC</i>	Dorsal	800pg	16 (19,5%)	66 (80,5%)	82
<i>Xotx5ΔRSbox</i>	Dorsal	800pg	63 (81,8%)	14 (18,2%)	77
<i>Xotx5-255ΔC- His-Rich</i>	Dorsal	800pg	73 (79,3%)	19 (20,7%)	92 ^g

Data were scored by χ^2 test for homogeneity; in the table are reported data resulting from: ^{a, b, c, d, e, f, g} 2 experiments. Amount of injected mRNA is indicated in picograms. Injection site is indicated. In brackets the relative percentage of embryos is indicated. *n*: number of embryos

4.3- Neural tissue induction

Xotx5 mis-expression in *Xenopus* embryos promotes ectopic neural tissue formation (Vignali et al., 2000), while *Xotx1* mis-expression does not have this effect. We investigated if this difference is also due to previously described primary structure differences between the two homeoproteins. We microinjected mRNA corresponding to *Xotx1* deleted constructs in *Xenopus* embryos and we checked them for ectopic neural tissue formation, performing whole mount *in situ* hybridization using *nrp-1* as neural tissue marker. Full length *Xotx1* and *Xotx5* were used as controls.

All three deleted construct tested (*Xotx1ΔHis*, *Xotx1ΔSer* and *Xotx1ΔHisΔSer*) were not able to promote ectopic neural tissue formation, when ventrally injected (Fig. 26 A and Tab. 5). To confirm data obtained in whole embryos we performed animal cap assays injecting the same deleted constructs, alongside with swap domain constructs, to test if neural inducing activity resides into protein N- or C-terminus. These data fully confirm the incapability of *Xotx1* C-terminus and of all three deleted constructs to promote neural fate ectopically (Fig. 26 B and Tab. 6).

Since neuralizing activity seems to reside in the protein C-terminal part, to localized XOTX5 region(s) involved in neural induction we injected embryos with *Xotx5-255ΔC* and with *Xotx5-210ΔC* and analyzed injected embryos for *nrp-1* mis-expression. Embryos microinjected with *Xotx5-210ΔC* do not express *nrp-1* at all (Fig. 26 C and Tab 5). Embryos microinjected with *Xotx5-255ΔC*, in rare cases, show only a very weak signal compared to control sibling embryos microinjected with *Xotx5*, and in most cases they do not show *nrp-1* expression at all (Fig. 26 C see dotted square, and Tab. 5),. We concluded that the OTX-tail seems to have a role in neural tissue induction by *Xotx5*. Further analysis will be anyway necessary to understand more about this aspect of *Xotx1* and *Xotx5* differential actions.

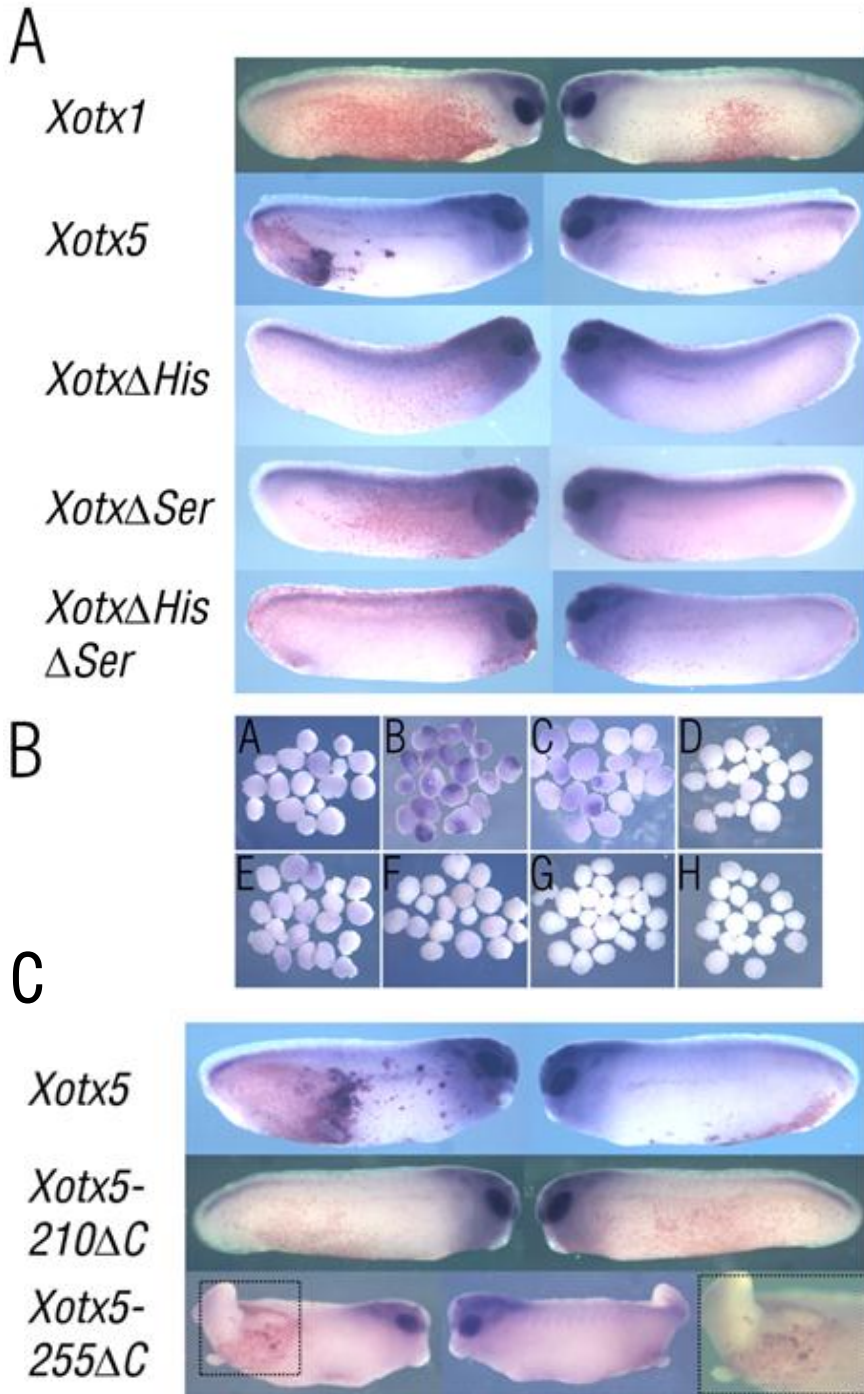


Fig. 26. Results of embryo microinjections and *nrp-1* *in situ* hybridizations: (A) 800pg of capped mRNAs corresponding to different constructs are ventrally microinjected in *Xenopus* embryos at 4-cells stage, embryos are grown to tailbud stage, and processed by *in situ* whole mount hybridization for *nrp-1* probe (neural tissue marker). (B) Animal caps are dissected from embryos injected with 800pg capped-mRNAs corresponding to the different constructs and *nrp-1* expression is detected by *in situ* hybridization. GFP is used as a microinjection tracer and GFP alone microinjection is used as a negative control. A: *Xotx1*; B: *Xotx5*; C: *Xotx1N5C*; D: *Xotx5N1C*; E: *Xotx1ΔHis*; F: *Xotx1ΔSer*; G: *Xotx1ΔHisΔSer*; H: GFP. (C) 800 pg of capped mRNAs corresponding to different constructs as indicated are ventrally microinjected in *Xenopus* embryos at 4-cells stage, embryos are grown to tailbud stage, and processed by WISH for *nrp-1* probe. Dotted square on *Xotx5-255ΔC* embryo on the extreme left corresponds to magnification on the extreme right.

Tab. 5. Results of *nrp-1* *in situ* hybridizations on whole injected embryo

Construct	dose	Ectopic neural tissue	NO Ectopic neural tissue	<i>n</i>
<i>Xotx1</i>	800pg	0 (0%)	144 (100%)	144
<i>Xotx5</i>	800pg	63 (58,3%)	45 (41,7%)	108
<i>Xotx1ΔHis</i>	800pg	0 (0%)	169 (100%)	169
<i>Xotx1ΔSer</i>	800pg	0 (0%)	214 (100%)	214
<i>Xotx1ΔHisΔSer</i>	800pg	0 (0%)	160 (100%)	160
<i>Xotx5-210ΔC</i>	800pg	0 (0%)	132 (100%)	132
<i>Xotx5-255ΔC</i>	800pg	18 * (27,7%)	47 (72,3%)	65

4-cells stage embryos have been ventrally microinjected, embryos have been grown until tailbud stage and then processed by *in situ* hybridization using *nrp-1* probe. *n*: number of embryos. Amount of injected mRNA is indicated in picograms. Brackets indicate the relative percentage of embryos. “*”:weak signal, see Fig. 26, dotted square. Lac Z has been used as injection tracer.

Tab. 6. Results of *nrp-1* *in situ* hybridizations on injected animal caps.

Construct	dose	<i>nrp-1</i> positive	<i>nrp-1</i> negative	n
<i>Xotx1</i>	800pg	0 (0%)	36 (100%)	36
<i>Xotx5</i>	800pg	18 (85,7%)	3 (14,3%)	21
<i>Swap1N5C</i>	800pg	17 (50%)	17 (50%)	34
<i>Swap5N1C</i>	800pg	0 (0%)	27 (100%)	27
<i>Xotx1ΔHis</i>	800pg	0 (0%)	35 (100%)	35
<i>Xotx1ΔSer</i>	800pg	1 (3,3%)	29 (96,7%)	30
<i>Xotx1ΔHisΔSer</i>	800pg	0 (0%)	33 (100%)	33
<i>GFP</i>	800pg	0 (0%)	42 (100%)	42

1-cell stage embryos have been microinjected, animal caps have been dissected from stage 9 embryos, grown until tailbud stage and then processed by *in situ* hybridization using *nrp-1* probe. *n*: number of embryos. Amount of injected mRNA is indicated in pictograms. In brackets relative percentage of animal caps are indicated. GFP has been used as injection tracer; GFP alone has been used as negative control.

5- Results section II

5.1- XOTX2 and XOTX5 transactivation domain

The yeast two hybrid system (Chien et al., 1991) is based on a simple strategy. A bait protein is fused in frame with the DNA binding domain (BD) of the Gal4 transcription factor, while potential prey proteins are fused in frame with the transactivation domain (AD) of the viral VP16 transcription factor; bait-prey interaction brings BD and AD in proximity allowing the transactivation of specific reporter genes containing a Gal 4 binding site into their regulating sequences; activated reporter genes allow yeast cells to grow on a specific selective medium.

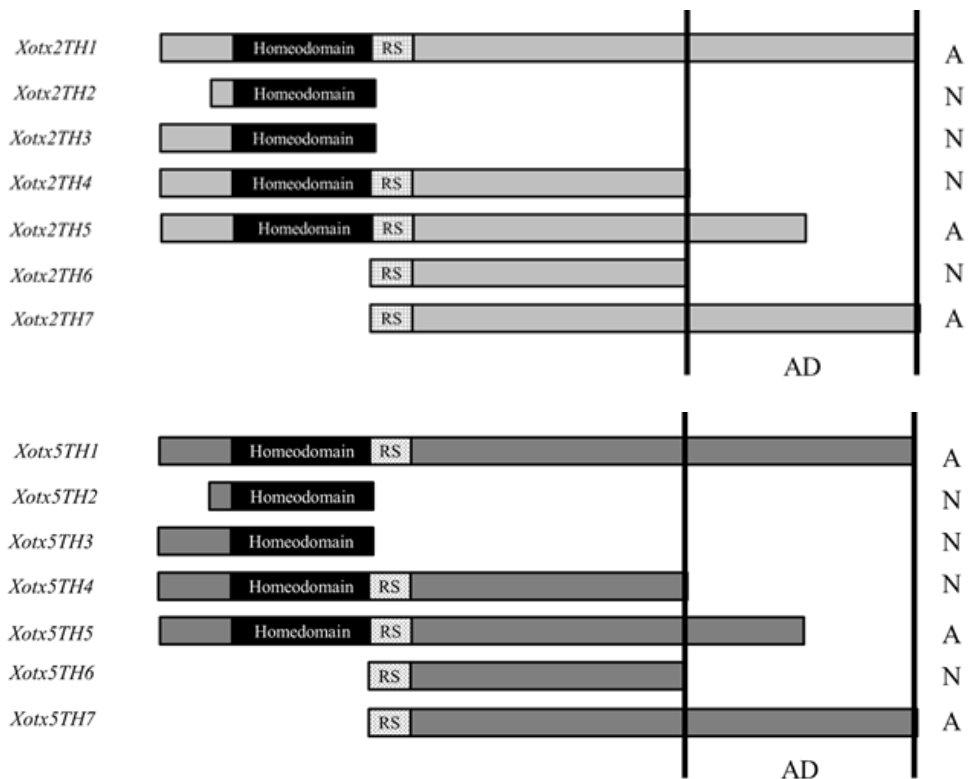


Fig. 27. XOTX2 and XOTX5 transactivation domains as detected in yeast auto-activation test. A: transcription auto-activation; N: no transcription transactivation; RS: retinal specificity box; AD: XOTX transactivation domain.

It is, therefore, necessary that bait protein does not contain a proper transactivation domain, to identify protein-protein interactions; if the bait is self-sufficient to induce reporter transactivation, bait-prey contact is no longer necessary to turn on reporter expression, and yeast cells can survive in the selective medium with the bait plasmid only.

We have used this simple strategy to isolate XOTX2 and XOTX5 transactivation domain(s): we have prepared 7 different XOTX2 and XOTX5 partial coding constructs (Fig. 21) and we have used them to transform yeast cells without any additional prey, thereby selecting XOTX portions sufficient to activate reporter activity in this auto-activation test. Yeast cells transformed with XOTX2 TH1, TH5 and TH7, have all been able to grow on selective medium; instead, yeast cells transformed with XOTX2 TH2, TH3, TH4 and TH6 have not been able to grow on selective medium. The same results have been obtained using corresponding XOTX5 constructs. We have concluded that XOTX2 and XOTX5 transactivation domains are both localized at their C-terminus. XOTX2 portion able to activate reporter transcription spans amino acids 174-288, while that of XOTX5 spans residues 174-290 (Fig. 27).

5.2- Two-hybrid screen for XOTX2 and XOTX5 potential interactors

To perform yeast two-hybrid screens to isolate XOTX2 and XOTX5 potential interactors we used XOTX2 TH4 and XOTX5 TH4 fragments: the longest TH fragments unable to autonomously activate reporter transcription. We have used a *Xenopus* oocyte library with the purpose of having a large spectrum of potential cofactors, since the *Xenopus* oocyte transcriptome is one of the largest. The oocyte library used has a complexity of $7,5 \times 10^6$ clones; thereby, for each bait, we had to screen a minimum of 15×10^6 clones (2-folds library's complexity); we have screened a total amount of 20×10^6 clones, a sufficient number to consider that the whole library was tested for

interaction with XOTX2/XOTX5. From the screenings we have isolated 116 XOTX candidate interactors: some have been isolated in both parallel screens, others with only one of the two baits. All 116 nucleotide sequences obtained from isolated prey plasmids, as well as predicted peptide sequences, were aligned using ClustaW (<http://www.ebi.ac.uk/Tools/msa/clustalw2/>). From this analysis we have been able to identify 74 peptide homology groups. For each group a sequence representative of the entire cluster was selected, and a yeast two hybrid assay has been used to confirm or test its interaction with both XOTX (interaction confirmation/cross-interaction tests). Surprisingly, all the 74 interactors were able to interact *in vitro* with both XOTX.

5.3- Potential interactor database search

Sequences selected for interaction confirmation and cross-interaction tests (see above) were also used to perform an extensive database search, using both nucleotide and amino acid BLAST alignment tool (<http://blast.ncbi.nlm.nih.gov/Blast.cgi>). The most interesting results are summarized below:

- Group 1: 11 independent clones. Amino acids homology ranging from 98 to 100%. Interaction with both XOTX2 and XOTX5. These sequences show a high level of homology with a predicted protein of unknown function of *X. tropicalis* (Fig. 28 A), that we named after one of our clone numbers as *c29*.
- Group 11: 1 clone, able to interact with both baits; this sequence matches with XGranulin-1 precursor (Fig. 28 B).
- Group 12: 6 independent clones. Amino acid homology 100%. Interaction with both XOTX2 and XOTX5. These sequences match with XUSF2 (Fig. 28 C).

- Group 13: 3 independent clones. Amino acid homology 100%, sequences differ only in length. Interaction with both XOTX2 and XOTX5. These sequences match with XUSF1 (Fig. 28 D).
- Group 14: 4 independent clones. Amino acid homology 100%, sequences differ only in length. Interaction with both XOTX2 and XOTX5. These sequences match with XGranulin-2 (Fig. 28 E).

Group 1 sequences raised our interest because they match with a so far undescribed hypothetical peptide; thereby it appeared to us very intriguing to try to characterize it.

Groups 12 and 13 seemed interesting to us because of the fact that upstream stimulatory factors (USF) have already been described as transcription factors of the bHLH family; thereby an interaction *in vivo* with XOTX transcription factors seemed to be likely.

Group 11 and 14 match with proteins of the Granulin family, several members of this class have been described as secreted factors, so that the interaction with transcription regulatory proteins may seem unlikely. Nevertheless homeoproteins contain Penetratin (Dom et al., 2003), and XOTX2 transcellular translocation phenomena have been described (Rebsam et al., 2008). We decided to go further with our investigation about Granulins, hypothesizing for them a possible extracellular interaction with XOTX.

Fig. 28. Potential interactors protein BLASTs. One amino acid sequence representative of the entire amino acid homology group was used to perform database search; most interesting output of protein BLAST are shown.

A: group 1; B: group 11; C: group 12; D: group 13; E: group 14.



B

granulin precursor [Xenopus laevis]

Sequence ID: [refNP_001080678.1](#) Length: 950 Number of Matches: 9[► See 1 more title\(s\)](#)

Range 1: 784 to 950		SeqFeat	Graphics	▼ Next Match	▲ Previous Match
Score	Expect	Method	Identities	Positives	Gaps
338 bits(866)	3e-107	Compositional matrix adjust.	166/167(99%)	166/167(99%)	0/167(0%)
Query 3	GGLSIPWFSRIPALRQGNHAYWCDSDFSQDGGQSCCRMVSGENGCCPIEKAVCCSDHLHC				62
Sbjct 784	GGLSIPWFSRIPALRQGNHAYWCDSDFSQDGGQSCCRMVSGENGCCPIEKAVCCSDHLHC				843
Query 63	CPAGYTCNVAAGSCEIPQGGVYKISFFGATSAALRLHYWCDAGTYCFDQGTCCRGRGGVW				122
Sbjct 844	CPAGYTCNVAAGSCEIPQGGVYKISFFGATSAALRLHYWCDAGTYCFDQGTCCRGRGGVW				903
Query 123	NCCLYIQGVCCPDMVHCCPYGVYVCLAGGASCARSMSRWDGKFSFPL				169
Sbjct 904	NCCLYIQGVCCPDMVHCCPYGVYVCLAGGASCARSMSRWDGKFSFPL				950

C

upstream transcription factor 2, c-fos interacting [Xenopus laevis]

Sequence ID: [refNP_001088700.1](#) Length: 310 Number of Matches: 1[► See 1 more title\(s\)](#)

Range 1: 153 to 310		SeqFeat	Graphics	▼ Next Match	▲ Previous Match
Score	Expect	Method	Identities	Positives	Gaps
330 bits(845)	2e-111	Compositional matrix adjust.	157/158(99%)	157/158(99%)	0/158(0%)
Query 1	LQAGGGFYVMMIPQVLPAGQQRSIAPRIFHFYSPKQGNRTFRDERRAQHNVEVERRR				60
Sbjct 153	LQAGGGFYVMMIPQVLPAGQQRSIAPRIFHFYSPKQGNRTFRDERRAQHNVEVERRR				212
Query 61	DKINWIVQLSKIIPDCNAESTKTAASKGGILSKACDYIRELRQTNQSVQETYPKAEERLQ				120
Sbjct 213	DKINWIVQLSKIIPDCNAESTKTAASKGGILSKACDYIRELRQTNQSVQETYPKAEERLQ				272
Query 121	MNELLRQQIEDQJENALLRAQLQGHGIEVVEESFRQ				158
Sbjct 273	MNELLRQQIEDQJENALLRAQLQGHGIEVVEESFRQ				310

D

upstream transcription factor 1 [Xenopus laevis]

Sequence ID: [refNP_001089471.1](#) Length: 299 Number of Matches: 1[► See 1 more title\(s\)](#)

Range 1: 111 to 299		SeqFeat	Graphics	▼ Next Match	▲ Previous Match
Score	Expect	Method	Identities	Positives	Gaps
396 bits(1017)	4e-137	Compositional matrix adjust.	189/189(100%)	189/189(100%)	0/189(0%)
Query 2	IEYTYFFTVVDSSTSTVWTHITDITLIQAGSTAPGQFYVMSQDVLQGGQSRSIAPR				61
Sbjct 111	IEYTYFFTVVDSSTSTVWTHITDITLIQAGSTAPGQFYVMSQDVLQGGQSRSIAPR				170
Query 62	IEYTYFFTVVDSSTSTVWTHITDITLIQAGSTAPGQFYVMSQDVLQGGQSRSIAPR				121
Sbjct 171	IEYTYFFTVVDSSTSTVWTHITDITLIQAGSTAPGQFYVMSQDVLQGGQSRSIAPR				230
Query 122	GILSKACDYIQELRQNLRLSEELQVVDQLQMNELLRQQVEDLQKHLLIRTLQRHGV				181
Sbjct 231	GILSKACDYIQELRQNLRLSEELQVVDQLQMNELLRQQVEDLQKHLLIRTLQRHGV				290
Query 182	EIIIKSDGR				190
Sbjct 291	EIIIKSDGR				299

E

granulin 2 [Xenopus laevis]

Sequence ID: [gbAAAY26493.1](#) Length: 724 Number of Matches: 7

Range 1: 511 to 714		SeqFeat	Graphics	▼ Next Match	▲ Previous Match
Score	Expect	Method	Identities	Positives	Gaps
401 bits(1031)	3e-133	Compositional matrix adjust.	200/204(98%)	202/204(99%)	0/204(0%)
Query 2	IFSCNDGQTCRRMGSVWGCCPIAQAVCCSDHWHCCPQSFCDTRGTGCVLGRMLPLGLMK				61
Sbjct 511	IFSCNDGQTCRRMGSVWGCCPIAQAVCCSDHWHCCPQSFCDTRGTGCVLGRMLPLGLMK				570
Query 62	VFLSSDQGWCDSEHSFCPSGTTCCPGEQGGWSSCCPLQEAVCCSDHWHCCPQSFCDTRGTGCVLGRMLPLGLMK				121
Sbjct 571	VFLSSDQGWCDSEHSFCPSGTTCCPGEQGGWSSCCPLQEAVCCSDHWHCCPQSFCDTRGTGCVLGRMLPLGLMK				630
Query 122	ICDLFPQKAAIISFSGTISAGRLDYWCDAGTYCSDDQTCRRGLGGAMHCCIYTWGVCCFD				161
Sbjct 631	ICDLFPQKAAIISFSGTISAGRLDYWCDAGTYCSDDQTCRRGLGGAMHCCIYTWGVCCFD				690
Query 182	MYBCCPYGVYVCLQWASGCRSSSP				205
Sbjct 691	MYBCCPYGVYVCLQWASGCRSSSP				714

5.4- DNA binding ability of potential interactors

A fundamental aspect to be tested is the capability of yeast cells transformed with preys alone to grow onto selective medium. A prey can be itself able to transactivate reporter transcription if it contains a DNA binding domain. We have transformed yeast cells with prey plasmids alone and checked their ability to survive in specific medium. None of our selected interactors is itself able to turn on reporter expression.

5.5- Expression profiles of potential interactors

5.5.1- RT-PCR

The first obvious condition necessary for two proteins to interact is that they have to be in the same place at the same time; in other words: they must be co-expressed.

First, we checked if selected potential interactors are expressed during *Xenopus* development. We have performed RT-PCR experiments, using specific primers, on cDNAs retro-transcribed from RNA extracted from *Xenopus* embryos at several developmental stages.

From 2-cell stage to gastrulation and early neurulation *c29* is expressed at a constant low level; at stage 15 we observe a little increase; during subsequent development, expression levels remain almost invariant till stage 37, when *c29* transcription increases to remain quite invariant till the last examined stage (42) (Fig. 29).

Xusf1 transcripts show a quite constant rising during the different developmental stages examined, from stage 2 to stage 37; at stage 39 *Xusf1* RNA decrease, to increase again at stage 42 (Fig. 29).

Xusf2 is expressed in a quite high constant manner from stage 2 and during gastrulation and early neurulation; during late neurula stage *Xusf2*

transcripts decrease, then increase at stage 23 to decrease again from stage 26 to stage 39. Finally we observe another rising during the last analyzed developmental stage (42) (Fig. 29).

Xgrn1 seems to be expressed in an almost invariant mode during whole *Xenopus* development (Fig. 29).

Xgrn2 expression is constant and low during all developmental stages from stage 15 to stage 37; at stages 2, 12 and 39 we observe a little increase, and two expression peaks at stages 9 and 42 (Fig. 29).

Moreover, we have checked expression of these cDNAs in fully differentiated *Xenopus* eye; *Xenopus* eyes have been dissected from stage 42 embryos, RNA has been extracted and retro-transcribed and RT-PCRs using specific primers have been performed. All analyzed XOTX potential partners are transcribed in completely differentiated *Xenopus* retinae. Dissected eyes comprised retinal pigmented epithelium and neural retina, so that we could not exactly determine in which of the two differentiated tissue the cDNAs are expressed (Fig. 30).

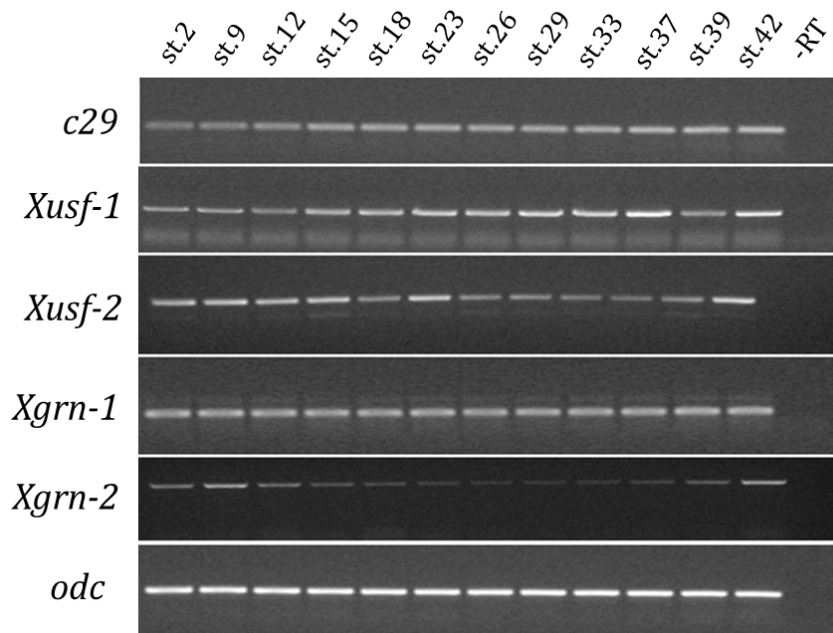


Fig. 29. Developmental expression of selected cDNAs as detected by RT-PCR analysis on whole embryos. RT-PCR analysis, performed on cDNAs retro-transcribed from RNAs extracted from *Xenopus laevis* embryos at different developmental stages. Developmental stages are indicated (st). *Odc* has been used as an internal reference.

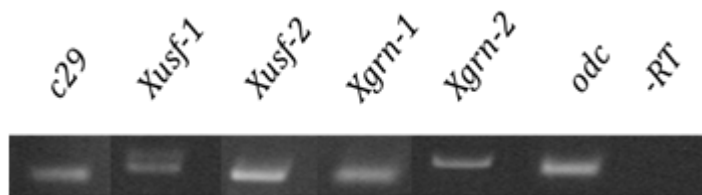


Fig. 30. Expression of selected cDNAs detected by RT-PCR analysis on *Xenopus* eyes. RT-PCR analysis, performed on cDNAs retro-transcribed from RNAs extracted from *Xenopus laevis* eyes dissected at stage 42. *Odc* have been used as an internal reference.

5.5.2- *In situ* hybridization

5.5.2.1- Early developmental stages

With the aim of determining the spatial expression of each of the 5 selected cDNAs during gastrulation and early neurulation, we have performed , *in situ* hybridizations on bisected *Xenopus* gastrulae and neurulae.

Results for each probe are reported below:

- *c29* transcripts are firstly detected in the migratory deep zone cells that are fated to give rise to prechordal mesendoderm; the expression seems to respect the boundary represented by the Brachet's cleft, similarly to *Xotx2* and *Xotx5*, but, differently from them, it does not seem to be expressed in dorsal bottle cells. At stage 15 and 20, *c29* begins to be expressed in the anterior neuroectoderm, becoming progressively restricted to the eyefield. In these regions *c29* expression domain seems included in *Xotx1* and *Xotx2* domains, while it seems complementary to *Xotx5* expression territory (Fig. 31).
- *Xgrn1* transcripts becomes detectable by *in situ* hybridization in the embryo animal pole already at stage 9; *Xgrn1* remains detectable in the ectodermal layer during gastrulation; *Xgrn1* mRNA seems to be partially coexpressed with *Xotx1* in the dorsal-anterior part of the ectoderm, while its expression appears complementary to those of

Xotx2 and *Xotx5*. During neurulation we detected only a weak expression in the neural plate (Fig. 31).

- *Xgrn2* expression profile substantially mirrors that of *Xgrn1* with few differences: at stage 10 *Xgrn2* transcripts are detectable in a deeper cell layer in respect of *Xgrn1*, and *Xgrn2* expression in neural territories looks more convincing (Fig. 31).

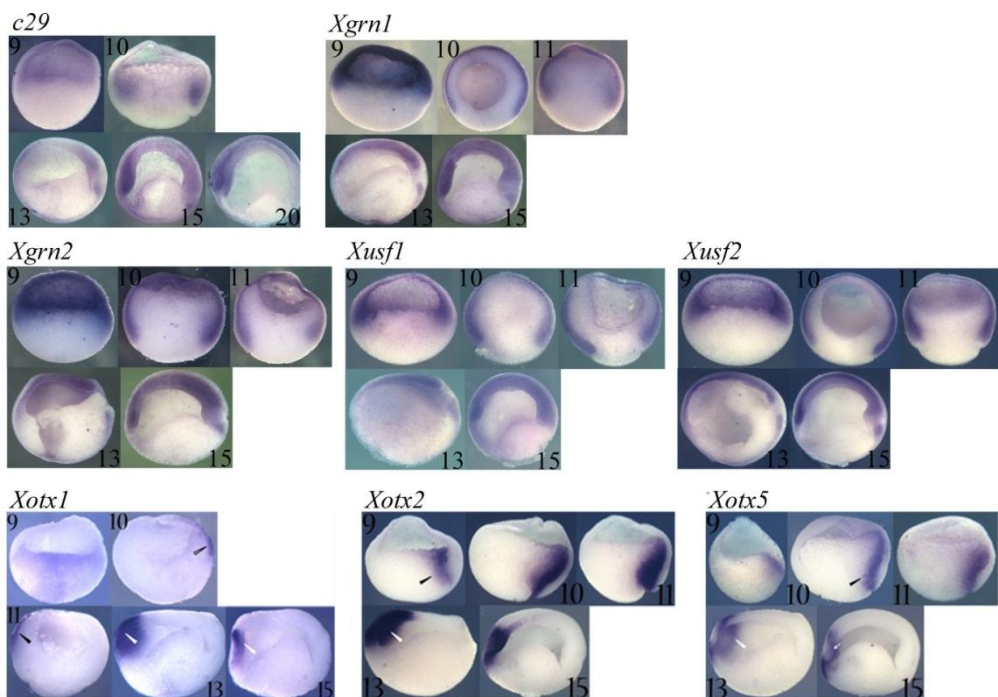


Fig. 31. Localization of *c29*, *Xusf1-2*, *Xgrn1-2* mRNAs in the early developing *Xenopus laevis* embryo. *In situ* hybridization of *Xenopus laevis* emi-gastrulae and emi-neurulae obtained with probes against: *c29*; *Xgrn1*; *Xgrn2*; *Xusf1*; *Xusf2*. *Xotx1*, *Xotx2* and *Xotx5* early expression profiles are also shown for comparison.

Xotx1: Empty black arrowhead: dorsal ectoderm; black arrowhead: presumptive anterior neuroectoderm; white arrowhead: anterior neural plate;

Xotx2: Black arrowhead: migratory deep zone; white arrowhead: anterior neural plate;

Xotx5: Black arrowhead: migratory deep zone; white arrowhead: anterior neural plate; white arrow: presumptive optic chiasma region. Embryos developmental stages are indicated.

- *Xusf1* and *Xusf2* show almost superimposable expression districts: both are expressed in the whole ectodermal layer during gastrulation, they are partially coexpressed with *Xotx1* in the dorsal-anterior part of the ectoderm, and complementary to *Xotx2* and *Xotx5*; later during neurulation they become visible in the neural plate, and especially *Xusf2* expression becomes stronger in the eyefield, thereby showing coexpression with *Xotx1* and *Xotx2* and complementarity to *Xotx5* (Fig. 31).

5.5.2.2- Later developmental stages

With the aim of determining potential XOTX partners expression districts during later developmental stages, we have performed, for each of the 5 selected clones, *in situ* hybridization on whole *Xenopus* embryos from late neurula (stage 20) to tailbud stage (stage 24, 28).

Results for each probe are reported below:

- *c29* is expressed in the forming eye vesicles, neural crest and in the anterior part of the neural tube at stage 20; at stage 24 this expression pattern persists and transcripts become more abundant in the eye vesicles; stage 28 embryos show *c29* strong expression in the eye, and a weaker expression in the otic cup and in branchial arches. Main sites of coexpression with *Xotx* are the eyefield and the anterior brain (Fig. 32).
- *Xusf1* and *Xusf2* expression districts are almost superimposable: at stage 20 they are expressed in the anterior part of the neural tube (including the eye vesicles) and in migrating neural crest; at stage 24 the expression persists quite invariant, with an intensified signal in the eye vesicles, especially for *Xusf2*; at stage 28 *Xusf* RNAs are detectable in the eyes, otic cups, branchial arches and in developing forebrain. At all examined developmental stages *Xusf2* expression

seems to be more intense than that of *Xusf1*. Main sites of coexpression with *Xotx* are the eyefield and the anterior brain (Fig. 32).

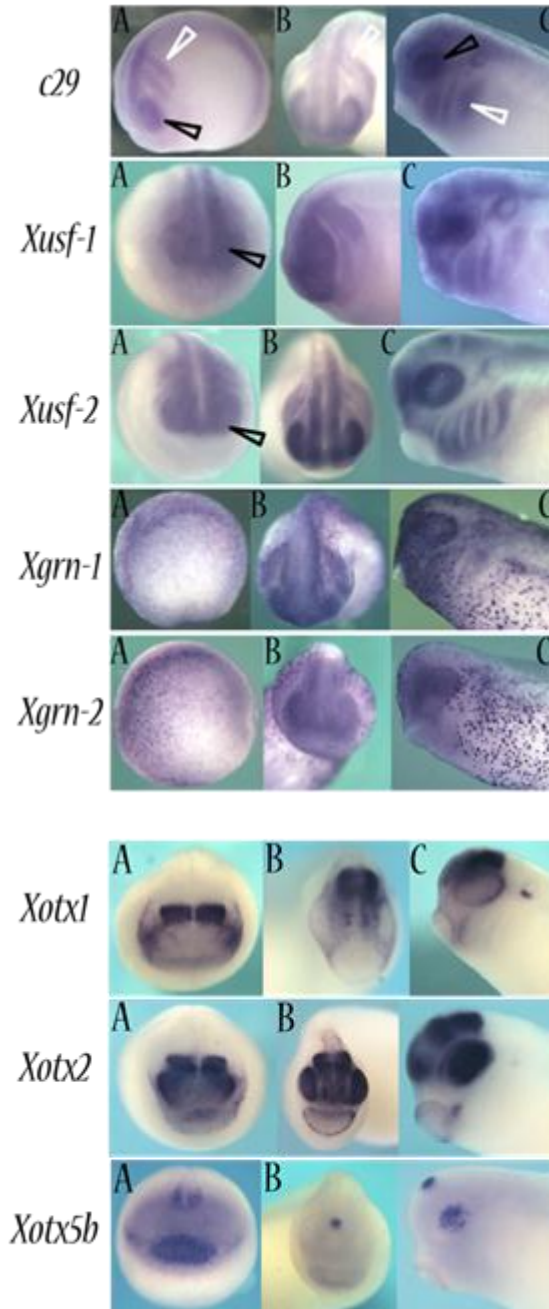


Fig. 32. Results of WISH of *c29*, *Xusf1/2*, *Xgrn1/2* in the developing *Xenopus laevis* embryo. Whole mount *in situ* hybridization of embryos at different developmental stages obtained with *c29*, *Xusf1-2*, *Xgrn1-2* probes; *Xotx1*, *Xotx2* and *Xotx5* later expression profiles are also shown for comparison. A: stage 20-21 embryos, B: stage 23-24 embryos, stage 28 embryos. White arrowhead: neural crest/branchial arches; black arrowhead: eyefield.

- Also *Xgrn1* and *Xgrn2* are quite coexpressed during *Xenopus* development. At stage 20 both genes show a weak expression in the dorsal region of the embryo; at stage 24 both are weakly expressed in the eye region and *Xgrn2* is also expressed in migrating neural crest; at stage 28 eye expression persists, but it is very weak for *Xgrn1*; at this stage *Xgrn2* is also expressed in branchial arches and pronephron. The main feature of both expression pattern is a constant dotted signal in the ectoderm, we hypothesize that those signal dots correspond to highly specialized ciliated cells localized in *Xenopus* developing ectoderm. A coexpression with *Xotx* can be found in the anterior part of the brain and in the eyefield, but especially for *Xgrn1* transcripts detectable in those regions are really a few (Fig. 32).

5.6- XOTX interaction domain(s) identification

To identify the precise XOTX portion(s) involved in the interaction with different potential partners, we have transformed yeast cells with prey plasmids and the different not-auto-activating fragments of bait proteins (TH2, TH3, TH4 and TH6 fragments, see above Fig. 27).

For each interactor we have obtained the same results, both using XOTX2 and XOTX5: TH 2 and TH 6 fragments do not interact with any prey, TH 3 and TH 4 interact with all tested preys. Because TH2 and TH6 are negative, this indicate that the XOTX portion they encode is not involved in the interaction; the regions of TH3 and TH4 that are relevant are therefore the “interaction domain”, that spans amino acids 1-25. The fragment corresponding to this region (TH 8, not shown) has been tested for interaction with preys. In this case the results have been ambiguous; the reason of this uncertainty may reside in TH 8 length: TH 8 fragment is too short and its fusion with AD sequence could alter its tertiary structure.

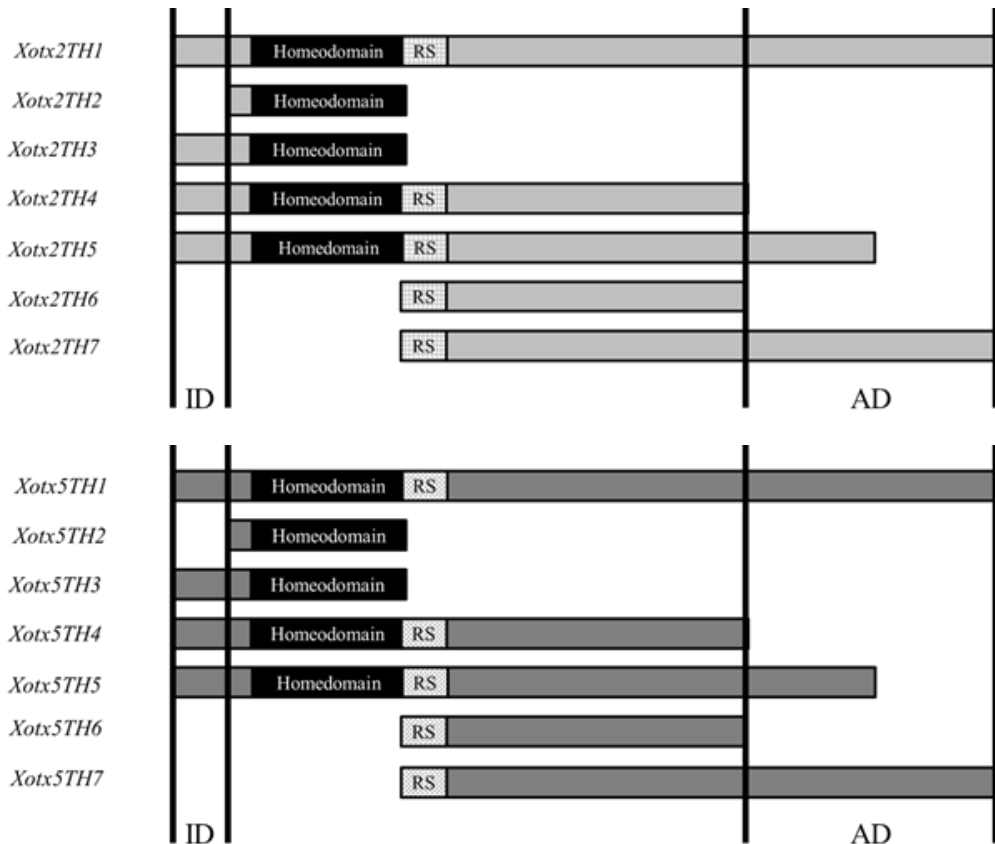


Fig. 33. XOTX2 and XOTX5 interaction and transactivation domains schematics: RS: retinal specificity box; AD: XOTX transactivation domain; ID: XOTX interaction domain.

5.7- XOTX2 and XOTX5 potential cofactors interaction with XOTX1

Since XOTX1 shows a high level of homology with XOTX2 and XOTX5 in the “interaction domain” region (Fig. 34), we decided to test the ability of selected XOTX2 and XOTX5 partners to interact also with XOTX1. To do this, we again used the two hybrid assay: we produced a XOTX1 TH4 construct and verified its incapability to transactivate reporter transcription; then we transformed yeast cells with XOTX1 TH4 fragment together with different preys. All tested preys (C29, XUSF1, XUSF2, XGRN1 and XGRN2) were able to interact *in vitro* also with XOTX1. Given that interactors expression patterns are partial superimposable also with that of *Xotx1*, we

conclude that an interaction of C29, XUSF1/2 and XGRN1/2 with XOTX1 is also possible *in vivo*.

```

XOTX2      MMSYLKQPPYAVNGLSLTASGMDLL
XOTX5      MMSYIKQPHYAVNGLTLAGTGMDLL
XOTX1      MMSYLKQPPYGMNGLGLTGPA MDLL
           ****:**** *.:*** *:...****

```

Fig. 34. XOTX1, XOTX2 and XOTX5 aminotermisus multialignment. “*”: identical residues; “.”: conserved substitution; “.”: semi-conserved substitution.

5.8- c29

5.8.1- C29 and XOTX2/XOTX5 *in vitro* interaction

We next verified the capability of C29 to interact *in vitro* with both XOTX2 and XOTX5 performing a GST-pull down assay (Fig. 35). For this, we produced C29 GST-fusion proteins in BL21 Bacterial cells, while both XOTX2 and XOTX5 were produced as myc-tagged forms in HEK 293T cultured cells. Baits were linked to a Glutation-Sepharose resin, and preys were added. After several washes the presence of preys linked to baits was detected by Western Blotting. We detected the presence of both XOTX-myc-tagged proteins linked to C29-GST fusion proteins: C29 is able to interact *in vitro* with both XOTX. Difference in myc-tagged protein quantity revealed in the two Western blotting is due to a different input of the two parallel experiments.

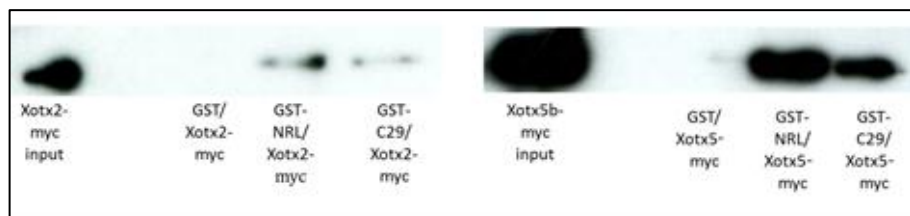


Fig. 35: Western blot following GST-pull down for C29-XOTX2/XOTX5 interaction assay. Ab1: anty-myc mouse; Ab2: GAM-Pod.

5.8.2- c29 localization in the *X. tropicalis* genome

By searching among databases, we have found several cDNA sequences corresponding to our clone *c29* isolated by two hybrid screen; thus it is possible that *c29* fragment really corresponds to a transcribed sequence. To confirm this, we have localized *c29* sequence into *Xenopus tropicalis* genome assembly (http://www.ensembl.org/Multi/blastview/BLA_MboVn22kj) and verified the presence of all sequence elements necessary to initiate mRNA transcription and to eukaryotic mRNA postranscriptional modification. We have localized *c29* hypothetical homologues on *Xenopus tropicalis* genomic scaffold GL172685.1 (Fig. 36 A); between *c29* 5' and 3' half we identified a long interposed region on *X.tropicalis* genome. We can thus hypothesize that *c29 X.tropicalis* homologue is encoded by a sequence made up of two exons divided by a long intronic sequence. By analyzing *X.tropicalis* sequence we have identified: a Kozak consensus sequence around our hypothetical initiation codon, exon-intron junction consensus sequences at hypothetical intron borders and a polyadenylation signal localized into hypothetical 3'-UTR. The hypothetical protein encoded by the *X.tropicalis* genomic sequence shows a high level of homology (96%) with C29 deduced protein (Fig. 36 B).

A

5' -CATTGGCCGAGTTCCCCATGGGTGAACCCTCatgATGqAGCTAAGTGCAAACTG
ACTAACAGAGACGGTAGTTGTCGTCCTGTTTTCAGTTTAGATGTGAGCGAACGTTGAAAGGA
CTGGCGAGTGGCCTGGAGCAGCTAAAAGGAGAAGTGTCCACCATTTTAACCGAGCTGGTG
TTACAAGAAAAGGGAGAGGGGGCACTGACATCTGGAGATCAGGAATCTGCAGGTCAGAGC
ATTATAATGAATTTGCTCTCAAAGGCTTTCCTGCGCTTCAGGGCAGCGAAGGGTCTCTGT
[...] TGAATGATATAACTGAGCACCATTATAAGCACGCATTTGGTAAGGTTTTTGTGTCT
TTTAAATATTATAAGTGAACCTTTTATCACTCTTTATTAGGTGAAGAAGATGACGAAGAT
GCAGATGAAAAAGATTTTGTCTGAAAATGGAGTAAGCAGTAATGGACCTCCTACTAAAAGA
AAGAAAAATCAGGATTGAATTGAATTTACTTGAACATTATTTTGGTCATCTCTTTGTAAA
TAATGCAGGTCCTTCTTTATACTGTATGCTCTGACTTGGACTAAAACCTAAGGATACAAT
TTTGTTCAGTATGTAATTTTCACTGTAAATGCACAAAAATCAAGGCATTTTAAATAA
TAAATACACCTTTTTCTAACTGCAGTTTTAGTTGAATAGTAACCATAGCTCAACTGCAGA
TTTTTCTTTTTTACAGATTCACAATTTTGTTCCTCTTGGATTTGGGTAGCGCGTATTA
AATAAACAAAACAGCAGCAGCTTTTTGTTGTTTTTTTACCTTTTCTGGAGTAAACCCAAA
TAAACTGTTTAAATAATATGGTTTGAGTCCAGGAAAAATAATTAACATGCTTTGGTGGGTA
CCTAAGGTTTTTTGAGTTGTACAGCAGTCTTCTTAGGGACAAGAAAACCTATGAGCAAC
AGAAGCATAACAGTAGGGGCAGCAAGAAAACAGAGTGGCCAGTTGGTGTTTTTGGGATAT
GTCAATTCGAGCATATATTTGCAAAACACAATCTTTTCAAGGTGGTATAGCTTGTGGTTG
TGCCACTTTACACAGGTATGGGACCTGTTATCCAGAATGCTGGGGACCTGGGGTTTTCCG
GATAAGGGATCTTTTCGTAATTTGAATCTCCATAACTTAAGTCTGCTAAAAATCATTTAA
ATATTA**AATAAA**CCCAACAGGCTGTTTTGCCTCCAATAAGGATTAATTATATCTTA
GTGGGATCAAGTACAAGGTACTGTTTTATTATTACAGAGAAAAGGAAATTATTTCT-3'

- CODING REGION
- NON CODING REGION
- Kozak sequence consensus:



- Initiation codon
- Exon-intron junction consensus sequence
- Poliadenilation signal

B

X. tropicalis hypothetical amino acid sequence:

MELSAELTNRDGSRRPFQFRCERTLKGLASGLEQLKGEVSTILTELVLQEKGEGALTSGDQESAGEEDD
 EDADEK DFAENGVSSNGPPTKRKNQD*

C29 deduced sequence:

MELSAELSNRDGSSRRPFQVRCERTLKGLANGLEQLKGEVSAVLTELVLQEKGEGALAAGDQEFAGEEED
 EEDTDEKDFSENGISSNGPPTKRKNIQD*

Alignement

tropicalis	MELSAELTNRDGSRRPFQFRCERTLKGLASGLEQLKGEVSTILTELVLQEKGEGALTSGD	60
laevis	MELSAELSNRDGSSRRPFQVRCERTLKGLANGLEQLKGEVSAVLTELVLQEKGEGALAAGD	60
	*****:*****.****.*****.*****.:*****:*****:*****:*****	
tropicalis	QESAGEEDE-DADEK DFAENGVSSNGPPTKRKNQD	96
laevis	QEFAGEEEDDEEDTDEKDFSENGISSNGPPTKRKNIQD	97
	** ****:* * :*****.***:*****.* **	

Fig. 36. *Xenopus tropicalis* genomic region containing *Xenopus laevis* c29 homologues: A: *X.tropicalis* genomic sequence aligning with *X.laevis* c29 sequence; see box legend; B: *X.tropicalis* deduced amino acid sequence and *X.laevis* predicted sequence alignment. Sequences multi-alignment has been obtained using ClustalW. “*”: identical residues; “.”: conserved substitution; “.”: semi-conserved substitution.

5.8.3- C29 *in silico* secondary structure prediction

Bioinformatics tool PsiPred (<http://www.bioinf.cs.ucl.ac.uk/psipred>) was used to *in silico* predict C29 secondary structure (Fig. 37). This tool allows predicting protein secondary structure based on amino acid sequence; we have deduced C29 hypothetical primary sequence starting from c29 nucleotide sequence, assuming the first “atg” triplet to be the initiation codon. PsiPred output shows the presence of a α -helix domain, predicted with a high level of confidence, separated by a coil region from a second shorter helix structure. This kind of structure is characteristic of several transcription factors (i.e. homeoproteins, bHLH factors). Since XOTX

NUCDISC: discrimination of nuclear localization signals	
pat4:	none
pat7:	PPTKRNK (3) at 88
pat7:	PTKRNKI (4) at 89
bipartite:	none
content of basic residues:	11.3%
NLS Score:	0.13
	82.6 %: nuclear
	17.4 %: mitochondrial

Fig. 38. C29 subcellular localization prediction. PSORT output is shown.

5.8.5- C29 sub-cellular localization

C29 is a novel hypothetical peptide, thus no antibody against it is as yet available. Therefore, to obtain indication about C29 subcellular localization we have prepared a C29 myc-tagged form, microinjected it as mRNA in *Xenopus* embryos, that were grown to tadpole stage; we then localized this fusion protein using an anti-myc antibody in embryo sections. Fusion proteins were mostly localized into nuclei (Fig. 39 A).

C29 is a small peptide; its predicted molecular weight is of about 10,5 kDa; thereby we could not exclude its free diffusion across nuclear pores. To verify if C29 nuclear localization is due to its NLS or to free diffusion, we prepared a truncated C29 myc-tagged form lacking C-terminal NLSs (C29-NLS-STOP-myc) and checked its subcellular localization. C29-NLS-STOP-myc proteins were diffused into cytoplasm (Fig. 39 A): hence we conclude that C29 NLS is necessary for its nuclear localization. To verify if this NLS could be also sufficient to drive a cytoplasmic protein into to the nucleus, we cloned it downstream of cytoplasmic RFP coding region and analyzed the subcellular localization of the resulting fusion protein RFP-C29NLS. Cytoplasmic RFP containing C29 NLS showed a strong nuclear

accumulation (Fig. 39 B). We conclude that C29 NLS could be necessary and sufficient to determine its nuclear localization *in vivo*.

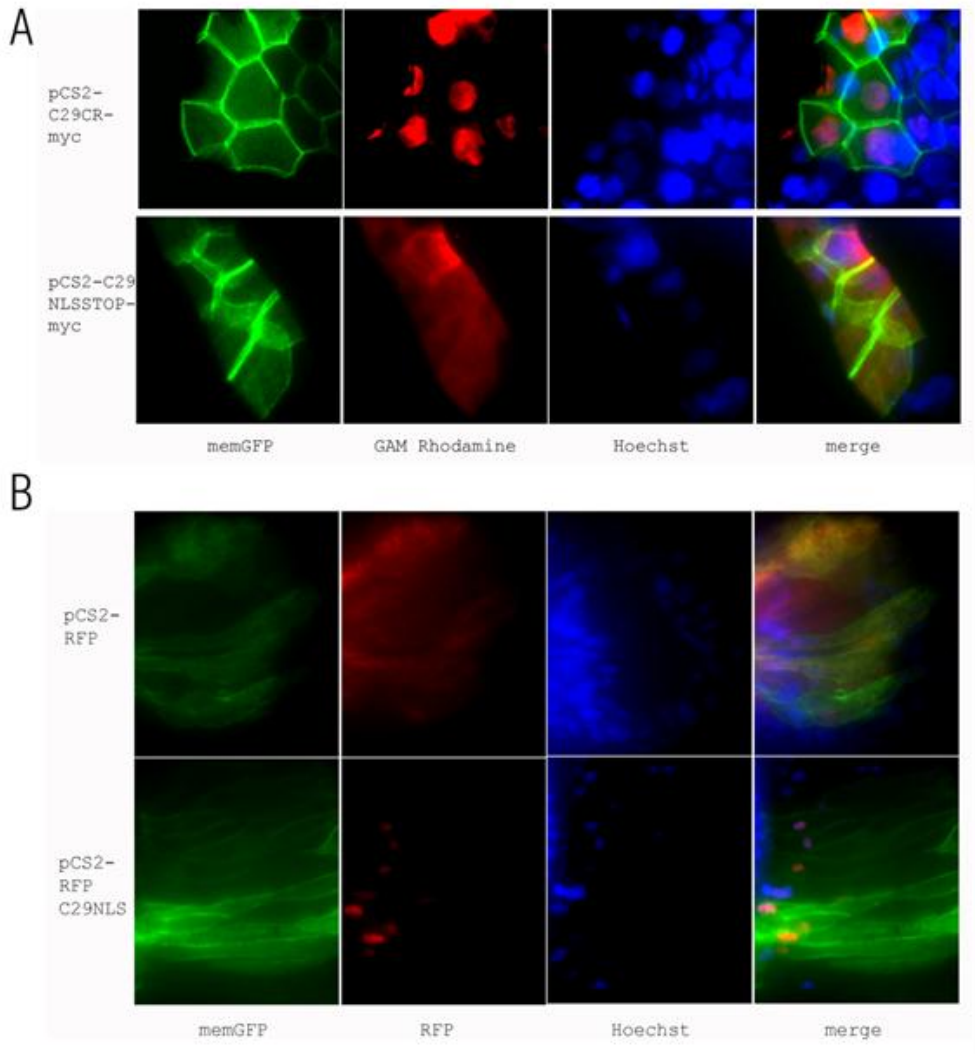


Fig. 39. C29 NLS functional analysis: embryos at 4-cell stage have been injected, grown till tadpole stage and then sectioned. Immunostaining has been performed on sections; Ab1: anti-myc mouse; Ab2: goat anti mouse Rhodamine. Injected constructs are indicated on the left; memGFP has been injected as tracer; Hoechst has been used as nuclei marker. Green fluorescence: (A, B) memGFP; Red fluorescence: (A) antibody conjugated rhodamine, (B) RFP; Blue fluorescence: (A, B) Hoechst staining.

complete disappearance of *nrp-1* signal on injected side with a frequency of 44,4% (Fig 41 and Tab 8).

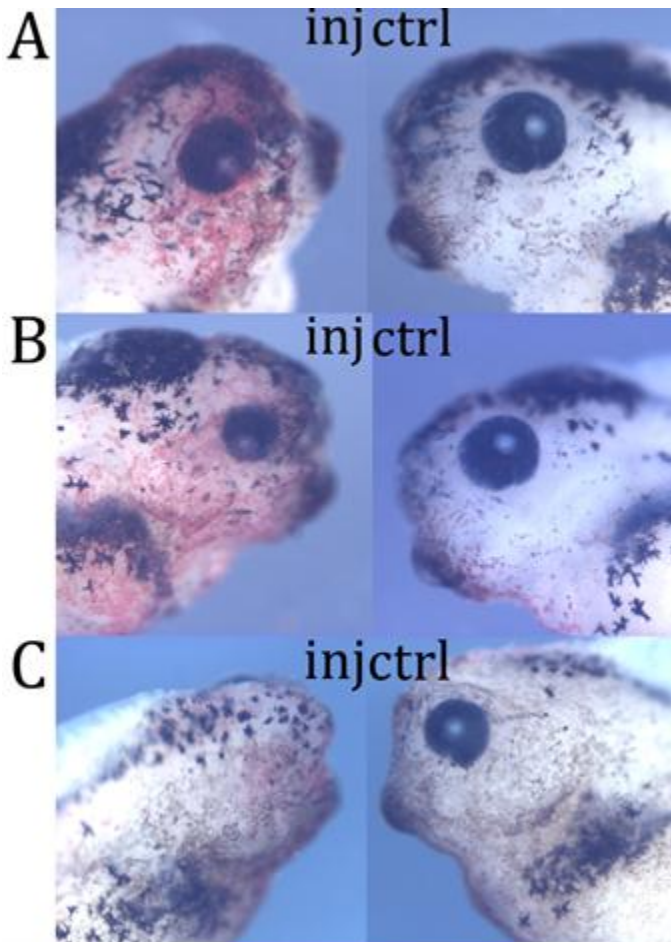


Fig. 40. Results of Moc29 microinjection. (A): coloboma; (B): microphthalmia; (C): anophthalmia. Lac Z is used as a tracer.

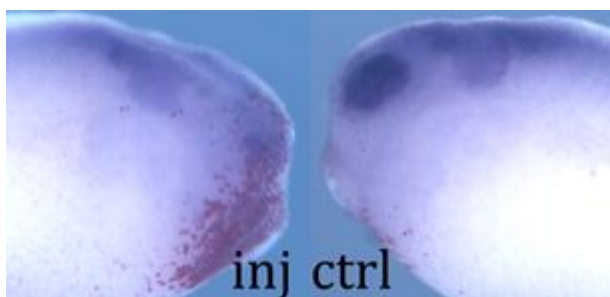


Fig. 41. Results of Moc29 microinjection and *nrp-1* WISH. Dorsal injection of 40 ng Moc29 and *nrp-1* WISH. Lac Z is used as a tracer. Note that *nrp-1* signal strongly decreases on injected side.

Tab. 7. Results of Moc29 embryos microinjections.

dose	site	defective/ absent eye	normal eye	<i>n</i>
40 ng	dorsal	82 (70,1%)	35 (29,1%)	117
20 ng	dorsal	31 (22%)	110 (78%)	141
		37 (27,6%)	97 (72,4%)	134
20 ng	dorsal bilateral	58 (77,3%)	17 (22,7%)	75
		27 (69,2%)	12 (30,8%)	39
5 ng	dorsal bilateral	21 (52,5%)	19 (47,5%)	40
		21 (53,8%)	18 (46,2%)	39

Moc29 injection doses are indicated in nanograms; injection site and number of injected blastomeres are shown; brackets indicate frequency of affected/normal embryos; each row corresponds to one independent experiments. *n*: number of injected embryos.

Tab. 8. Results of Moc29 embryos microinjections and *npr-1* WISH.

dose	site	npr-1 reduction	NO npr-1 teduction	<i>n</i>
40 ng	dorsal	24 (44,4%)	30 (55,6%)	54

Moc29 injection dose is indicated in nanograms; injection site is shown; brackets indicate frequency of affected/normal embryos; each row corresponds to one independent experiments. *n*: number of injected embryos.

To confirm Moc29 specificity we have prepared a sensor construct harbouring Moc29 target sequence fused with GFP coding region. We microinjected the sensor construct alone or together with Moc29 and checked embryos for green fluorescence from mid-gastrula stage to tadpole stage. After the microinjection of sensor plasmid alone we detected GFP fluorescence from mid gastrula stage to tadpole stage, while after sensor and Moc29 coinjection we never observed fluorescent signal (Fig. 42). We conclude that Moc29 binding blocks GFP mRNA translation *in vivo*; thus observed phenotype may be due to a specific *c29* block of translation. Rescue experiments in which *c29* function is recovered by *c29* coding region mRNA are now ongoing.

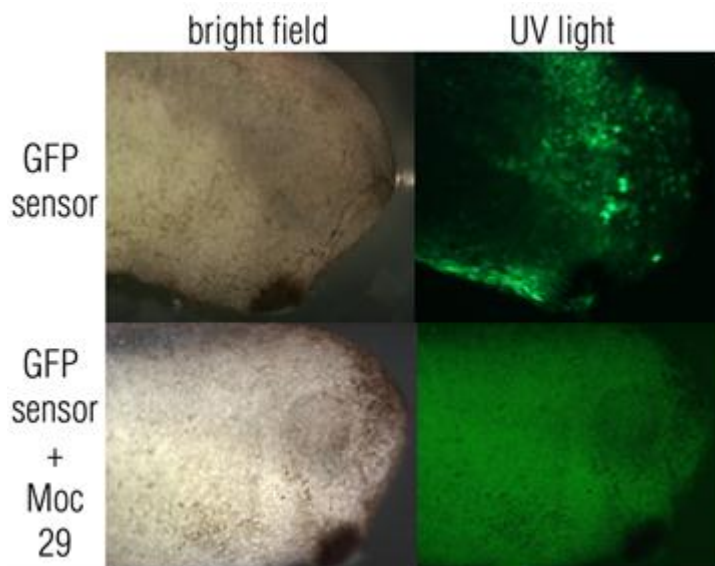


Fig. 42. results of GFP sensor and Moc29 injection.

After 100 pg sensor injection GFP green fluorescent signal is detected; after 100 pg GFP sensor and 10 ng Moc29 coinjection any fluorescence is detected.

5.9- *Xusf2*

5.9.1- XUSF2 and XOTX2/XOTX5 *in vitro* interaction

We have verified the capability of XUSF2 to interact *in vitro* with both XOTX2 and XOTX5 performing a GST-pull down assay (Fig. 43). XUSF2 GST-fusion proteins were produced in BL21 Bacteria cells and both XOTX2 and XOTX5 as myc-tagged forms in HEK 293T cultured cells. Baits were linked to a Glutathione-Sepharose resin, and preys were added. After several washes the presence of preys linked to baits was detected by Western Blotting. We detected the presence of both XOTX-myc tagged proteins linked to XUSF2-GST fusion proteins: XUSF2 resulted able to interact *in vitro* with both transcription factors.

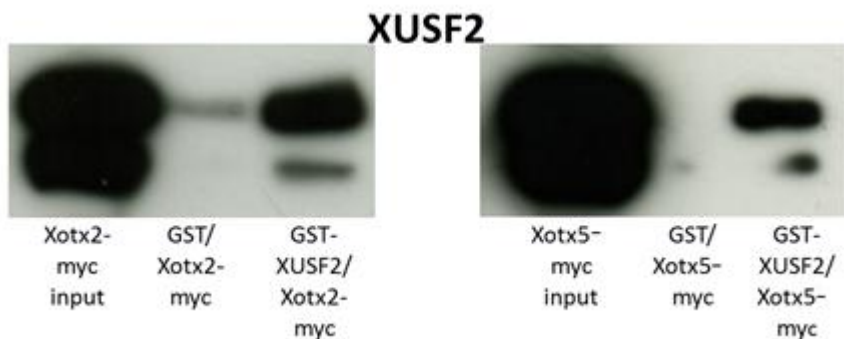


Fig. 43. Western blot following GST-pull down for XUSF2-XOTX2/XOTX5 interaction assay. Ab1: anty-myc mouse; Ab2: GAM-Pod.

5.9.2- XUSF2 and XOTX2/XOTX5 antagonistic action on Rhodopsin promoter

XUSF2 is a transcription factor of the basic-helix-loop-helix-leucine zipper (bHLH-zip) family. The regulating proteins of this class bind to E-box cis-regulating elements. *Xenopus laevis* Rhodopsin promoter contains this kind of regulating sequences, therefore USF2 could be able to promote Rhodopsin transcription. XOTX2 and XOTX5 are both able to synergize with NRL to bind and transactivate Rhodopsin promoter (Mitton et al., 2000; Whitaker and Knox, 2004; Peng and Chen, 2005; Onorati et al., 2007). Therefore we hypothesized that XOTX and XUSF2 can synergize to transactivate the *Xenopus* Rhodopsin promoter. We investigated our hypothesis by monitoring their ability to activate a *Xenopus* rhodopsin promoter (XOP) driving green fluorescent protein (GFP) expression in HEK 293T cultured cells. As previously described (Mitton et al., 2000; Whitaker and Knox, 2004; Peng and Chen, 2005; Onorati et al., 2007), we verified that XOTX and NRL are able to synergize on XOP, since cells transfected with both plasmids showed a higher level of GFP expression in respect to cell transfected with XOTX only. Interestingly XOTX and XUSF2 cotransfection has the opposite result: GFP expression levels strongly decreases in cotransfected cells in respect to cell transfected with XOTX only. We conclude that XOTX and XUSF2 can operate in an antagonistic fashion on the *Xenopus* opsin promoter. Besides, we noted a stronger inhibition of XUSF2 on XOTX5 in respect to XOTX2 (see Fig. 44 and 45 for relative percentage of GFP positive cells).

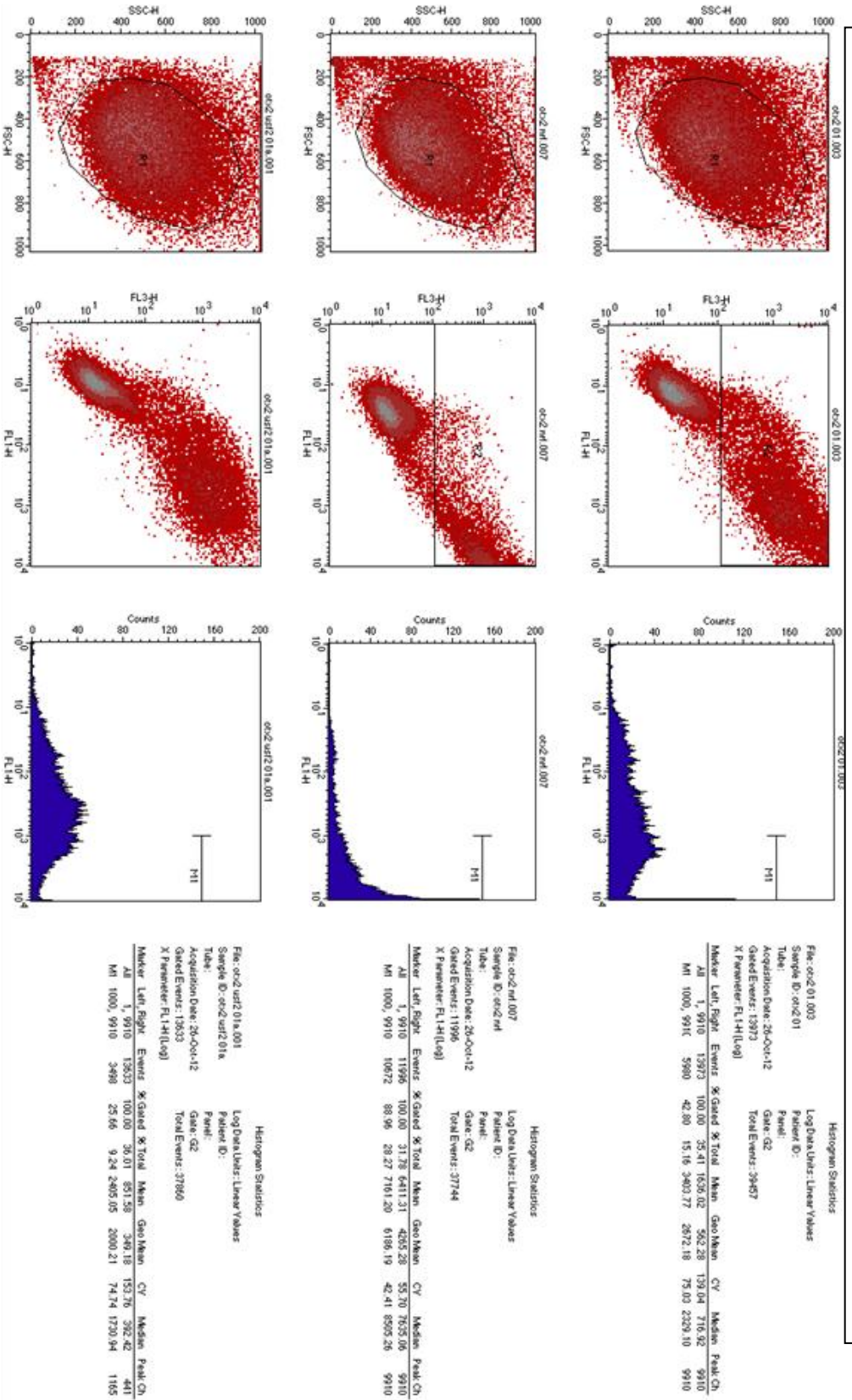
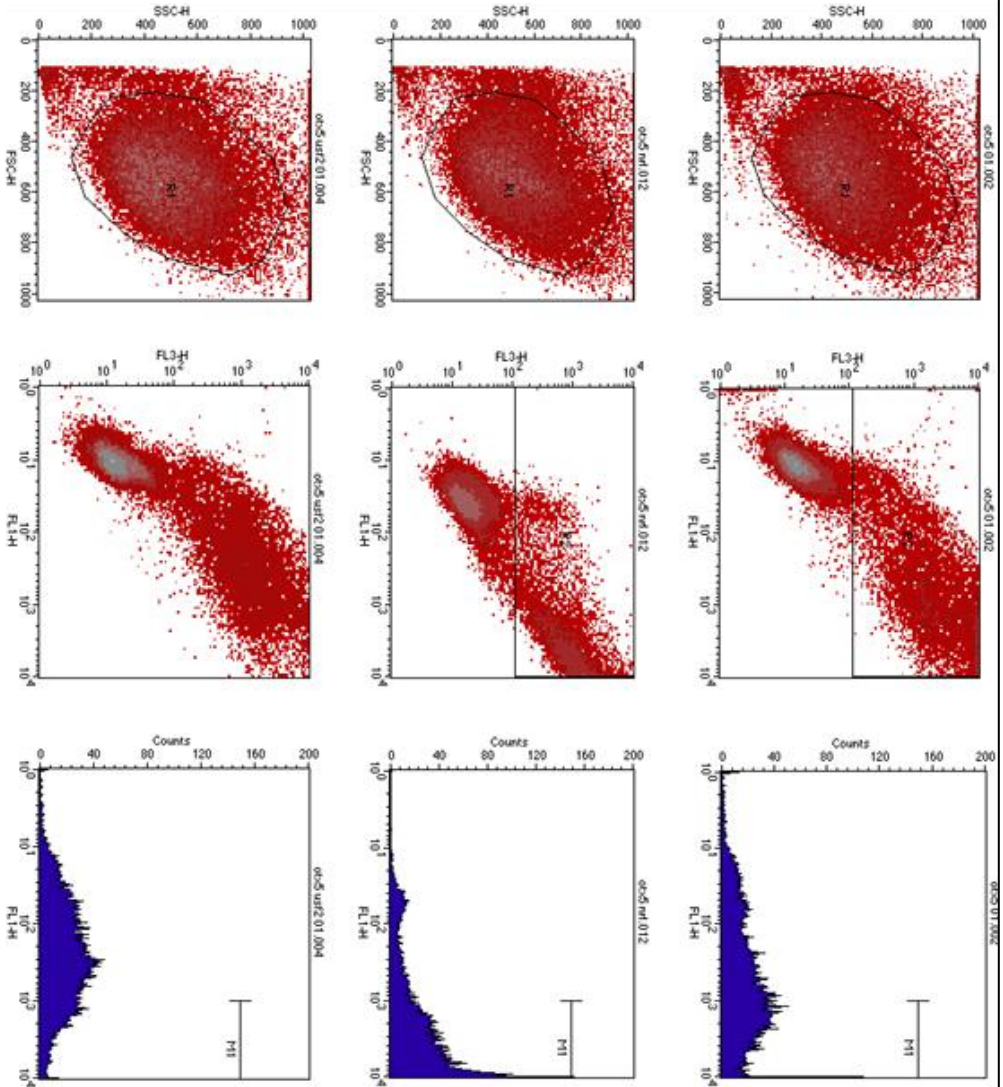


Fig. 45. Graphs images of transfected HEK 293T cells.
 The cotransfection of Xclx5 with Xrf1 and Xus2 elicits different level of GFP fluorescence. RFP represents the control for the transfection. Green fluorescence is scored together with Red fluorescence. First dot plot represents the selected cell population; second dot plot represents red versus green fluorescence; a graph shift to the right corresponds to GFP activation increase; a graph shift to the left corresponds to GFP activation decrease; the last graph represents established fluorescence gate. Table: percentage of GFP positive cells are reported (with the help of Dr. Michele Bertocchi and Luca Pandolfini).



Histogram Statistics

File: o45:01.002	Log Data Units: Linear Values
Sample ID: o45:01	Parameter ID:
Tube:	Gate: G2
Acquisition Date: 28-Oct-12	Gate: G2
Gate Events: 13118	Total Events: 38214
X Parameter: FL1-H [Log]	
Marker Left Right	Events % Gate % Total Mean GeoMean CV Median Peak Ch
A1 1, 9910 13118 100.00 34.33 1625.41 535.80 148.46 704.14 9910	
M1 1000, 9910 5505 42.19 14.48 3427.49 2684.89 75.10 2350.14 9910	

Histogram Statistics

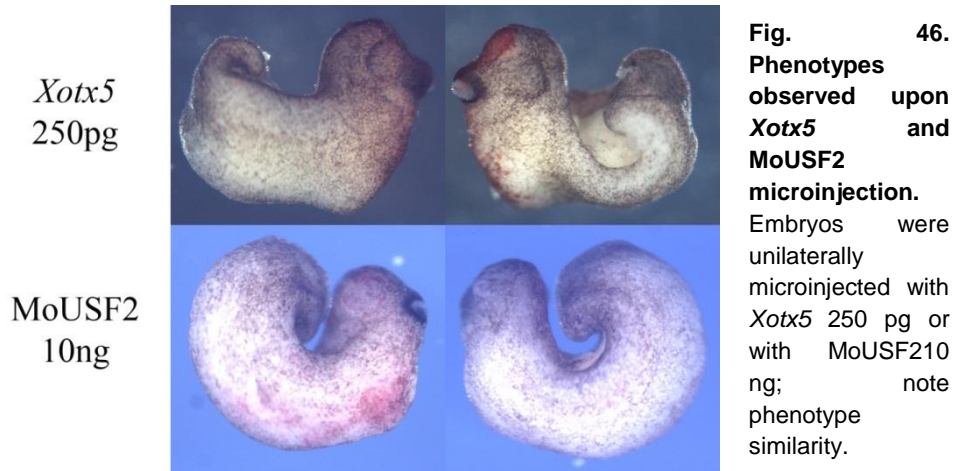
File: o45:rd1012	Log Data Units: Linear Values
Sample ID: o45:rd1	Parameter ID:
Tube:	Gate: G2
Acquisition Date: 28-Oct-12	Gate: G2
Gate Events: 15721	Total Events: 39691
X Parameter: FL1-H [Log]	
Marker Left Right	Events % Gate % Total Mean GeoMean CV Median Peak Ch
A1 1, 9910 15721 100.00 39.82 5301.50 2081.01 69.93 5093.88 9910	
M1 1000, 9910 12939 82.30 32.61 6366.10 5288.24 50.36 6792.53 9910	

Histogram Statistics

File: o45:rd201004	Log Data Units: Linear Values
Sample ID: o45:rd201	Parameter ID:
Tube:	Gate: G2
Acquisition Date: 28-Oct-12	Gate: G2
Gate Events: 13407	Total Events: 36627
X Parameter: FL1-H [Log]	
Marker Left Right	Events % Gate % Total Mean GeoMean CV Median Peak Ch
A1 1, 9910 13407 100.00 36.60 6711.75 243.82 175.27 259.46 278	
M1 1000, 9910 2530 18.87 6.91 2438.23 2002.20 76.65 1700.08 1197	

5.9.3- XUSF2 and XOTX5 microinjection experiments: preliminary data

To check the capability of XUSF2 and XOTX5 to antagonize also *in vivo*, we injected *Xotx5* alone and together with *Xusf2* mRNAs in *Xenopus* embryos, and monitored the two typical phenotypes obtained upon *Xotx5* microinjection: posterior defect induction (Fig. 46) and ectopic cement gland formation. The dorsal microinjection of 250 pg of *Xotx5* causes posterior defects (Fig. 46) with a frequency of 82,7%, while upon the coinjection of *Xotx5* with *Xusf2* the frequency of this phenotype strongly decreases, down to 39,3% (Tab. 9). Almost the same 50% reduction is observed after ventral microinjection (Tab. 9). On the other hand, we do not observed almost any difference of ectopic cement gland frequency between embryos injected with *Xotx5* or with *Xotx5+Xusf2* (Tab. 10). The dorsal microinjection of 10 ng of oligo antisense Morpholino against *Xusf2* 5'UTR (MoUSF2) causes posterior defects analogous to those observed upon *Xotx5* microinjection (Fig. 46), with a frequency of 33,6%, while upon microinjection of the same dose of mis-matched MoUSF2 (MisMoUSF2), used as negative control, we observed this phenotype with a lower frequency (15,3%) (Tab. 11). Consistent results have been obtained by reducing MoUSF2 and MisMoUSF2 to 5 ng. All these data taken together suggest the possibility of the existence of an antagonistic interaction between XOTX5 and XUSF2 in modulating convergent extension, while this interaction does not have any effect on XOTX5 cement gland inducing capability.



Tab. 9. Results of *Xotx5* injection and of *Xotx5* and *Xusf2* coinjection.

Exp. n°	Injected constructs	Injection site	Posterior defect	NO posterior defect	<i>n</i>
1	<i>Xotx5</i> 250pg	Dorsal	67 (82,7%)	14 (17,3%)	81
	<i>Xotx5</i> 250pg+ <i>Xusf2</i> 250pg	Dorsal	42 (39,3%)	65 (60,7%)	107
2	<i>Xotx5</i> 250pg	Ventral	31 (22,2%)	109 (77,8%)	140
	<i>Xotx5</i> 250pg+ <i>Xusf2</i> 250pg	Ventral	29 (13,2%)	192 (86,8%)	221

Embryos are scored for posterior defects. Injected doses and injection sites are indicated; in brackets embryos percentages are shown; *n*: number of embryos.

Tab. 10. Results of *Xotx5* injection and of *Xotx5* and *Xusf2* coinjection.

Exp. n°	Injected constructs	Injection site	Ectopic cement gland	NO ectopic cement gland	<i>n</i>
1	<i>Xotx5</i> 250pg	Ventral	53 (37,9%)	87 (62,1%)	140
	<i>Xotx5</i> 250gp+ <i>Xusf2</i> 250pg	Ventral	100 (45,3%)	121 (54,7%)	221
2	<i>Xotx5</i> 125pg	Ventral	40 (26%)	114 (74%)	154
	<i>Xotx5</i> 125pg+ <i>Xusf2</i> 250pg	Ventral	20 (37%)	34 (63%)	54

Embryos are scored for ectopic cement glands formation. Injected doses and injection sites are indicated; in brackets embryos percentages are shown; *n*: number of embryos.

Tab. 11. Results of MoUSF2 and MisMoUSF2 microinjection.

Exp. n°	Injected constructs	Injection site	Posterior defect	NO posterior defect	<i>n</i>
1	MoUSF2 10ng	Dorsal	38 (33,6%)	75 (66,4%)	113
	MisMoUSF2 10ng	Dorsal	13 (15,3%)	72 (84,7%)	85
2	MoUSF2 5ng	Dorsal	23 (13,7%)	145 (86,3%)	168
	MisMoUSF2 5ng	Dorsal	9 (7,6%)	110 (92,4%)	119

Embryos are scored for posterior defects. Injected doses and injection sites are indicated; in brackets embryos percentages are shown; *n*: number of embryos.

6- Discussion section I: cemnt gland, convergent extension and neural tissue

We have performed a molecular dissection analysis of the XOTX1 and XOTX5 proteins in order to identify the molecular domains involved in their inability/ability to promote CG and neural tissue formation, and responsible for their capability to inhibit convergent extension movement at a different extent.

A first set of injections with swapped constructs where the C-terminal parts of XOTX1 and XOTX5 were exchanged, clearly showed that the CG promoting activity relies on the C-terminal part. To map the functional domains of XOTX5 required for CG induction, we prepared a series of C-terminal deletion constructs. Injections of their mRNAs showed that the region corresponding to aa 210-255 contains the most active CG promoting domain (CGboxD1, that is largely co-extensive with the His-rich region of XOTX1); its removal causes a strong reduction of CG frequency in injected embryos, as well as a consistent decrease of CG markers in animal cap assays. Another region (CGboxD2, aa 177-209), is also involved in CG promoting activity: its removal causes a further decrease of *Xag* and *Xcg* expression in animal cap explants, and the almost complete disappearance of ectopic CG on whole embryos.

Furthermore, our results showed that the XOTX1 His-rich region exerts the major inhibitory function on CG promoting capability: when this region is removed, the *Xotx1 Δ His* construct becomes able both to elicit ectopic CG development in whole embryos and to turn on expression of CG markers in animal cap assays. However, results in whole embryos and in animal caps show clearly that *Xotx1 Δ His* is not as efficient as *Xotx5*, that induces a higher frequency of ectopic CGs and a higher activation of *Xag* and *Xcg* in animal caps. This is due to the fact that the His-rich region of XOTX1 is contained within the XOTX1 region aligning with XOTX5 CGboxD1 (Fig. 23): when the His-rich region is deleted, we do not actually “restore” the XOTX5

CGboxD1 sequence, because at the same time we are deleting non-His residues conserved between the two proteins that may play a crucial role in CG inducing action; this could explain why the CG promoting activity is not fully rescued in *Xotx1ΔHis*. In addition, also the XOTX1 Ser-rich region may exert a similar, though weaker, inhibitory function on this potential *Xotx1* activity: in fact, *Xotx1ΔSer* is able to weakly activate *Xag* expression in the animal cap assay, though it remains unable to transactivate *Xcg* or to promote the formation of ectopic CGs on whole embryos. This is also confirmed by the fact that *Xotx1ΔHisΔSer* seems more effective than *Xotx1ΔHis* in inducing *Xag* expression in injected caps. However, also *Xotx1ΔHisΔSer*, like *Xotx1ΔHis* does not have the full activity of *Xotx5*, again suggesting that coextensive deletion of non-His residues in *Xotx1ΔHisΔSer* may compromise the CGboxD1 activity. Therefore, we conclude that *Xotx1* His-rich region strongly inhibits *Xotx1* adhesive organ formation capability, while the Ser-rich region may exploit only a much weaker inhibition.

The strong inhibitory action of His-rich region could be the result of disrupting the structure of a CG inducing domain within the XOTX C-terminal; besides, the His stretch could also turn a CG promoting domain into a CG repressing domain. We showed that the XOTX1 His-rich region acts as a domain actively repressing the potential of XOTX proteins to promote CG, rather than being only a simple disruptor of the CGboxD1; in fact, while *Xotx5-255ΔC*, harboring both CGboxD1 and CGboxD2, works as efficiently as *Xotx5*, the *Xotx5-255ΔC-His-rich* construct is completely unable to promote ectopic CG in whole embryos, and only weakly induces CG markers in animal caps.

These data suggest that the His-rich region has an active repressive role on the XOTX domains responsible for CG promoting activity. On the whole, the analysis of the CG activating and repressing domains in XOTX1 and XOTX5 provide a molecular explanation of their diverse actions.

Our data regarding *Xotx5* CG promoting domains are quite coherent with those obtained by Gammill and Sive (2001). They showed that *Xag* is more

weakly induced by *Xotx2* after the removal of its 81 C-terminal residues, almost corresponding to our CGboxD1 plus the OTX-tail; besides, they demonstrated that *Xag* is not induced at all after the removal of the 129 C-terminal *Xotx2* residues, a region comprising our CGboxD1, CGboxD2 plus six aa residues N-terminal to CGboxD2. The main difference between our results and those of Gammill and Sive (2001) is that the removal of the OTX-tail from XOTX5 does not cause a diminution of the transactivation capability on *Xag* and *Xcg*, while they observed such a reduction after removing the XOTX2 OTX-tail.

Xotx1 and *Xotx5* share a similar effect on gastrulation movements, but *Xotx1* is less efficient than *Xotx5* in inhibiting convergent extension. All constructs used in the present study are able to induce gastrulation defects when misexpressed. Interestingly, we observed an increase of posterior defect frequency following the microinjection of *Xotx1ΔHis*, compared to *Xotx1*, while the microinjection of *Xotx1ΔSer* does not show any significant variance in respect of full length construct. Consistent with this, the misexpression of *Xotx1ΔHisΔSer* completely resemble the microinjection of *Xotx1ΔHis*. So, we speculate that the His-rich region has an inhibitory effect also on *Xotx1* gastrulation defect inducing capability, while Ser-rich domain does not affect at all this function of *Xotx1*.

The deletion of XOTX5 OTX-tail does not have any effect on its ability to inhibit convergent extension, since the microinjection of *Xotx5-255ΔC* does not show almost any significant variation in inducing gastrulation defects in respect of *Xotx5*; the small difference observed in the percentage of embryos showing posterior defects it is probably due to different batches of embryos used in different experiments. Similarly, the microinjection of the shorter construct, *Xotx5-210ΔC*, lacking the OTX-tail together with CGboxD1, also has the same effect of *Xotx5*. These results led us to conclude that CGboxD1 is not involved in *Xotx5* convergent extension inhibiting activity. On the contrary, the deletion of *Xotx5* CGboxD2 seems to affect it: embryos microinjected with *Xotx5-177ΔC* show posterior defects

with a significantly lower frequency compared to *Xotx5* injected ones. Anyway, the ability of *Xotx5* to inhibit convergent extension is completely lost when the C-terminal deletion reaches the homeodomain. We conclude that CGboxD2 is involved in regulation of gastrulation movements, but there are other regions upstream of it involved in this activity.

Xotx1ΔHis does not completely reproduce *Xotx5* efficiency in eliciting posterior defects; thus, *Xotx1* lower efficiency in respect of *Xotx5* cannot be due only to the His-rich region. Besides, since the CGboxD1 seems not to be involved in regulation of gastrulation movement, the removal of non-His residues in the *Xotx1ΔHis* construct is not responsible for its minor efficiency in respect of *Xotx5*. On the other hand, in spite of XOTX1 high similarity to XOTX5 at level of the CGboxD2 and upstream of it, the differences in their efficiency in causing posterior defects can be due to few sequence differences between the two homeoproteins in this region, that may be directly involved in convergent extension inhibition.

We conclude that *Xotx5* CGboxD1 is a functional domain more specifically involved in mediating the CG promoting activity and not that on convergent extension, while CGboxD2 may be also relevant for inhibition of convergent extension; in addition, we can hypothesize that in XOTX1, the His-rich region exerts its inhibitory effect on convergent extension by acting on CGboxD2, plus, eventually, additional N-terminal region(s).

The insertion of the His-rich region downstream to *Xotx5-255ΔC* does not affect its convergent extension effect, contrary to what we observe for CG promoting activity. We may not exclude that the His-rich region has different actions when positioned in diverse parts of the XOTX protein.

We also demonstrated that the RS box is not involved at all in gastrulation movement regulation, since its removal does not influence *Xotx5* posterior defect induction.

Our results clearly show that the XOTX1 specific His-rich region exerts a crucial function in differentiating XOTX actions. The comparison of OTX related proteins from different species suggests the importance of the His-

rich region during evolution. Histidine stretches, in almost the same position, are present in all OTX1 proteins and are considered a distinctive character of this orthology group, being absent in other OTX proteins of Gnathostomes and in OTX of all other organisms (Germot et al., 2001). It is strongly probable that these OTX1 peculiar regions appeared, for instance as insertions, in an *Otx1* ancestral gene, that initially had functional characters similar to other *Otx*. It is interesting to note that the microinjection of *Drosophila otd* in *Xenopus* embryos leads to the formation of ectopic adhesive organs (Lunardi and Vignali, 2006), suggesting that the ability to activate the genetic pathways that are involved in *Xenopus* CG formation is an ancestral property of OTX/OTD proteins, that XOTX1 has lost upon the appearance of the histidine stretch; also human *Otx1* does not induce CG (Andreazzoli et al., 1997), while, on the contrary, human *Otx2* does (Pannese et al., 1995). An interesting aspect of *Otx1* function comes out from experiments in mouse; in this organism *Otx1* is involved in the development of the lateral semicircular canal of the inner ear, the absence of which is not rescued either by *Otx2* or by *otd* (Acampora et al., 1996; 1998; Morsli et al., 1999). It may be possible that *Otx2* inability to rescue *Otx1*^{-/-} defects could be due to the absence of the His-rich region. Given that the His-rich region is the most conserved divergent character between *Otx1* and the other *Otx*, these data taken together can suggest the hypothesis that the His-rich region is implicated in modulating two different genetic pathways: the insertion of the histidine rich region inhibits *Otx1* capability to induce CG formation and, on the other hand, makes it able to activate the genetic pathway responsible for the development of the inner ear semicircular canal. From this point of view the insertion of the His-rich region in OTX1 could be an interesting case where evolution of a new part of protein has led both to gain and loss of functions on the ancestral protein. However, we cannot exclude that the Ser-rich region may play a novel evolutionary role in OTX1; even though our experiments may suggest for it a minor role, this may be due to the specific aspects investigated in our experimental system.

Another functional difference between *Xotx1* and *Xotx5* is that, while *Xotx5* is able to elicit ectopic neural tissue formation in whole embryos if misexpressed, *Xotx1* does not. None of the *Xotx1* deleted constructs used in the present study are able to induce neural markers either in whole injected embryos or in animal cap assays. We can speculate that XOTX1 incapability to induce neural differentiation, differently from what previously seen, is not due to an inhibitory effect of XOTX1 specific regions (His-rich or Ser-rich region), since their removal from XOTX1 protein does not lead to a recovery of neural induction capability. An interesting result coming out from our very preliminary investigation is that the removal of XOTX5 OTX-tail seems to be sufficient to abrogate, almost completely, *Xotx5* neural inducing activity. Our results are consistent with data obtained by Gammil and Sive, (2001): the deletion of the OTX-tail seems to abolish, almost completely, XOTX2 neuralizing activity. At the level of the OTX-tail XOTX1 and XOTX5 show a high homology level; in fact, they differ only for 6 conserved substitutions and a AlaSer couple present in XOTX1 and absent in XOTX5. So far, we can only hypothesize a differential neural induction ability mostly due to these few differences, but further analyses will be necessary to verify this hypothesis.

Xotx5-255ΔC is, anyway, still able to induce *nrp-1* expression, although at a very lower level compared to full length *Xotx5*; therefore, other protein domain(s) contained in this construct may be partially involved in *Xotx5* neural inducing activity.

Consistent with published data, *Xotx5* is weakly able to trigger *nrp-1* expression in animal cap experiments, indicating that *Xotx5* may be not sufficient to neuralize naïve ectoderm (Vignali et al., 2000), differently from *Xotx2*, that seems to be able to activate general and anterior neural markers in ectoderm explants (Gammill et al, 2000). These different results may be due to a real differential activity of the two transcription factors, as well as to different experimental approaches used by the two groups. So far we can conclude that, in whole embryos, *Xotx5*, differently from *Xotx1*, is able to

trigger neuralization and that most of this activity resides in *Xotx5* Otx-tail. Our data also show that the RS box, on the contrary, is not involved at all in *Xotx5* neuralizing action.

In conclusion, we have highlighted molecular domains of XOTX1 and XOTX5 proteins that explain some of their different activities in living *Xenopus* embryos. Interestingly, these domains are differently involved in mediating convergent extension and CG and neural tissue promoting effects; moreover, they are physically separated from the RS box that mediates the diverse cell fate abilities of XOTX2 and XOTX5 (Onorati et al., 2007). These data show that XOTX proteins have a modular structure with domains that can mediate different aspects of their activities in a rather independent way.

7- Discussion section II: XOTX potential interactors

By performing a molecular dissection of XOTX2 and XOTX5 transcription factors we have isolated their transactivation domain (AD) in their C-terminal half: XOTX2 AD spans residues 174-288 and XOTX5 AD spans residues 174-290. Sequence divergences between XOTX5 and Mammalian CRX are notably, and we cannot establish a precise correspondence between XOTX5 transactivation domain that we have isolated and CRX activation domain AD1 and AD2 described by Chen et al., (2002). Approximately, our AD corresponds to AD1, the most active transactivation domain described by Chen et al. (2002); thus, in our experimental system, XOTX5 region corresponding to AD2, that plays a minor role in CRX transactivation activity, seems not to be comprised in our AD domain. These results imply that while for Chen et al., (2002) WSP domain is involved in transactivation by CRX, this seems not to be the case for XOTX5. Differences can be due to diverse experimental approaches used in the two studies, or may be also due to a functional difference between the two transcription factors due to their notable sequence divergence.

Beside the AD domain, we have characterized the XOTX regions involved in the interaction with two hybrid- (TH-)isolated potential partners (referred to as interaction domain, ID). This domain is localized at XOTX N-terminus; at this level, the sequence homology between the three XOTX is high. This is consistent with the fact that all selected preys interact with all tested XOTX: the conserved interaction domain mediates the interaction with common partners.

Since we isolated 74 XOTX2 and XOTX5 common partners, we have not gained any proof supporting our initial hypothesis on RS box mechanism of action: the RS box could modulate XOTX interaction with different cofactors, and different protein complexes could be able to bind different target sequences. Nevertheless, we cannot exclude our initial hypothesis, since a cofactor able to interact *in vitro* with both XOTX may *de facto* interact *in vivo*

with only one XOTX, if it colocalized with it but not with the other. Immunohistochemistry experiments could localize potential cofactors in specific retinal cellular population, thereby confirming or rejecting this hypothesis. Analogously, we cannot exclude our second model of RS box functioning: sequence divergences at RS box level could confer to XOTX2 and XOTX5 diverse and specific DNA binding capability, allowing them to bind and transactivate different genetic pathways. A chip assay performed using XOTX specific binding sequences could clarify this second point.

We decided to go on investigating TH-isolated XOTX potential interactors, in fact, as previously explained, we cannot exclude that an *in vitro* common interactor can be *in vivo* a partner specific for one only; besides, XOTX proteins exploit several common actions during *X. laevis* development, thereby a common interactor could be involved in this kind of processes.

Based on database search we have selected 5 out of 74 XOTX potential partners for further analyses: *granulin 1* and *2* (*grn1* and *grn2*), *upstream stimulatory factor 1* and *2* (*usf1* and *usf2*), and *c29* a hypothetical novel peptide.

Since Granulins (GRN) have been described as secreted proteins, it may seem hard to hypothesize an interaction between them and XOTX nuclear proteins. Nevertheless, XGRN intracellular functions have also been described (Mainul Hoque et al., 2003), as well as Penetratin-mediated XOTX2 transcellular translocation phenomena (Rebsam et al., 2008 and references therein); therefore their interaction, both inside and outside the cell, could take place. The first condition necessary for protein-protein interaction is their colocalization; antibodies against GRN in *Xenopus* are not available, thus we decided to investigate their transcripts distribution first. Our results showed a very interesting expression profile for *grn1* and *grn2* in *Xenopus* epidermis ciliated cells, but almost no expression has been detected in *Xotx* expression territories. Based on these results we dropped investigating GRN/XOTX potential interaction.

Upstream stimulatory factors (USF) are ubiquitously expressed transcription factors (Gregor et al., 1990; Sirito et al., 1994; Corre and Galibert, 2005). In Vertebrates two USF isoforms have been described: USF1 and USF2, which shared the conserved helix-loop-helix domain. These two transcription factors bind to E-box consensus sites as homo- or hetero-dimers (Ferred'Amare et al., 1994). USFs caught our interest for four major reasons: 1) they are transcription factors and several interactions of USF1 with tissue-specific or general transcription factors have been reported (Andrews et al., 2001; Ge et al., 2003; Liu et al., 2004); 2) gene-targetting studies in mouse suggested that *Usf* genes are important for embryonic development and brain function (Sirito et al., 1998); 3) several bHLH factors are involved in retinogenesis (Hatakeyama and Kageyama, 2004); 4) specific promoters, such as that of rhodopsin, contains both XUFS and XOTX binding sites.

As previously described for *Xgrn* genes, we first investigated *Xusf1* and *Xusf2* expression patterns during frog development. The two *Xusf* genes show a high level of sequence homology and they differ most at the N-terminus; hence we have designed two specific probes targeting *Xusf1* and *Xusf2* mRNA 5' region. Our results concerning *Xusf1* and *Xusf2* expression profiles substantially coincide with those of Fujimi et al. (2008) and we found that the major site of overlap between *Xotx* and *Xusf* expression is the developing nervous system.

Generally *Xusf2* expression is stronger than that of *Xusf1*, thus we decided to concentrate on *Xusf2* for functional analyses.

GST-pull down assays confirm the capability of XUSF2 to interact, almost *in vitro* with both XOTX2 and XOTX5.

Promoter transactivation assays suggested an antagonistic relationship between XUSF2 and XOTX5 and XOTX2: XOP activation level is higher in the presence of *Xotx5* alone and lower in case of *Xotx* cotransfection with *Xusf2*. Preliminary functional data coming from *Xenopus* microinjections substantially confirm this kind of interaction for XUSF2 and XOTX5: embryos coinjected with the two transcription factors show a decrease of posterior

defects in respect to embryos injected with *Xotx5* only. On the other hand, if we compare ectopic cement gland formation we do not observe any substantial difference between the two treatments. Therefore it may be possible that XOTX5/XUSF2 antagonistic interaction could be specific and affect only certain transcription pathways in *Xenopus* developing embryos. *Xusf2* knockdown experiments, once again, confirm the hypothesis of XUSF antagonistic action on XOTX5, since if *Xusf2* is removed we observe the same phenotype observed upon *Xotx5* overexpression: inhibition of convergent extension; also in this case, the cement gland developmental pathway seems not to be affected. Till now we can assert to have convincing evidence of the existence of an antagonistic intercourse between these two transcription factors, and we can speculate that XUSF2 can modulate XOTX function in cellular contexts-dependent way, since convergent extension inhibition seems to be influenced, but not cement gland induction. From two hybrid and GST-pull down assays we do not have any evidence of a diverse relationship between USF2 and XOTX2 and XOTX5, but from promoter transactivation assays we highlighted a stronger inhibition of XUSF2 on XOTX5 in respect to XOTX2; further analysis comparing those two interactions *in vivo* will better clarify this point, and shed light on a possible involvement of XUSF2 in mediating XOTX2 and XOTX5 different retinal functions.

We described and characterized the expression and nuclear localization of a putative novel protein, C29. The first reason why *c29* sequences caught our interest is because its sequence was shared by eleven independent clones. From database surveys, we found that this sequence is highly homologous to an hypothetical protein of *X. tropicalis*; beside this, we localized *c29* homologous sequences on *X.tropicalis* assembled genome and found that this genomic sequence has all elements necessary for a genomic region to be transcribed and translated: initiation codon, stop codon, Kozac consensus sequence, exon-intron junction consensus at hypothetical intron borders and polyadenylation signal at 3'UTR. Moreover, C29 *in silico*

predicted secondary structure contains a helix motif scored with a high level of confidence. This kind of secondary structure is characteristic of several transcription factors from Bacteria to Eukaryotes, and it is often involved in DNA binding: i.e. homeodomain recognition helix. Obviously, to be a transcription factor a protein has to be able to localize into the nucleus; two partially overlapping NLSs have been localized *in silico* at C29 C-terminus. These hypothetical NLSs are necessary and sufficient to drive the protein into the nucleus: their removal causes C29 delocalization to the cytoplasm, while their insertion in cytoplasmatic RFP drives it into the nuclear compartment. Thus, several evidences addressed that C29 may function as a transcription factor in *Xenopus*. Its expression pattern is largely coextensive with those of *Xotx*: mainly they are coexpressed in the anterior nervous system and especially in the developing eye. Preliminary functional analyses have shown a knock-down phenotype consistent with *c29* expression pattern: the main feature of Moc29 injected embryos is a defective eye, with abnormalities ranging from total anophthalmia to coloboma. The eye field is the main expression site of *c29* during development, therefore it may be possible that *c29* could be involved in eye development. Moreover, *c29* is also expressed in the neural crest, that contributes to eye development and optic cup closure (Gage and Zacharias, 2009). Therefore, loss-of-function results are again coherent with the expression pattern. *Xotx* genes are also expressed in the developing eye, are necessary for the normal development of the eye (Martinez-Morales et al., 2001) and are involved in retinal cells differentiation (Vicgian et al., 2003). Rescue experiments recovering Moc29 phenotype by injecting *c29* mRNA are ongoing in our lab, to check Moc29 specificity, as well as the analysis of several neural and eye specific markers, to check the molecular effects of *c29* loss-of-function. It will be interesting to further characterize C29 functions *in vivo*, since it has several characters making it a developmentally interesting peptide.

8- Conclusions

A molecular dissection analysis of XOTX1 and XOTX5 transcription factors has allowed us to identify the molecular domains responsible for their ability/inability to promote cement gland and neural fate and to inhibit convergent extension movements at a different extent. A bipartite CGbox, localized in XOTX5 C-terminal half is responsible for its cement gland inducing capability; the more C-terminal domain (CGboxD1) is more effective in CG promoting activity in respect to the more N-terminal one (CGboxD2); in XOTX1, a histidine stretch inserted in CGboxD1 disrupts its continuity and converts it in a CG inhibition domain, making XOTX1 unable to induce the adhesive organ. A serine rich region localized downstream to XOTX1 homeodomain synergies with the histidine stretch in inhibiting XOTX1 CG promoting capability. CGboxD1 seems to be a highly specialized domain, since it is not involved in convergent extension inhibition; on the contrary, CGboxD2 seems to be involved also in this XOTX function, together with other more N-terminal regions. The lower effectiveness of *Xotx1* compared to that of *Xotx5* in this respect is due, at least in part, to the histidine rich region, and possibly also to sequence divergences in CGboxD2 region, as well as in other upstream regions. The different neural induction capability of the two XOTX seems to be due to few amino acid divergences in their OTX-tail, while XOTX1 serine and histidine rich regions seem to be not at all involved in this activity.

We have shown that XOTX1, XOTX2 and XOTX5 can interact *in vitro* with XUSF1 and XUSF2, and we have demonstrated that XUSF2 intercourse with XOTX2 and XOTX5 is an antagonistic one, confirming this observation also *in vivo* for XOTX5. A possible involvement of this interaction, in regulating different developmental processes involving *Xotx* gene is hypothesizable.

Moreover XOTX1, XOTX2 and XOTX5 can interact *in vitro* with a novel predicted peptide (C29), harbouring a predicted helix secondary structure and two functional and overlapping NLSs. Phenotypes resulting upon *c29*

loss-of-function are coherent with its expression in the eye and brain region, and make feasible its involvement in eye developmental processes, possibly in synergy with XOTX proteins.

The XOTX interaction domain with the potential partners isolated from the two-hybrid screen is localized at their N-terminus, while their transactivation domain is C-terminal.

In this study we have gained new insights about XOTX differential actions during *Xenopus* development; in particular, we have characterized different XOTX functional domains responsible for these diverse functions, as well as XOTX potential partners that may be involved in regulating their common and divergent developmental functions. On the whole, we have contributed shedding light onto the molecular bases of XOTX mechanism of action.

9- Bibliography

Acampora D, Mazan S, Lallemand Y, Avantaggiato V, Maury M, Simeone S, Brulet P: Forebrain and midbrain regions are deleted in *Otx2*^{-/-} mutants due to a defective anterior neuroectoderm specification during gastrulation. *Development* 1995, 121:3279-3290.

Acampora D, Mazan S, Avantaggiato V, Barone P, Tuorto F, Lallemand Y, Brule P, Simeone A: Epilepsy and brain abnormalities in mice lacking *Otx1* gene. *Nat Genet* 1996, 14:218-222.

Acampora D, Avantaggiato V, Tuorto F, Barone P, Reichert H, Finkelstein R, Simeone A: Murine *Otx1* and *Drosophila otd* genes share conserved genetic functions required in invertebrate and vertebrate brain development. *Development* 1998, 125:1691-1702.

Acampora D, Simeone A: Understanding the roles of *Otx1* and *Otx2* in controlling brain morphogenesis. *TINS* 1999, 22:116-122.

Acampora D, Avantaggiato V, Tuorto F, Barone P, Perera M, Corte G, Simeone A: Differential transcriptional control as the major molecular event in generating *Otx1*^{-/-} and *otx2*^{-/-} divergent phenotypes. *Development* 1999a, 126:1417-1426.

Acampora D, Gulisano M, Broccoli V, Simeone A: *Otx* genes in brain morphogenesis. *Progress in Neurobiology* 2001, 64:69-95.

Andreazzoli M, Pannese M, Boncinelli E: Activating and repressing signals in head development: the role of *Xotx1* and *Xotx2*. *Development* 1997, 124:1733-1743.

Andrews GK, Lee DK, Ravindra R, Lichtlen P, Sirito M, Sawadogo M, Schaffner W: The transcription factors MTF-1 and USF-1 cooperate to regulate mouse metallothionein-I expression in response to the essential metal zinc in visceral endoderm cells during early development. *Embo J* 2001, 20:1114-1122.

Ang SL, Jin O, Rhinn M, Daigle N, Stevenson L, Rossant J: Targeted mouse *Otx2* mutation leads to severe defects in gastrulation and formation of axial mesoderm and to deletion of rostral brain. *Development* 1996, 122:243-252.

Baas D, Bumsted KM, Martinez JA, Vaccarino FM, Wikler KC, Barnstable CJ: The subcellular localization of *Otx2* in cell-type specific and developmentally regulated in the mouse retina. *Brain Res Mol Brain Res* 2000, 78:26-37.

Bachiller D, Macias A, Doboule D, Morata G: Conservation and functional hierarchy between mammalian and insect Hox/HOM genes. *EMBO J.* 1994, 13:1930-1941.

Blitz IL, Cho KWY: Anterior neuroectoderm is progressively induced during gastrulation: the role of the *Xenopus* homeobox gene *orthodenticle*. *Development* 1995, 121:993-1004.

Boncinelli E, Gulisano M, Broccoli V: *Emx* and *Otx* homeobox genes in the developing mouse brain. *J Neurobiol* 1993, 24(10):1356-1366

Boothby KM, Roberts A: The stopping response of *Xenopus laevis* embryos: behavior, development and physiology. *J Comp Physiol A* 1992a, 170:171-180.

Boothby KM, Roberts A: The stopping response of *Xenopus laevis* embryos: Pharmacology and intracellular physiology of rhythmic spinal neurons and hindbrain neurons. *J Exp Biol* 1992b, 169:65-85.

Bouillet P, Chazauad C, Oulad-Abdeghani M, Dolle P, Chambon P: Sequence and expression pattern of the *Stra7* (*Gbx2*) homeobox-containing gene induced by retinoic acid in P19embryonal carcinoma cells. *Dev-Dynam.* 1995, 204:3723-4382.

Bovolenta P, Mallamaci A, Briata P, Corte G, Boncinelli E: implication of OTX2 in pigmented epithelium determination and neural retina differentiation. *J Neurosci* 1997, 17:4243-4252.

Bouwmeester T, Kim S, Sasai Y, Lu B, De Robertis EM: Cerberus is a head-inducing secreted factor expressed in the anterior endoderm of Spemann's organizer. *Nature* 1996, 382(6592):595-601.

Boyl PP, Signore M, Annino A, Martinez Barbera JP, acampora D, Simeone A: *Otx* genes in the development and evolution of the vertebrate brain. *Int. J.DevlNeuroscience* 2001, 19:353-363.

Bradley L, Wainstock D, Sive H: Positive and negative signals modulate formation of the *Xenopus* cement gland. *Development* 1996, 122:2739-2750.

Broccoli V, Boncinelli E, Wurst W: The caudal limit of *Otx2* expression positions the isthmic organizer. *Nature* 1999, 401:164-168.

Bruce AE, Shankland M: Expression of the head gene *Lox22-Otx* in the leech *Holobdella* and the origin of bilaterian body plan. *Dev. Biol.* 1998, 201:101-112.

Chalmers AD, Welchman DA, Papalopulu N: intrinsic differences between the superficial and deep layers of the *Xenopus* ectoderm control primary neuronal differentiation. *Cell dev* 2002, 2:171-182.

Chapman G, Rathjen P: Sequence and evolutionary conservation of the murine Gbx2 homeobox gene. *FEBS Lett* 1995, 364:289-292.

Chatelain G, Fossat N, Brun G, Lamonerie T: Molecular dissection reveals decreased activity and not dominant negative effect in human OTX2 mutants. *L Mol Med* 2006, 84:604-615.

Chen S, Wang QL, Nie Z, Sun H, Lennon G, Copeland NG, Gilbert DJ, Lenkins NA, Zack DJ: Crx, a novel Otx-like paired-homeodomain protein, binds to and transactivates photoreceptor cell-specific genes. *Neuron* 1997, 19:1017-1030.

Chen S, Wang QL, Xu S, Liu I, Lili Y, Wang Y, Zack DJ: Functional analysis of cone-rod homeobox (CRX) mutations associated with retinal dystrophy. *Human Molecular Genetics* 2002, 11(8):873-884.

Chien CT, Bartel PL, Sternglanz R, Fields S: the two-hybrid system: a method for identify and clones genes for proteins that interact with a protein of interest. *Proc Natl Acad Sci* 1991, 88:9578-9582.

Cho KWY, Blumberg B, Steinbeisser H, De Robertis EM: Molecular nature of Spemann's organizer: the role of the *Xenopus* homeobox gene gooseoid. *Cell* 1991, 67:1111-1120.

Choen SM, Jurgens G: Mediation of *Drosophila* head development by gap-like segmentation genes. *Letters to Nature* 1990, 346:482-485

Cohen SM, Jurgens G: Drosophila headlines. Trends Genet 1991, 7:267-272.

Corbo JC, Lawrence KA, Karlstetter M, Myers CA, Abdelaziz M, Dirkes W, Weigelt K, Seifert M, Benes V, Fritsche LG, Weber BH, Langmann T: CRX XhiP-seq reveals the cis-regulatory architecture of mouse photoreceptors. Genome Res 2010, 20:1512-1525.

Corre S, Galibert MD: Upstream stimulating factors: highly versatile stress-responsive transcription factors. Pigment Cell Res 2005, 18:337-348.

Crews ST, Thomas JB, Goodman CS: The Drosophila single-minded gene encodes a nuclear protein with sequence similarity to the per gene product. Cell 1988, 52:143-151.

Davies SN, Kitson DL, Roberts A: The development of the peripheral trigeminal innervation in Xenopus embryos. J Embryol Exp Morph 1982, 70:215-224.

Deblandre GA, Wettstein DA, Koyano-Nakagawa N, Kintner C: A two-step mechanism generates the spacing pattern of the ciliated cells in the skin of Xenopus embryos. Development 1999, 126:4715-4728.

Decembrini S, Andreazzoli M, Vignali R, Barsacchi G, Cremisi F: Timing the generation of distinct retinal cells by homeobox proteins. PLoS Biol 2006, 4(9):e272.

denHollander AI, Roepman R, Koenekoop RK, Cremers FP: Lebercongenital amaurosis: genes, proteins and disease mechanisms. Prog Retin Eye Res 2008, 27:391-419.

Dom G, Shaw-Jackson C, Mathis C, Boufflux O, Picard JJ, Prochinatez A, Mingeot-Leclercq MP, Brasseur R, Rezsosazy R: Cellular uptake of antennapedia penetratin peptides is a two-step process in which phase transfer precedes a tryptophan-dependent translocation. *Nucleic Acids* 2003, 31:556-561.

Drysdale T, Elison R: Cell migration and induction in the development of the surface ectodermal pattern of *Xenopus laevis* tadpole. *Dev Growth Differ* 1992, 34:51-59.

Eagleson GW, Harris WA: Mapping of the presumptive brain region in the neural plate of *Xenopus laevis*. *J Neurobiol* 1990, 21:427-440.

Fainsod A, Steinbeisser H, De Robertis EM: On the function of BMP4 in patterning the marginal zone of the *Xenopus* embryo. *EMBO J* 1994, 13:5015-5025.

Fei Y, Hughes TE: Nuclear trafficking of photoreceptor protein CRX: the targeting sequence and pathologic implications. *Invest Ophthalmol Vis Sci* 2000, 41:2849-2856.

Ferre-D'Amare aR, Pognonec P, Roeder RG, Burley SK: Structure and function of the b/HLH/Z domain of USF. *Embo J* 1994, 13:180-189.

Finkelstein R, Smouse D, Capaci MT, Spradling AC, Perrimon N: The orthodenticle gene encodes a novel homeodomain protein involved in the development of the *Drosophila* nervous system and ocellar visual structure. *Genes and development* 1990, 4:1516-1527.

Finkelstein R, Perrimon N: The orthodenticle gene is regulated by bicoid and torso and specifies *Drosophila* head development. *Nature* 1990, 346:485-488.

Fritsch B, Barald K, Lomax M: Early embryology of the vertebrate ear. In: Rubel EW, Popper AN, Fay RR (Eds.) *Springer Handbook of Auditory Research. Development of the Auditory System*, vol. 12 Springer, New York 1986, pp. 80-145.

Freund CL, Gregory-Evans CY, Furukawa T, Papoiannou M, Loose J, Ploder L, Bellingham J, Ng D, Herbrick JAS, Duncan A, Scherer SW, Tsui LC, Loutradis-Anagnostou A, Jacobson SG, Cepko CL, Bhattacharya SS, McInnes RR: Cone-rod dystrophy due to mutation in a novel photoreceptor-specific homeobox gene (CRX) essential for maintenance of the photoreceptor. *Cell* 1997, 91:543-553.

Freund CL, Wang QL, Chen S, Muskat BL, Wiles CD, Sheffield VC, Jacobson SG, McInnes RR, Zack DJ, Stone EM: De novo mutations in the CRX homeobox gene associated with Leber congenital amaurosis. *Nat Genet* 1998, 18:311-312.

Fujimi TJ, Aruga J: Upstream stimulatory factors, USF1 and USF2 are differentially expressed during *Xenopus* embryonic development. *Gene Expression Patterns* 2008, 8:376-381.

Furukawa T, Morrow EM, Cepko CL: Crx, a novel otx-like homeobox gene, shows photoreceptor-specific expression and regulates photoreceptor differentiation. *Cell* 1997, 91:531-541.

Furukawa T, Morrow EM, Li T, Davis FC, Cepko CL: Retinopathy and attenuated circadian entrainment in Crx-deficient mice. *Nat Genet* 1999, 23:466-470.

Gage PJ, Zacharias AL: Signalling "cross-talk" is integrated by transcription factors in the development of the anterior segment in the eye. *Developmental Dynamics* 2009, 238:2149-2162.

Galliot B, de Vargas C, Miller D: Evolution of homeobox genes: Q50 paired-like founded the paired class. *Dev Genes Evol* 1999, 209:186-197.

Gammil LS, Sive H: Identification of otx2 target genes and restrictions in ectodermal competence during *Xenopus* cement gland formation. *Development* 1997, 124:471-481.

Gammil LS, Sive H: Identification of otx2 and BMP4 signalling correlates with *Xenopus* cement gland formation. *MechDev* 2000, 92:217-226.

Gammil LS, Sive H: Otx2 expression in the ectoderm activates anterior neural determination and is required for *Xenopus* cement gland formation. *Developmental Biology* 2001, 240:223-236.

Gamse J, Sive H: Vertebrate anteroposterior patterning: the *Xenopus* neuroectoderm as a paradigm. *Bioessays* 2000, 22:976-986.

Garstang W: The morphology of the Tunicata, and its bearing on the phylogeny of the Chordata. *Q.J. Microsc. Sci.* 1928, 72:51-187.

Ge Y, Jensen TL, Matherly LH, Taub JW: Physical and functional interactions between USF and Sp1 proteins regulate human deoxycytidine kinase promoter activity. *J Biol Chem* 2003, 278:49901-49910.

Gerhart J, Danilchik M, Doniach T, Roberts S, Rowning B, Stewart R: Cortical rotation of the *Xenopus* egg: consequence for the anteroposterior pattern of embryonic dorsal development. *Development* 1989, 107 Supplement: 37-51.

Germot A, Lecointre G, Poulinec JL, Le Mentec C, Giradot F, ;azan S: Structural evolution of Otx genes in craniates. *Mol Biol Evol.* 2001, 18:1668-1678.

Gilbert FS: *Developmental Biology* 6th edition. Swarthmore College Sunderland (MA): Sinauer Associates; 2000.

Gregor PD, Sawadogo M, Roeder RG: The adenovirus major late transcription factor USF is a member of the helix-loop-helix group of regulatory proteins and binds to DNA as a dimer. *Genes Dev* 1990, 4:1730-1740.

Hamburger V: *The heritage of experimental embryology: Hans Spemann and the Organizer.* Oxford: Oxford University Press, 1988.

Harland RM: *In situ* hybridization: an improved wholemount method for *Xenopus* embryos. *Methods Cell Biol* 1991, 36:675-685.

Hatakeyama J, Kageyama R: Retinal cell fate determination and bHLH factors. *Semin Cell Dev Biol* 2004, 15(1):83-89.

Hawley SH, Wunnenberg-Stapleton K, Hashimoto C, Laurent MN, Watabe T, Blumberg BW, Cho KW: Disruption of BMP signals in embryonic *Xenopus* ectoderm leads to direct neural induction. *Genes Dev* 1995, 9:2923-2935.

Hemmati-Brivanlou A, Frank D, Bolce M, Brown B, Sive H, Harland R: Localization of specific mRNA in *Xenopus* embryos by whole-mount in situ hybridization. *Development* 1990, 110:325-330.

Henderson RH, Williamson KA, Kennedy JS, Webster AR, Holder GE, Robson AG, FitzPatrick DR, van Heyningen V, Moore AT: A rare de novo non-sense mutation in OTX2 causes early onset retinal dystrophy and pituitary dysfunction. *Mol Vis* 2009, 15:2442-2447.

Henning AK, Peng GH, Chen S: Regulation of photoreceptor gene expression by Crx-associated transcription factor network. *Brain Res* 2008, 1192:114-133.

Hirth F, Therianos S, Loop T, Gehring T, Reichert H, Furukubo-Tokunaga K: developmental defects in brain segmentation caused by mutations of the homeobox gene orthodenticle and empty spiracles in *Drosophila*. *Neuron* 1995, 15:769-778.

Hunt P, Gulisano M, Cook M, Sham MH, Faiwlla A, Wilkinson D, Boncinelli E, Krumlauf R. A distinct Hox code for the branchial region of the vertebrate head. *Nature* 1991, 353: 861-864

Issacs HV, Andreazzoli M, Slack JMW: Anteroposterior patterning by mutual repression of orthodenticle and caudal-type transcription factors. *Evolution Development* 1999, 1:143-152.

Jacobson SG, Cideciyan AV, Huang Y, Hanna DB, Freund CL, Affatigato LM, Carr RE, Zack DJ, Stone EM, McInnes RR: Retinal degenerations with truncation mutations in the cone-rod homeobox (CRX) gene. *Invest Ophthalmol Vis Sci* 1998, 39:2417-2426.

Jamrich M, Sato S: Differential gene expression in the anterior neural plate during gastrulation of *Xenopus laevis*. *Development* 1989, 105:779-786.

Jurgens G, Lehmann R, Schardin M, Nusslein-Volhard C: Segmental organization of the head in the embryo of *Drosophila melanogaster*. *Wilhem Roux's Arch. Dev. Biol.* 1986, 195:359-377.

Kablar B, Vignali R, Menotti L, Pannese M, Andreazzoli M, Polo C, Giribaldi MG, Boncinelli E, Barsacchi G: Xotx genes in the developing brain of *Xenopus laevis*. *Mech. Dev.* 1996, 55:145-158.

Keller R, Shih J, Sater A: The cellular basis of the convergence and extension of the *Xenopus* neural plate. *Dev Dyn* 1992, 193:199-217.

Knecht AK, Good PJ, Dawid IB, Harland RM: Dorsal-ventral patterning and differentiation of noggin-induced neural tissue in the absence of mesoderm. *Development* 1995, 121:1927-1936.

Koike C, Nishida A, Ueno S, Saito H, Sanuki R, Sato S, Furukawa A, Aizawa S, Matsuo I, Suzuki N, Kondo M, Furukawa T: Functional roles of Otx2 transcription factor in postnatal mouse retinal development. *Mol Cell Biol* 2007, 27:8318-8329.

Kuroda H, Hayata T, Eisaki A, Asahima M: Cloning a novel developmental regulating gene, Xotx5: its potential role in anterior formation in *Xenopus laevis*. *Dev. Growth Diff.* 2000, 42:87-93.

Lacalli T: Apical organs, epithelial domains, and the origin of the chordate central nervous system. *Am. Zool.* 1994, 34:533-541.

Lahder R, Mohun TJ, Smith JC, Snape AM: Xom: a *Xenopus* homeobox gene that mediates the early effects of BMP4. *Development* 1996, 122:2385-2394.

Lanjuin A, VanHoven MK, Bargmann CI, Thompson JK, Sengupta P: otx/otd homeobox genes specify distinct sensory neuron identities in *C.elegans*. *Developmental Cell* 2003, 5:621-633.

Lewin B: *Gene VIII*, Benjamin-Cummings Pub Co. 2003.

Li Y, Brown SJ, Hausdorf B, Tautz D, Denell RE, Finkelstein R: Two orthodenticle-related genes in the short-germ beetle *Tribolium castaneum*. *Dev. Genes Evol.* 1996, 206:35-45.

Li X, Chen S, Wang Q, Zack D, Snyder SH, Borjigin J: A pineal regulatory element (PIRE) mediates transactivation by the pineal/retina-specific transcription factor CRX. *Proc. Natl. Acad. Sci* 1998, 95:1876-1881.

Liu M, Whetstine JR, Payton SG, Ge Y, Flatley RM, Matherly LH: Roles of USF, Ikaos and Sp proteins in the transcriptional regulation of the human reduced folate carrier B promoter. *Biochem* 2004, 383:249-257.

Livesey FJ, Cepko CL: Vertebrate neural cell-fate determination: a lesson from the retina. *Nat Rev Neurosci* 2001, 2:109-118.

Lunardi A, Vignali R: *Xenopus* Xotx2 and *Drosophila* otd share similar activities in anterior patterning of the frog embryo. *Dev Genes Evol* 2006, 216(9):511-521.

Mainul Hoque, Tara M. Young, Chee-Gun Lee, Ginette Serrero, Michael B. Mathews, and Tsafi Pe'ery. The growth factor granulin interacts with cyclin

T1 and modulates P-TEFb-dependent transcription. *Mol Cell Biol.* 2003 23(5): 1688-1702.

Maliki J, Bogarad LD, Martin MM, Ruddle FH, McGinnis W: Functional analysis of the mouse homeobox gene HoxB9 in *Drosophila* development. *Mech. Dev.* 1993, 42:139-150.

Marchant L, linker C, Ruiz P, Guerrero N, Mayor R: The inductive properties of mesoderm suggest that the neural crest cells are specified by a BMP gradient. 1998, 198:319-329.

Martinez S, Wassef M, Alvarado-Mallart RM: Induction of a mesencephalic phenotype in the 2-day-old chick prosencephalon is preceded by the early expression of the homobox gene *en*. *Neuron* 1991, 6:971-981.

Martinez-Morales JR, Signore M, Acampora D, Simeone A, Bovolenta P: *otx* genes are required for tissue specification in the developing eye. *Development* 2001, 128:2019-2030.

Martinez-Morales JR, Dolez V, Rodrigo I, Zaccarini R, Leconte L, Bovolenta P, Saule S: OTX2 activates the molecular network underlying retina pigment epithelium differentiation. *J Biol Chem* 2003, 278:2172-21731.

Matsuo I, Kuratani S, Kimura C, Takeda N, Aizawa S: Mouse *Otx2* functions in the formation and patterning of rostral head. *Genes Dev* 1995, 9:2646-2658.

Mayor R, Morgan R, Sargent M: Induction of the prospective neural crest of *Xenopus*. *Development* 1995, 121:767-777.

Meinhart H: Cell determination boundaries as organizing regions for secondary embryonic fields. *Dev Biol* 1983, 96:375-385.

Millet S, Campbell K, Epstein DJ, Losos K, Harris E, Joyner A: A role for Gbx2 in repression of Otx2 and positioning the mid/hindbrain organizer. *Nature* 1999, 401:161-164.

Mitton KP, Swain PK, Chen S, Xu S, Zack DJ, Swaroop A: The leucine zipper of NRL interacts with the CRX homeodomain. A possible mechanism of transcriptional synergy in rhodopsin regulation. *J Biol Chem* 2000, 275:29794-29799.

Morgan R, Hooiveld MHW, Pannese M, Dati G, Broder F, Delarue M, Thiery JP, Boncinelli E, Durston AJ: Calponin modulates the exclusion of Otx-expressing cells from convergence extension movements. *Nature cell biology* 1999, 1(7):404-408.

Mori H, Miyazaki S, Morita I, Nitta H, Mishina M: Different spatio-temporal expression of three Otx homeoprotein transcripts during zebrafish embryogenesis. *Mol. Brain Res* 1994, 27:221-231.

Morsli H, Tuorto F, Choo D, Postiglione MP, Simeone A, Wu DK: Otx1 and Otx2 activities are required for the normal development of the mouse inner ear. *Development* 1999, 126:2335-2343.

Nicols LL Jr, Alur RP, Booblan E, Sergveev YV, Caruso RC, Stone EM, Swaroop A, Johnson MA, Brooks BP: Two novel CRX mutant proteins causing autosomal dominant Leber congenital amaurosis interact differently with NRL. *Hum Mutat* 2010, 31:E1472-E1483.

Newport J, Kirschner M: A major developmental transition in early *Xenopus* embryos. II. Control of the onset of transcription. *Cell* 1982, 30:687-696.

Nieuwkoop PD: Activation and organization of the central nervous system in amphibians. Part II. Synthesis of a new working hypothesis. *J Exp Zool* 1952, 120:83-108.

Nieuwkoop PD, Faber J: Normal table of *Xenopus laevis*. Amsterdam: North Holland Publishing Company, 1967.

Nieuwkoop PD: The organization center of the amphibian embryo: its spatial organization and morphogenetic action. *Adv Morphogen* 1973, 10:1-39.

Nishida A, Furukawa A, Koike C, Tano Y, Aizawa S, Matsuo I, Furukawa T: Otx2 homeobox gene controls retinal photoreceptor cell fate and pineal gland development. *Nat Neurosci* 2003, 6:1255-1263.

Omori Y, Katoh K, Sato S, Muranishi Y, Chaya T, Onishi A, Minami T, Fujikado T, Furukawa T: Analysis of transcriptional regulatory pathways of photoreceptor genes by expression profiling of the Otx2-deficient retina. *PLoS One* 2011, 6:e19685.

Onichtchiuk D, Gawantka V, Doshc R, Delius H, Hirschfeld K, Blumenstock C, Niehrs C: The Xvent-2 homeobox gene is part of the BMP4 signalling pathway controlling dorsoventral patterning of *Xenopus* mesoderm. *Development* 1996, 122:3045-3053.

Onorati M, Cremisi F, Liu Y, He R, Barsacchi G, Vignali R: A specific box switches the cell fate determining activity of XOTX2 and XOTX5b in the *Xenopus* retina. *Neural Development* 2007, 2:12.

Pannese M, Polo C, Andreazzoli M, Vignali R, Kablar B, Barsacchi G, Boncinelli E: The *Xenopus* homologue of *Otx2* is a maternal homeobox gene that demarcates and specifies anterior body regions. *Development* 1995, 121:707-720.

Papalopulu N, Kinter C: *Xenopus* distal-less related homeobox genes are expressed in the developing forebrain and are induced by planar signals. *Development* 1993, 117:961-975.

Peng GH, Chen S: Chromatin immunoprecipitation identifies photoreceptor transcription factors target in mouse models of retinal degeneration: new findings and challenges. *Vis Neurosci* 2005, 22:575-586.

Plouhinec JL, Sauka-Spengler T, Germot A, Le Mentec C, Cabana T, Harrison G, Pieau C, Sire JY, Veron G, Mazan S: The mammalian *Crx* genes are highly divergent representatives of the *Otx5* gene family, a gnanthostome orthology class of orthodenticle-related homeogenes involved in the differentiation of retinal photoreceptors and circadian entrainment. *Mol Biol Evol* 2003, 20:513-521.

Rebsam A, Mason CA: *Otx2*'s incredible journey. *Cell* 2008, 134(3):386-387.

Reichert H, Simeone A: Conserved usage of gap and homeobox genes in patterning the CNS. *Curr. Opin. Neurobiol.* 1999, 9:589-595.

Rivolta C, Berson EL, Dryja TP: Dominant Leber congenital amaurosis, cone-rod degeneration, and retinitis pigmentosa caused by mutant versions of the transcription factor *CRX*. *Hum Mutat* 2001, 18:488-498.

Roberts A, Blight AR: anatomy, physiology and behavioural role of sensory nerve endings in the cement gland of embryonic *Xenopus*. Proc R Soc Lond B 1975, 192:111-127.

Royet J and Finkelstein R: Establishing primordia in the *Drosophila* eye-antennal imaginal disc: the roles of decapentaplegic, wingless and hedgehog. Development 1997, 124:4793-4800.

Rubenstein JLR, Shimamura K, Martinez S, Puelles L: Regionalization of the prosencephalic neural plate. Annu. Rev. Neurosci. 1998, 21:445-477.

Sasai Y, Lu B, Steinbeisser H, De Robertis EM: Regulation of neural induction by Chd and Bmp-4 antagonistic patterning signals in *Xenopus*. Nature 1995, 377:757.

Schmidt JE, von Dassow G, Kimelman D: Regulation of dorsal-ventral patterning: the ventralizing effect of the novel *Xenopus* homeobox gene *Vox*. Development 1996, 122:1711-1721.

Sharman AC, Brand M: Evolution and homology of the neuron system: cross-phylum rescues of *otd/Otx* genes. TIG 1998: 14:211-214.

Simeone A, Acampora D, Gulisano M, Stornaiuolo A, Boncinelli E: Nested expression domains of four homeobox genes in developing rostral brain. Nature 1992, 358:687-690.

Simeone A, Acampora D, Mallamaci A, Stornaiuolo A, D'Apice MR, Nigro V, Boncinelli E: A vertebrate gene related to orthodenticle contains a homeodomain of the bicoid class and demarcates anterior neuroectoderm in the gastrulating mouse embryo. EMBO L 1993, 12:2735-2747.

Simeone A: positioni the isthmic organizer where Otx2 and Gbx2 meet. Trends Genet 2000, 16:237-240.

Sirito M, Lin Q, Maity T, Sawadogo M: Ubiquitous expression of the 43- and 44-kD forms of transcription factor USF in mammalian cells. Nucleic Acids Res 1994, 22:427-433.

Sirito M, Lin Q, Deng JM, Behringer RR, Sawadogo M: Overlapping roles and asymmetrical cross-regulation of the USF proteins in mice. Proc Natl Acad Sci USA 1998, 95:3758-3763.

Sive HL, Bradley LC: A sticky problem: the Xenopus cement gland as a paradigm for anterior patterning. Dev Dyn 1996, 205:265-280.

Smith KM, Gee L, Blitz IL, Bode HR: CnOtx a member of the Otx gene family, has a role in cell movements in hydra. Dev. Biol. 1999, 212:392-404.

Sohoki MM, Sullivan LS, Mintz-Hittner HA, Birch D, Hechenlively JR, Freund CL, McInnes RR, Daiger SP: A range of clinical phenotypes associated with mutation in CRX, a photoreceptor transcription-factor gene. Am J Hum Genet 1998, 63:1307-1315.

Spemann H: Embryonic development and induction. New Haven, Conn: Yale University Press, 1938.

Stornaiuolo A, Bayascas JR, Salo E, Boncinelli E: A homeobox gene of the orthodenticle family is involved in antero-posterior patterning of regenerating planarians. Int. J. Dev. Biol. 1998, 42:1153-1158.

Suzuki A, Theis RS, Yamaji n, Song JJ, Wozney J, Murakami K, Ueno N: A truncated BMPreceptor affects dorsal-ventral patterning in the early *Xenopus* embryo. *Proc Natl Acad Sci USA* 1994, 91:10255-10259.

Swaarop A, Wang QL, Wu W, Cook J, Coatsn C, Xu S, Chen S, Zack DJ, Sieving PA: Leer congenital amaurosis caused by a homozygous mutation (R90W) in the homeodomain of the retinal transcription factor CRX: direct evidence for the involvement of CRX in the development of photoreceptor function. *Hum Mol Genet* 1999, 8:299-305.

Swain PK, Chen S, Wang QL, Affatigato LM, Coats CL, Brady KD, Fishman GA, Jacobson SG, Swaroop A, Stone E, Sieving PA, Zack DJ: Mutations in the cone-rod homeobox gene are associate with the cone-rod dystrophy photoreceptor degeneration. *Neuron* 1997, 19:1329-1336.

Tahayato A, Sonnevile R, Pichaud F, Wernet MF, Papatsenko D, Beaufils P, Cook T, Desplan C: Otd/Crx, a dual regulator for the specification of ommatidia subtypes in the *Drosophila* retina. *Dev Cell* 2003, 5:391-402.

Terrell ID, Xie B, Workman M, Mahato S, Zelhof A, Gebelein B, Cook T: OTX2 and CRX rescue overlapping and photoreceptor-specific functions in the *Drosophila* eye. *Developmental Dynamics* 2012, 241:215-228.

Torres M, Giraldez F: The development of the vertebrate inner ear. *Mech Dev.* 1998, 71:5-21.

Ueki T, Kuratani Y, Hirano S, Aizawa S: Otx cognates in a lamprey, *Lampetra japonica*. *Dev Gene Evol.* 1998, 208:223-228.

Umesono Y, Watanabe K, Agata K: Distinct structural domains in the planarian brain define by the expression of evolutionary conserved homeobox genes. *Dev. Genes Evol.* 1999, 209:31-39.

Van Evercooren A, Picard JJ: Surface changes during development and involution of the cement gland of *Xenopus laevis*. *Cell Tissue Res* 1978, 194:303-313.

Vandendries ER, Johnson D, Reinke R: Orthodenticle is required for photoreceptor cell development in the *Drosophila* eye 1996,173:243-255.

Viczian A, Vignali R, Zuber ME, Barsacchi G, Harris WA: *Xotx5b* and *Xotx2* regulates photoreceptors and bipolar fates in the *Xenopus* retina. *Development* 2003, 130:1281-1294.

Vignali R, Colombetti S, Lupo G, Zhang W, Stachel S, Harland RM, Barsacchi G: *Xotx5b*, a new member of the *Otx* gene family, may be involved in anterior and eye development in *Xenopus laevis*. *Mechanism of Development* 2000, 96:3-13

von Bubnoff A, Schmidt L, Kimelman D: The *Xenopus laevis* homeobox gene *Xgbx2* is an early marker of antero-posterior patterning in the ectoderm. *Mech Dev.* 1995, 54:149-160.

Wada S, Katsuyama Y, Sato Y, Itoh C, Saiga H: *Hroth* an orthodenticle-related homeobox gene of the ascidian, *Halocynthia roretzi*: its expression and putative roles in the axis formation during embryogenesis. *Mech. Dev.* 1996, 60:59-71.

Wang JC, Harris WA: The role of combinational coding by homodomain and bHLH transcription factors in retinal cell fate specification. *Dev Biol* 2005, 285:101-115.

Wardle FC, Wainstock DH, Sive H: Cement gland-specific activation of the Xag1 promoter regulated by co-operation of putative Ets and ATF/CREB transcription factors. *Development* 2002, 129:4387-4397.

Wardle F, Sive HL: What's your position? The *Xenopus* cement gland as a paradigm of regional specification. *Hypothesis* 2003, 25:717-726.

Wassarman KM, Iewadoski M, Campbell K, Joyner AL, Rubenstein JLR, Martinez S, Martin GR: Specification of the anterior hindbrain and establishment of a normal mid/hindbrain organizer dependent on *gbx2* gene function. *Development* 1997, 124:2923-2934.

Weimann JM, Zhang YA, Lewin ME, Devine WP, Brulet P, Mc-Connell SK: Cortical neurons require *Otx1* for the refinement of exuberant axonal projections to subcortical targets. *Neuron* 1999, 24:819-831.

Weinstein DC, Hemmati-Brivanlou A: Neural induction. *Ann Rev Cell Dev Biol* 1999, 15:411-433.

Wharton KA, Johansen KM, Xu T, Artavanis-Tsakonas S: Nucleotide sequence from the neurogenic locus *Notch* implies a gene product that shares homology with proteins containing EGF-like repeats. *Cell* 1985a, 43:567-581.

Wharton KA, Yedvobnick B, Finnerty VG, Artavanis-Tsakonas S: A novel family of transcribed repeats shared by the *Notch* locus and other developmentally regulated loci in *D. melanogaster*. *Cell* 1985b, 40:55-62.

Whitaker SL, Knox BE: Conserved transcriptional activators of the *Xenopus* rhodopsin gene. J Biol Chem 2004, 279:490-498.

Wieschaus E, Nusslein-Volhard C, Jurgens G: Mutations affecting the pattern of the larval cuticle in *Drosophila melanogaster*. 3. Zygotic loci on the X-chromosome and 4th chromosome. Wilhem Roux's Arch. Dev. Biol. 1984, 193:296-307.

Wieschaus E, Perrimon N, Finkelstein R: Orthodenticle activity is required for the development of medial structures in the larval and adult epidermis of *Drosophila*. Development 1992, 115:801-811.

Williams NA, Holland PWH: Old head on young shoulders. Nature 1996, 383:490.

Williams NA, Holland PWH: Gene and domain duplication in the chordate Otx family: insights from amphioxus Otx. Mol Biol Evol 1998, 15:600-607.

Wilson PA, Lagna G, Suzuki A, Hemmati-Brivanlou A: Concentration-dependent patterning of the *Xenopus* ectoderm by BMP4 and its signal transducer Smad1. Development 1997, 124:3177-3184.

Xu RH, Kim J, Taira M, Zhan S, Sredni D, Kung HF: A dominant negative bone morphogenetic protein 4 receptor causes neutralization in *Xenopus* ectoderm. Biochem Biophys Res Commun 1995, 212:212-219.

Younossi-Hartenstein A, Green P, Liaw GJ, Rudolph K, Lemgyel J, Hartenstein V: Control of early neurogenesis of the *Drosophila* brain by the head gap genes *tll*, *otd*, *ems* and *btd*. Dev. Biol. 1997, 182:270-283.

Zhao JJ, Lazzarini RA, Pick L: The mouse Hox1.3 gene is functionally equivalent in the Drosophila Sex comb reduced gene. *Genes Dev* 1993, 7:343-354.

10- Ringraziamenti

Grazie ai miei genitori che, fin dal principio, hanno messo le basi affinché io arrivassi qui, dai corvi neri al mio ottimo ragù. Grazie a tutti coloro che considero la mia famiglia, perchè tutto ciò che è stato ha fatto sì che arrivassi qui. Grazie a Robert, e a tanti dei Prof che ho incontrato, che mi hanno fatto innamorare di questo lavoro, al punto di decidere di dedicargli una bella parte della mia vita. Grazie a Jiali Liu, Federico Cremisi, Michele Bertacchi e Luca Pandolfini per la preziosa collaborazione. Grazie ad Alvaro Galli per tutto quello che ho imparato sui lieviti. Grazie a Michele Castelli per il lavoro ed il tempo trascorso insieme. Grazie alla Fontina, passata e presente, che ha fatto da cornice a questi anni difficili e bellissimi. Grazie a Giulia e a Martina, per tutte le nostre chiacchiere e le nostre risate, grazie perchè ho potuto avere delle amiche e non solo delle colleghe. Grazie ai miei studentelli Luca e Davide, se è vero che ho insegnato qualcosa a loro è sicuramente vero che ho imparato tantissimo anche io, e sicuramente ci siamo divertiti. Grazie a Simone, perchè chi ti vuole bene ti fa piangere, ma anche tanto ridere. Grazie alla mia piccola grande “squadra”, sapete chi siete, che mi ha fatto nascere ancora, insieme ci siamo. Grazie a te, Maurizio, che mi hai sorretta, protetta e lasciata camminare, con la mia mano nella tua siamo arrivati fino qui, grazie al nostro amore, adesso, ci siamo. E grazie a tutta la gioia che mi regalano i nostri piccoli grandi tesori, io, te, e, e.